ABSTRACT

Title of Thesis:	DESIGN AND PERFORMANCE EXPLORATION OF A SCALED-UP MILLIGRAM-SCALE FLAME CALORIMETER
	Kyra Cromwell Reed, Master of Science, 2024
Thesis Directed By:	Assistant Professor Fernando Raffan-Montoya, Fire Protection Engineering

Fire causes thousands of lost lives and injuries, as well as billions of dollars of property damage, each year. It is critical to understand the fire hazard associated with materials used in the built environment. One method to evaluate the flammability properties of a material is through bench-scale and milligram-scale testing with apparatus such as the Milligram-Scale Flame Calorimeter (MFC). The MFC has previously been used to test samples ranging from 30 mg – 50 mg in mass. The small samples were useful for testing materials under development or materials cost prohibitive to test at larger sizes, but presented some difficulties in testing, including in sample preparation and as inconsistency in the results of testing on inhomogeneous materials. Furthermore, the small size of the MFC caused difficulty in heater manufacturing, requiring laborious by-hand construction. The size of the MFC crucible and apparatus was increased in this work to allow testing on larger sample masses, ranging in size from 90 mg – 150 mg, and for the exploration of five alternate heater manufacturing techniques. The MFC was rebuilt with a larger heater and optimized to create the best possible test conditions for this work. Tests were conducted on five polymers: polymethyl methacrylate (PMMA), polyethylene (PE), polyvinyl chloride (PVC), and polyether ether ketone (PEEK), and on a wood-based material: oriented strand board (OSB). The tests showed general consistency when materials were tested at different sample

masses and sample presentations. The results for the heat release rate and heat of combustion of the materials also aligned well with testing conducted using the previous version of the MFC apparatus. The updates to the MFC conducted in this work constitute an improvement to the versatility of the apparatus, allowing for testing on larger sample masses, but future work is needed to resolve flow and exhaust issues that caused some inconsistency in the test results and to further explore and develop alternate heater manufacturing techniques.

DESIGN AND PERFORMANCE EXPLORATION OF A SCALED-UP MILLIGRAM-SCALE FLAME CALORIMETER

by

Kyra Cromwell Reed

Thesis submitted to the Faculty of the Graduate School of the
University of Maryland, College Park, in partial fulfillment
of the requirements for the degree of
Master of Science
2024

Advisory Committee:

Assistant Professor Fernando Raffan-Montoya, Chair
Professor Stanislav Stoliarov
Assistant Professor Shuna Ni

Acknowledgments

First, I would like to thank my parents for their love and support this year. It wasn't always easy, but I am so grateful that I had you to lean on during the harder days. Thank you for the encouraging sticky notes on the mirror, the meals made just because I like them, and the hours spent watching the Great British Baking Show to relax. And don't worry, now that I'm done, I promise I'll move out! Thank you so much for your love, your time, and your support.

I would like to thank my advisor, Dr. Fernando Raffan-Montoya. I am truly grateful to have had this experience which has taught me a lot, not just about experimental work and the MFC specifically, but also about myself. I know that I will carry this experience forward with me throughout my career and I am so thankful to have had your encouragement, support, and kind words throughout this year. I am proud to have been your student and I am excited to see where future research on the MFC goes.

Next, I would like to thank Dr. Stanislav Stoliarov for his support throughout this process. Your comments, questions, and suggestions during meetings challenged me to think more deeply about my work and made me a stronger student and researcher. Thank you for your time and your guidance.

I would also like to extend a huge thank you to Thomas Roche, who spent time throughout this year teaching me about the MFC, on topics from running tests to post-processing data. Your working knowledge of the MFC was critical to my success in my thesis and your generosity with your time, throughout the year, but particularly at the end of this process with sample preparation and the high volume of tests, was immensely helpful and I can't thank you enough.

I would also like to extend a thank you to all the other graduate students who have been a part of my experience this year. As I'm sure you know, I love talking to you all. You've made the office

enjoyable and each one of you is kind and smart, and I can't wait to see the things we all go on to do in the future. And thank you for being so supportive of the holiday decorations in the office this year, I like to think that it brought a little extra fun to the space.

I would also like to thank Dr. Shuna Ni for her time serving as a part of my thesis committee. Additionally, I would like to thank the entirety of the FPE department for their kindness and support during my time as a student, both as a graduate and as an undergraduate. I have loved being part of such a special community.

Finally, to my friends outside of FPE, thank you for your support and love, and for understanding at the end of this process when I spent all my time writing or in the lab. Thank you for cheering me on.

Contents

List of Figures

List of Tables

List of Abbreviations

MFC – Milligram-Scale Flame Calorimeter

MCC – Microscale Combustion Calorimeter

FPA – Fire Propagation Apparatus

HRR – Heat release rate

pHRR – Peak heat release rate

HOC – Heat of combustion

MLR – Mass loss rate

NDIR – Nondispersive Infrared

FLIR – Forward Looking Infrared

NiCr – Nickel chromium

NPT – National Pipe Tapered

PTFE – Polytetrafluoroethylene

OD – Outer diameter

ID – Inner diameter

PMMA – Polymethyl methacrylate

PE – Polyethylene

PVC – Polyvinyl chloride

PEEK – Polyether ether ketone

OSB – Oriented strand board

SLPM – Standard liters per minute

sccm – Standard cubic centimeters per minute

1. Introduction

Local fire departments respond to over 1.5 million fires in the United States each year. These fires cause thousands of civilian deaths and injuries, as well as billions of dollars of property damage each year. NFPA reports that 35% of these fires occurred in structures but that fires in structures caused 77% of deaths, 88% of injuries, and 83% of property damage [1]. Although there has been a significant reduction in the number of fires and fire related deaths, injuries, and damages since 1980, the last five years have seen a new increase in the number of fires. The number of deaths and injuries from fire has been steady for approximately a decade, showing that improvement in fire safety in structures has slowed in recent years.

Synthetic materials, such as plastics, including polyurethane and polyester, and engineered wood, are known to burn more quickly than traditional materials, such as solid wood and cotton. The Fire Safety Research Institute conducted several comparison burns between near identical rooms furnished with synthetic and traditional materials. The room furnished with synthetics reached flashover in an average of 4 minutes and 50 seconds, whereas the naturally furnished rooms did not reach flashover conditions during the 30-minute experiments [2]. This discrepancy between the time to flashover suggests that the synthetic materials are more flammable, and the increase in their use may be correlated with the increased number of fires in the United States.

Particularly as the materials used in the home evolve to reflect new manufacturing techniques, it is important to understand how the materials will burn. Similarly, as construction techniques change to be more economical and environmentally friendly, such as the increase in wood frame construction, it is critical to understand the way in which the construction materials and the material contents of the structure will burn. Developing an understanding of material flammability

is critical to improving fire safety and reducing the number of fires, fire deaths, injuries, and damage occurring each year in the United States.

1.1 Material Flammability

Flammability is evaluated using a variety of parameters including ignitability, flame spread, mass loss rate (MLR), heat release rate (HRR), heat of combustion (HOC), and smoke and soot yield. These parameters describe how quickly a material ignites, the rate at which it burns, and the intensity at which it burns, as well as the products produced during combustion. These flammability parameters can be examined and tested through various bench-scale and milligram-scale flammability tests and apparatuses. Commonly used tests and apparatuses include cone calorimetry, the Fire Propagation Apparatus, the Microscale Combustion Calorimetery, and the Milligram-Scale Flame Calorimeter. Understanding the applications and limitations of these test methods is important for selection of the most appropriate testing method for the overall best understanding of a material's flammability.

1.1.1 Cone Calorimetry

The cone calorimeter is the best-known flammability test apparatus, and cone calorimetry is the most widely used method to measure the heat release rate of materials [3]. There are many variations on the basic design of the cone calorimeter that allow for different test parameters, experimental setups, and sample sizes. The typical bench-scale cone calorimeter exposes materials to controlled levels of external radiant heating, usually 10 to 100 kW-m^{-2} [4], as well as, optionally, an external ignition source, usually a spark plug. Materials may be oriented either horizontally or

vertically, and a wide range of materials can be tested using the cone calorimeter. The typical bench-scale cone calorimeter and involved instruments are depicted in Figure 1.1.

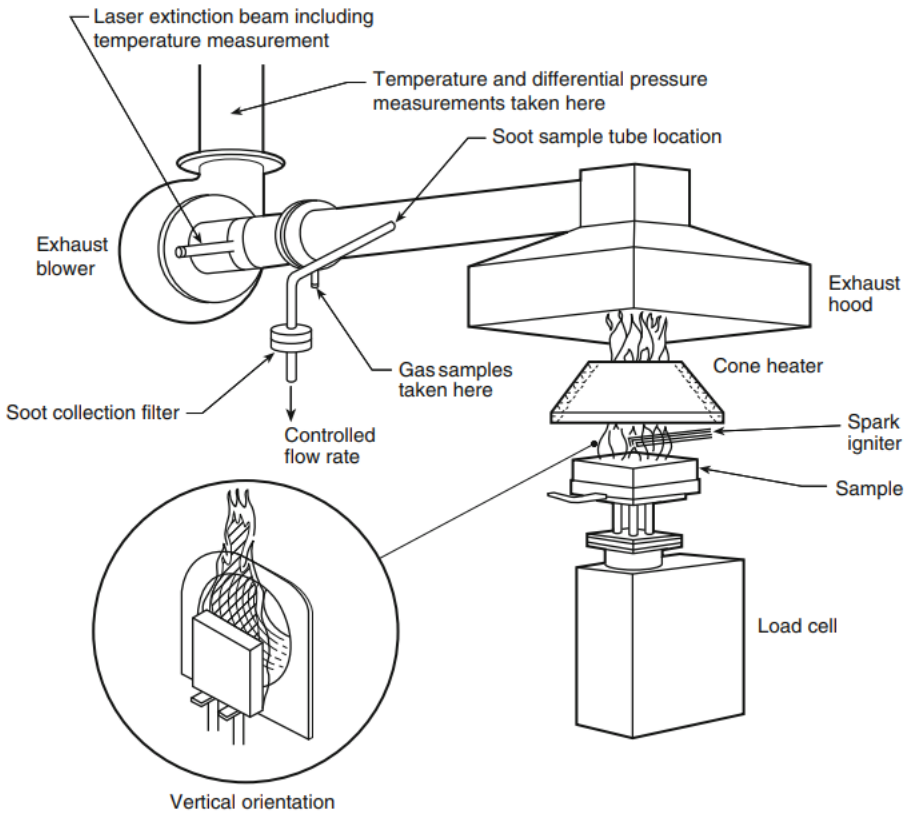

Figure 1.1 Experimental setup for cone calorimeter tests [5]

Oxygen consumption calorimetry is used to determine the heat release rate as it varies in time by measuring the exhaust air flow rate and the concentration of oxygen in the exhaust gases. This method is based on empirical observations by Huggett that for most materials 13.1 ± 0.6 kJ-kg^{-1} of energy is released per kilogram of oxygen consumed, which allows for the calculation of HRR when a known amount of oxygen is consumed [6]. The method is also utilized to calculate the peak heat release rate (pHRR) of a sample and the time-averaged HRR.

A mass balance can also be integrated into the setup of the cone calorimeter providing mass data over time on the sample. This is used to calculate MLR as it varies over time and the average

MLR. To find the HOC of a sample per unit mass, the HRR curve can be integrated over time and divided by the total mass lost during the test. The cone calorimeter can also be used to determine a material's time to ignition when exposed to radiant heating and the char yield of a tested material. When multiple tests at varying heat fluxes are conducted, the critical heat flux for ignition (Q''_{crit}) can also be determined, as can the ignition temperature of a test material. This makes cone calorimeter particularly versatile in measuring a variety of flammability parameters for many types of materials.

The cone calorimeter also has applications for determining smoke yield and visibility during burning as described and standardized in ASTM E1354 [3]. The smoke extinction coefficient is determined from cone tests using light extinction measurements and calculated using Bouger's law. The smoke extinction coefficient is a popular optical property used to evaluate the smoke produced by a fire, and it can be used to determine the mass of smoke generated by a fire, meaning that cone testing can be used in this manner to determine smoke yield.

There are some limitations inherent in cone calorimetry. First, is that the size of samples required for cone testing is large, even at the bench-scale. Typical bench-scale samples are 100 mm by 100 mm square and up to 50 mm thick with masses between 30 to 50 grams. This means that cone calorimetry may not be suitable for use in material or product development where producing samples of this scale may be cost or labor prohibitive. A second limitation is the negative impact of sample swelling on the uniformity of the radiation received across the sample surface. This swelling impacts the ability to analyze test results as the heat flux profiles across the surface vary and cannot be accurately known for data analysis. Additionally, sample swelling may interfere with the performance of the external ignition source. Thus, it is a challenge to properly test highly intumescent samples in the cone calorimeter. Similarly, other types of materials, such

as fabrics, are less suitable for cone testing due to their material properties. For example, previous experience has shown burning lightweight fabrics does not result in significant oxygen depletion in cone testing, resulting in higher signal to noise ratios and greater uncertainty in the data.

1.1.2 Fire Propagation Apparatus

The Fire Propagation Apparatus (FPA) is another bench-scale apparatus used to evaluate the flammability of materials. Samples are exposed to radiant heat fluxes up to 65 KW-m^{-2} supplied by infrared tungsten heating lamps and ignited using an ethylene-air pilot flame [7]. The oxygen environment around the sample can also be controlled to simulate both an under- and an over-ventilated fire condition, a significant advantage of the FPA compared to other test apparatus. The ability to control the atmosphere composition and flow rate also allows for the close emulation of conditions seen in real fires. The FPA has been standardized in accordance with ASTM E2058 [8], which calls for three tests to obtain different flammability characteristics of a tested material. The FPA can be used to determine the time to ignition, the chemical and convective HRR, the mass loss rate, the HOC, and the smoke production. Materials are tested in both a horizontal orientation, with a 101.6 mm square sample with a maximum thickness of 25.4 mm, and in a vertical orientation, with a 101.6 mm by 305 mm rectangular sample with a thickness ranging from 3 to 13 mm. The apparatus is shown in Figure 1.2.

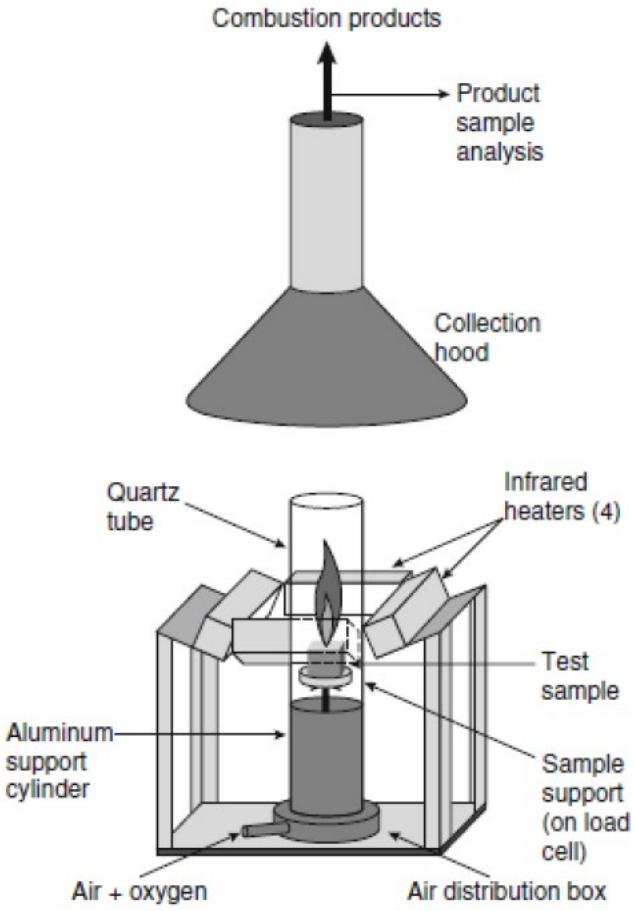

Figure 1.2 Experimental setup for fire propagation apparatus tests [10]

The FPA is versatile and offers the ability to determine a variety of flammability parameters, but FPA testing is not trivial and testing in triplicate means that FPA testing can be time consuming and labor intensive. The FPA is also unsuitable for material development testing or testing of expensive materials. Because a minimum of three tests is desired for adequate test data, the large sample size required for each test may be cost prohibitive when testing novel materials or additives.

1.1.3 Microscale Combustion Calorimetry

Developed by the Federal Aviation Administration and standardized in ASTM D7309, Microscale Combustion Calorimetry (MCC) is a test method that can be used to determine the maximum HOC

of a material, as well as other intrinsic material properties [10]. The MCC has been used for screening flame retardants for plastics [11]. Milligram-sized samples, ranging from 1 to 10 mg, are placed in a ceramic crucible that is inserted into a pyrolyzer heated by 0.5 to 2 °C per second to a maximum standard temperature of 750 °C [12]. MCC tests do not involve flaming combustion, and MCC tests force complete combustion of all fuel, meaning there is no particulate matter and little to no CO expected in the combustion products.

There are two options of MCC test methods. The first involves a pyrolyzer that heats the sample in an inert, typically nitrogen environment. Volatiles produced by the heated sample are carried by the inert purge gas to a separate combustion chamber where there is sufficient oxygen and heat for complete combustion. In this method, there is no smoldering at the sample and, as with all MCC tests, no flaming combustion at any point in the test. The second MCC test method flushes the volatiles produced by the heated sample into the combustion chamber using dry air. This allows for smoldering combustion at the sample surface during testing, but no flaming combustion in this version of an MCC test. The MCC apparatus is shown in Figure 1.3.

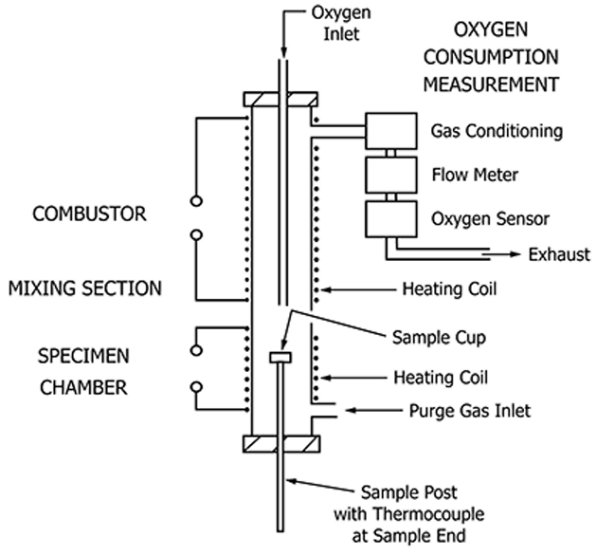

Figure 1.3 Experimental setup of Microscale Combustion Calorimeter (MCC) [13]

In both cases, air flow and oxygen levels are measured throughout the test for use in determining HRR through oxygen consumption calorimetry. The HOC is calculated by integrating the HRR curve over time for the duration of the test. The HOC is also typically normalized by initial sample mass or by volatilized mass. The volatilized mass is found by subtracting the final sample mass from the initial sample mass, which also allows the char yield to be determined from the final sample mass.

The MCC is useful for providing information on HRR and HOC for low mass samples, making it suitable for use during product or material development or for testing of expensive materials, but it has some inherent limitations. The MCC forces complete combustion of all volatilized fuel, meaning only the maximum HOC can be found using this test method. Forcing complete combustion means no particulate matter is expected in the combustion products of an MCC test, and as such, MCC tests are limited in their ability to accurately predict material behavior in real fire conditions where complete combustion is unlikely and smoke is expected to be generated. Furthermore, there is no flaming combustion in an MCC test, which means that even qualitatively it is difficult to use an MCC test to predict the behavior of a tested material in a real-flame situation. A final drawback of the MCC is that the test materials are completely enclosed for the duration of testing, and therefore, there is no ability to visually observe the condensed phase processes or the pyrolysis process during an MCC test.

1.1.4 Milligram-Scale Flame Calorimeter

The Milligram-Scale Flame Calorimeter (MFC) is a bench-scale flammability test method that can be used to find the pHRR, HRR, HOC, and char and soot yields of tested samples. The MFC uses oxygen consumption calorimetry, like the cone calorimeter and the MCC, to determine the HRR and HOC. The MFC was originally developed to measure gas-phase activity of flame-retardant

additives used with thermoplastics [13]. The MFC has since also been used to examine additive flame retardants in small fabric samples of 30 - 50 mg, a much smaller scale than that used for the cone calorimeter and on a similar order of magnitude to the test samples used in MCC testing. In its current iteration, the heating profile used in the MFC mirrors the profile seen in cone tests, leading to the possibility of strong comparisons between cone tests and MFC tests done at a smaller scale.

There have been several iterations of the design of the MFC, with the most recent updates being conducted by DeBeer [9] and Roche [14]. A schematic diagram of the most recent MFC design, prior to this work, is shown in Figure 1.4.

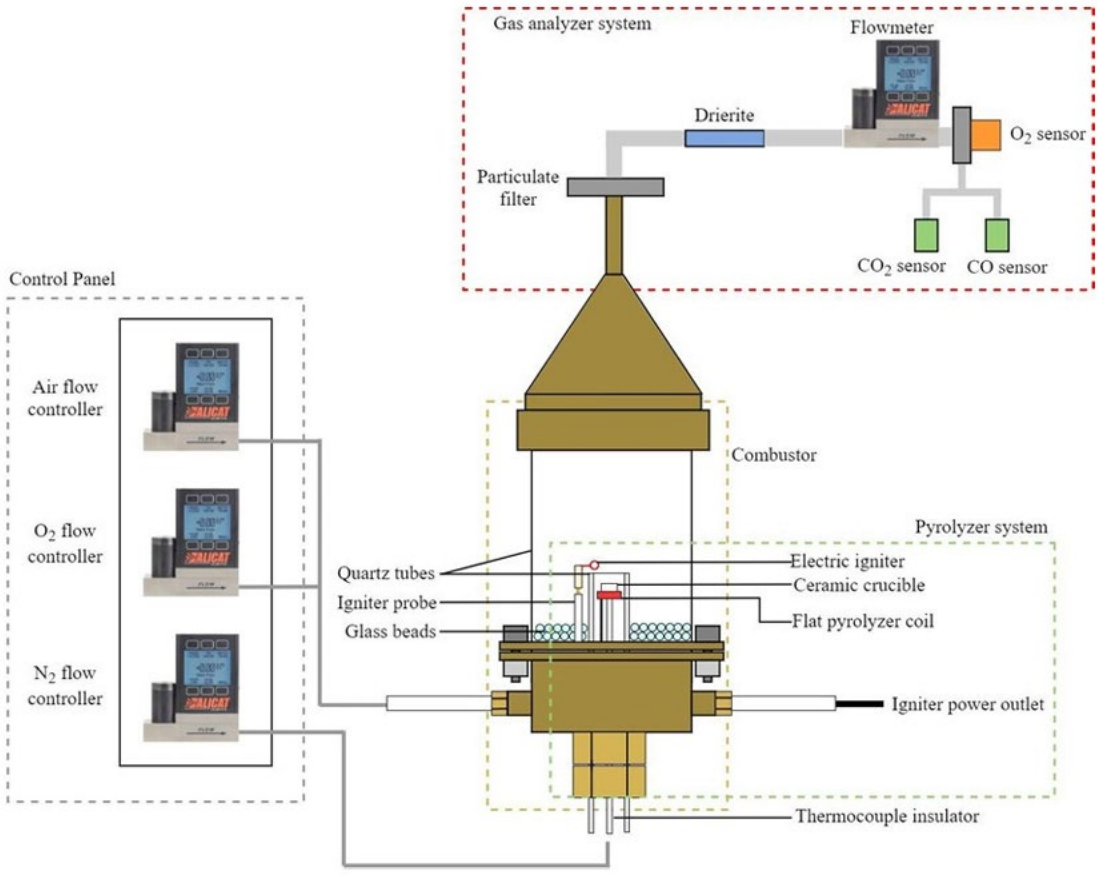

Figure 1.4 Experimental setup for Milligram-scale Flame Calorimeter (MFC) [9]

Test samples are placed in a ceramic crucible that sits on a ceramic hot plate containing a NiCr wire heating coil and a thermocouple. The thermocouple bead sits level with the top of the ceramic flat plate and makes direct contact with the bottom of the crucible. A schematic of the current pyrolyzer and crucible developed by DeBeer is shown in Figure 1.5. Samples are heated through conduction from a hot plate using two nonlinear heating ramps, first to a consistent initial sample temperature 47 ℃ then to a final temperature of 695 ℃ during the pyrolysis ramp [9] [14].

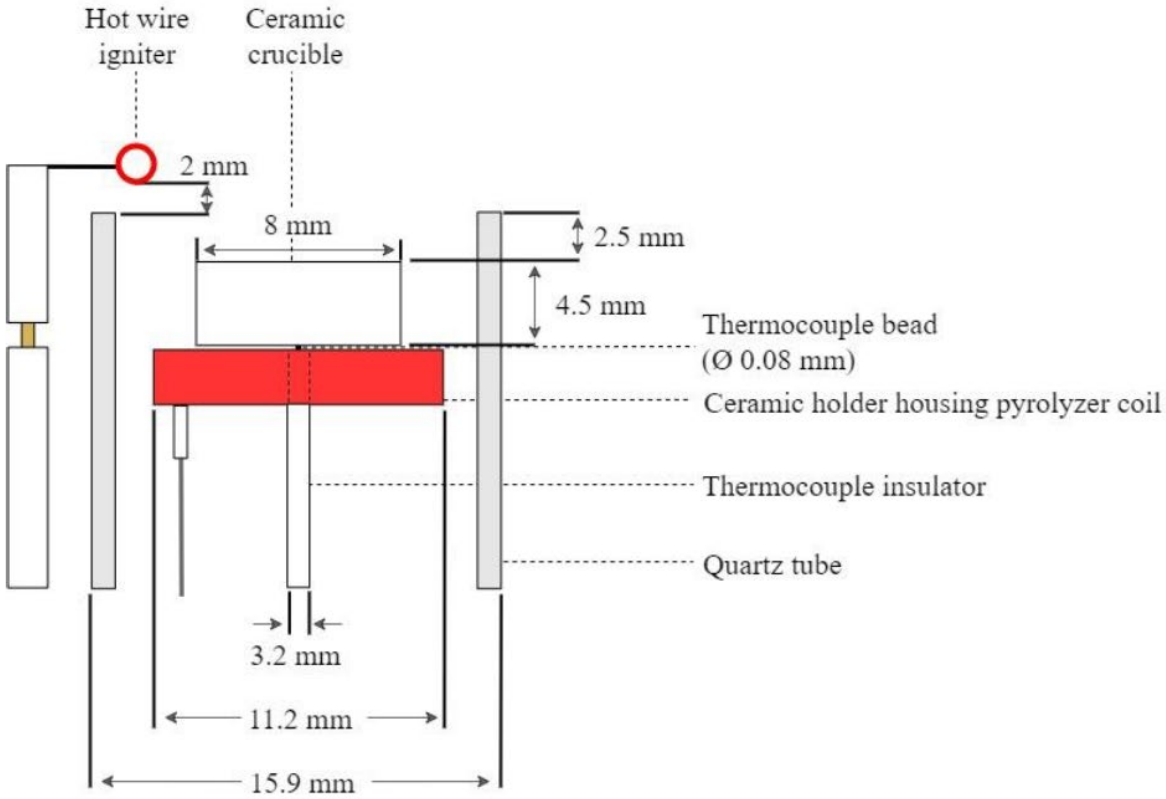

Figure 1.5 Schematic of MFC pyrolyzer, crucible, and igniter developed by DeBeer [10]

As the temperature increases during the second ramp, the sample pyrolyzes producing volatile gases that are pushed upward by nitrogen flowing through the inner quartz tube seen in Figure 1.4 and Figure 1.5. When the gases leave the inner quartz tube and enter the air environment of the outer quartz tube, they encounter an electric igniter that is turned on to allow a laminar, axisymmetric, diffusion flame to be established. The igniter is turned off after 5 seconds of steady

flaming to allow the test to reflect a self-sustaining flame. The products of combustion are carried downstream by the air co-flow through a 2-micron filter, which captures solid and liquid matter present in the combustion products. The mass of the filter is measured before and after a test to determine the soot yield [9] [14].

Then, the gasses flow through a ¼" tube filled with a desiccant to remove the moisture from the flow. Finally, the gases pass through a flowmeter to measure the total flow rate out of the MFC and sensors for oxygen, carbon monoxide, and carbon dioxide. An electrochemical oxygen sensor (Teledyne R17a) and Nondispersive Infrared (NDIR) CO and CO_2 sensors are used to measure gas concentration after combustion. During tests, a camera focused on the flame is used to record the test, providing visual information on ignition time, burning duration, and flame behavior that can be used to corroborate and build on the measurements recorded by the sensors [9] [14].

The MFC can measure many flammability parameters in a single test. Furthermore, the small sample size significantly reduces the amount of material required to conduct tests, making the MFC ideal for testing materials that may be expensive, difficult to produce, or in a material development phase. This is a significant advantage compared to the cone calorimeter or the FPA. Unlike the MCC, there is flaming combustion in MFC tests meaning that MFC tests can provide a more accurate description of the HRR and HOC when a material burns in real-flame conditions. Furthermore, complete combustion is not forced in MFC tests, increasing the accuracy of the measured soot yield to a real fire condition as compared to MCC tests, which force complete combustion. Additionally, MFC tests measure smoke yield gravimetrically by capturing combustion products in a filter for measurement rather than determining smoke yield through optical measurements, as done in cone calorimeter testing. Measuring the actual mass of the combustion products is a more direct method to determine smoke yield. Finally, the MFC is also

able to easily provide data on other aspects of flaming combustion such as flame height making it also useful for developing more qualitative descriptions of material behavior when burning.

1.2 Drawbacks of the MFC

However, the small design of the MFC prior to this work had several drawbacks that for some sample materials made the test method less effective and made construction of parts of the apparatus time consuming.

1.2.1 Size of Samples

In the design of the MFC prior to this work, the crucible used to hold sample materials has an 8 mm OD and a height of 4.5 mm. Samples must completely fit inside the crucible to be tested in the MFC as a sample that intumesces, chars, or bubbles out of the crucible can spill onto the pyrolyzer or be carried out of the inner quartz tube and become exposed to air prematurely. Often samples need to be significantly shorter than the crucible height to avoid the effects of intumescing, charring, or bubbling out of the crucible. Additionally, samples also must weigh between 30 - 50 mg, meaning that particularly low-density materials were not suitable for testing in the MFC. Other materials, such as fabrics like cotton and nylon, need to be layered to be tested in the MFC to achieve the desired mass for testing. While layering is an effective method, it did tend to lead to problems with bubbling for some types of samples, such as nylon.

1.2.2 Ease of Sample Production

For materials that could meet the size and mass requirements for testing in the MFC, the small sample size creates other problems in the process of sample preparation. Some materials can be ground into a powder for testing, but many materials cannot be ground into powder and need to be cut to size. For many materials, cutting a sample smaller than 8 mm in diameter is challenging.

For fabrics, it requires the use of a fabric hole punch, which is effective but produces inconsistently shaped samples.

Other samples are even more difficult to prepare. Tests on oriented strand board (OSB) found that while a cork drill bit could be used to cut samples to small cylinders of the correct diameter, the small size of the sample led to breaking, cracking, and chipping in the larger piece of material. The small sample pieces were also prone to breaking and cracking during the drilling process making it difficult to achieve consistent height and mass across samples. Because the drilled pieces were inconsistent, it was necessary to further cut or shave them by hand to achieve a consistent mass between 30 to 50 mg for all samples used for testing. Hand cutting the samples also sometimes resulted in breakage of the sample into pieces too small for testing. Producing samples for just a few tests in this method was time-consuming and laborious.

Furthermore, cutting non-circular shapes to fit into the crucible was not easily achievable due to the small size of the crucible. Cutting materials, rather than grinding, hole-punching, or drilling them may be an easier method of sample preparation, however, it is not easily achievable for most materials at the current crucible size.

1.2.3 Inhomogeneous Materials

The MFC is intended to offer an alternative to testing a larger sample mass, but for some materials the small sample size required for testing in the MFC means that tests are not representative of a larger piece of material. Many materials are non-homogeneous and have inconsistencies in properties, such as density, throughout a large sample. Perhaps more importantly, given the development of the MFC to examine the effects of flame retardants, treatment of materials with flame retardants is often inconsistent and uneven across the surface and through the body of a large piece of material.

Larger bench-scale testing, such as a cone test, uses a sample large enough to include inhomogeneities in material properties or inconsistency in material treatment. The results of that test using the cone or the FPA would reflect the effects of the sample inconsistency. Running multiple MFC tests using samples from various locations in a larger piece of material can provide some information on how an inhomogeneous material may burn, however, an individual MFC test is unlikely to provide sufficient information on how an inhomogeneous material will burn.

Furthermore, as described previously, the difficulty of producing small enough samples for use in the previous MFC design meant that sample sections were selected based on their likelihood to create a good sample. This often meant the exclusion of areas with a high degree of inhomogeneity given concerns about breaking or chipping, meaning that even across multiple tests it would be difficult to understand how the inhomogeneity of a material affects pHRR, HRR, HOC, and soot yield.

1.2.4 Preservation of Characteristic Length

As mentioned previously, the design of the MFC requires samples to fit in the 8 mm OD crucible. While this sample size has been suitable for materials such as fabrics, wood, and plastics, there are materials for which there is interest in flammability testing where this sample size may not be appropriate, such as for materials where preserving the characteristic length is important to understanding burning behavior. Characteristic length is particularly important in testing biomass fuels, such as pine needles, which are the subject of significant research interest due to the increasing prevalence and severity of wildfires.

1.2.5 Pyrolyzer Construction

The pyrolyzer design prior to the updates in this work is a NiCr wire coil inside of a small 11 mm OD ceramic plate. A 10 cm length of wire is coiled manually three times into the plate, which

requires great care to avoid electrical shorting. Making a pyrolyzer coil requires significant time and effort. Then, the thermocouple probe must be inserted into the plate and aligned vertically so the bead sits parallel to the top of the plate. Finally, a plaster must be applied to the plate to hold the wire coil and the thermocouple probe in place. Along with calibration, the entire process to build a pyrolyzer can take several days. This process was developed because it was not possible to manufacture heaters of the desired 11 mm OD size.

1.3 Objectives

Increasing the size of the crucible and heater used in the MFC will address the five drawbacks of the MFC design to increase versatility and usability of the MFC. Increased crucible size would allow for testing of lower density materials and reduced need for layering of fabric materials. This would allow for improved ability to test on intumescent materials, as well as for testing samples of larger mass. Using a larger sample size would also make it easier for all materials to be cut to size with greater repeatability. For materials that require drilling cylindrical samples, larger sizes would be significantly easier to drill, and the size increase would reduce the chances of breaking, cracking, and chipping in the prepared sample and in the piece of larger material. For all materials, a larger crucible also means an increased ability to use non-circular sample shapes as larger shapes will fit into the crucible. The increased ability to test non-circular samples also would allow the MFC to be used to test materials where preserving the characteristic length is important to the burning behavior. Increasing the size of the MFC would give it the ability to be used for biomass flammability testing, giving it increased relevance in the expanding field of wildfire research.

Increasing the size of the MFC will also improve the manufacturability of the pyrolyzer, which is currently constructed manually. An increased size will allow for new manufacturing techniques to be explored. The hand coiled NiCr wire method could also still be utilized for pyrolyzer

construction and would be easier to construct at a larger scale, particularly in terms of achieving a sufficient number of coils for heating while avoiding electrical shorting.

The MFC has great utility as a milligram-scale test method, particularly for use with materials under development, but there are several significant drawbacks and challenges involved with the apparatus. Primarily the constraints on the use of the MFC come from the small size of the crucible and pyrolyzer system. Additionally, the construction of the pyrolyzer is completed by hand and is time-consuming, creating a significant manufacturing challenge for replacing this part of the MFC in a simple and repeatable way.

The objectives of this study are as follows:

- Design and build a larger pyrolyzer and crucible system
- Explore manufacturing techniques to produce pyrolyzers more quickly and with increased repeatability
- Characterize new pyrolyzer system using a range of materials with diverse combustion performance

Increasing the size of the crucible will allow for greater ease in sample preparation, as well as increased utility with low-density, intumescing, or inhomogeneous materials and materials where preservation of the characteristic length is important for understanding burning behavior. Increasing the crucible size requires increasing the size of the pyrolyzer. To do this, the current method of coiling nickel chromium wires into a ceramic plate will be applied at a larger scale, but several other methods of heater manufacturing will also be explored to simplify and optimize the production of this crucial part of the MFC apparatus. The alternate methods will be evaluated on their repeatability, reliability, durability, ease of manufacture, and cost. Increasing the heater size will involve increasing the size of the inner quartz tube of the apparatus, as well as the base,

supports, and supply flow components of the MFC, which will require the re-calibration of flow rates and conditions for successful testing. The changes to the MFC pyrolyzer will address the challenges inherent in the MFC design and make it a more versatile apparatus and expand its potential in the research world.

2. Design Exploration

This work explores modifications that could be made to the MFC test apparatus to address the drawbacks discussed in detail in Chapter 1.2. One of the major drawbacks is the small sample size required for use with the previous version of the MFC. The limitations on sample size also create concerns with testing highly intumescent materials, inhomogeneous materials, and materials with geometries that must be maintained during testing. The size of the crucible in which test samples are placed was increased in this work to address the drawbacks of the previous version of the MFC. In the previous iteration of the MFC, samples in sizes ranging from 30 mg to 50 mg could be tested and this sample mass was increased to a target sample size of 90 mg to 120 mg for the current study. This size increase maintains the order of magnitude of sample mass in the tens of milligrams, a desirable feature of the original MFC. Because the drawbacks in the previous iteration of the MFC mainly arose from the small diameter of the crucible and not the height of the crucible, the size of the crucible was changed by increasing the diameter only.

Another drawback of the previous version of the MFC is that pyrolyzer construction was laborious and limited to manual methods, due to the small size of the pyrolyzer. Increasing the crucible size also necessitated an increase in pyrolyzer size, so new methods of pyrolyzer construction will be explored and evaluated for their feasibility moving forward with this larger version of the MFC.

2.1 Crucible Size Increase

The crucible size could be altered by changing the height of the crucible walls, the diameter of the crucible, or by changing both. The height of the crucible walls has not caused issues in the previous version of the MFC, so the height of the crucible walls was maintained while the diameter was increased. Increasing only the crucible diameter to increase sample mass addresses the problems

seen in previous experience with highly intumescent or bubbling samples in the original, smaller MFC. The increased crucible diameter relieves the constriction on the path of the volatiles as they leave the crucible, which allows highly intumescent or bubbling materials to be tested without concerns that the materials will expand or bubble out of the crucible and onto the pyrolyzer plate or quartz tube. Additionally, for materials that may need to be layered to achieve enough sample mass, such as fabrics, a larger crucible diameter allows for fewer layers to be used to achieve the desired sample mass. With fewer layers, fabric samples will more closely resemble the way in which the material is used during full-scale applications. Finally, for all materials, a larger crucible diameter enhances the thermal contact between the crucible and the pyrolyzer plate, allowing for improved heating.

The increased area of the crucible also addresses several of the other drawbacks in the previous iteration of the MFC. Sample preparation was challenging due to the small diameter that samples needed to be cut to fit within the crucible. A larger diameter will allow for cutting larger samples, making it simpler to cut repeatable samples and easier to cut samples in non-circular shapes. Furthermore, the previous iteration of the MFC struggled to capture the effects of inhomogeneity in a material due to the small sample area. The larger crucible size will allow for samples with an increased surface area, which better reflects the overall characteristics of the material. Larger sample sizes will be particularly beneficial for testing and understanding the burning behavior of materials like OSB or materials with a surface treatment, such as a flame retardant. Furthermore, increased crucible area also allows sample characteristic length to be maintained while testing. For example, with some materials, such as biomass like grass or pine needles, it is important to preserve the original geometry of the material during testing, even at the reduced scale used for MFC tests, to better understand the material burning behavior. Though the new, larger crucible

will not fit an entire leaf or pine needle, it will allow for a portion of the material to be tested while still retaining the key geometry of the original piece of biomass, something that is not possible with the original MFC crucible or other small-scale methods, like the MCC. Because the crucible size was being changed, it was also possible to alter the crucible in other ways to further improve MFC testing. The thickness of the crucible walls and floor was decreased from the previous version of the MFC. This improves heat transfer between the pyrolyzer plate and the sample resulting in minimized heat loss to the ceramic of the crucible. A dimensioned drawing of the new crucible is shown in Figure 2.1.

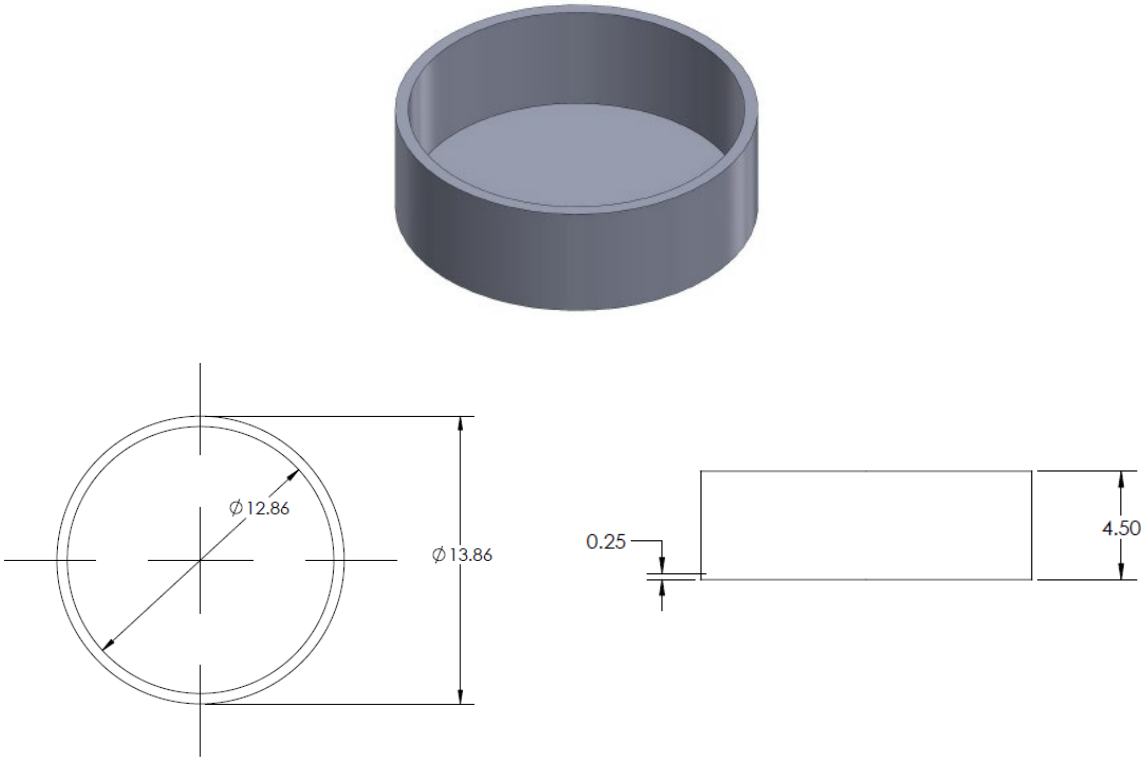

Figure 2.1 Dimensioned drawing of updated crucible design for larger version of the MFC.

The increased diameter of the crucible required the pyrolyzer diameter to be increased. Since new pyrolyzer construction methods were to be explored and a new pyrolyzer was to be built, the pyrolyzer plate was also updated to improve on the previous iterations. The thickness of the walls of the pyrolyzer plate was increased to reduce the fragility of the piece. Additionally, the height of the walls was increased to allow for greater flexibility in the size of wire used for pyrolyzer construction and for greater flexibility in the techniques that could be used in pyrolyzer coil construction. Finally, the hole in the center of the pyrolyzer plate where the thermocouple rod is inserted was closed. In the previous iteration of the MFC, described and pictured in Chapter 1.1.4, it was necessary to carefully place and adjust the location and angle of the thermocouple rod to ensure that the thermocouple bead was located flush with the face of the pyrolyzer plate. Closing this hole with an 0.5 mm thin layer of ceramic allows for consistent placement of the thermocouple bead between multiple pyrolyzers, increasing the reliability and repeatability of the temperature profile measurements from that thermocouple. During manufacturing of this part, it was initially produced with this hole left open, and, due to time constraints, tests in this study were run with the plate with the hole open, as in the pyrolyzer plate of the previous version of the MFC. A dimensioned drawing of the updated pyrolyzer plate is shown in Figure 2.2.

Increasing the size of the crucible and pyrolyzer plate also required the size of the inner quartz tube to be increased to fit the new pyrolyzer assembly. A schematic of the new dimensions of the crucible, pyrolyzer, and inner quartz tube is shown in Figure 2.3. The dimensions of the crucible, pyrolyzer, and quartz tube in the new apparatus are shown in Table 2.1, along with the dimensions of the same parts in the previous iteration of the MFC for comparison.

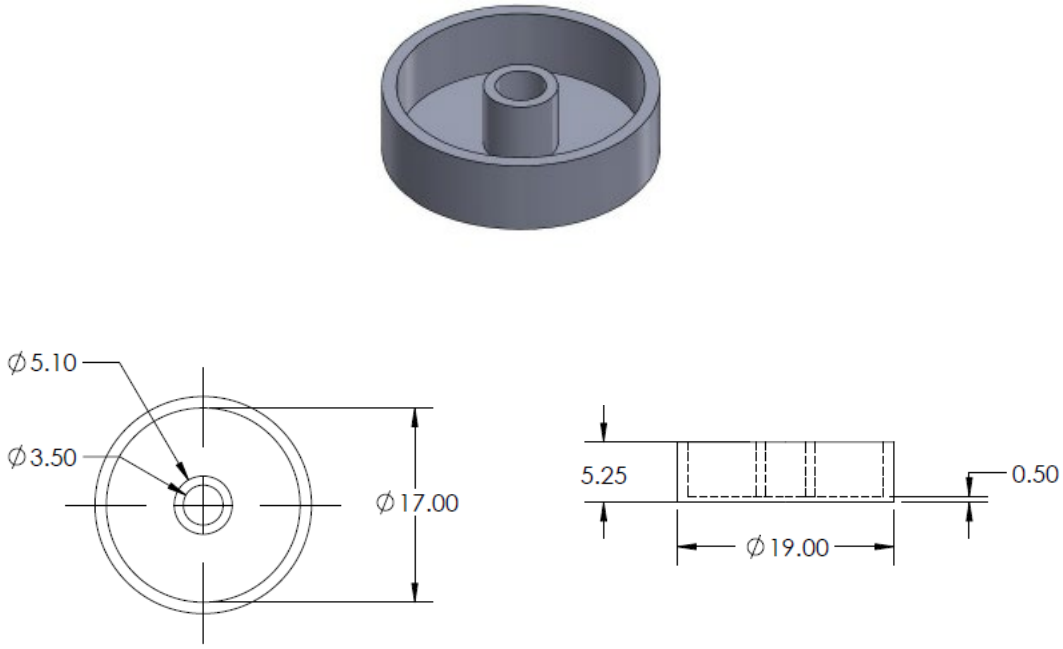

Figure 2.2 Dimensioned drawing of updated pyrolyzer plate design for larger version of the MFC.

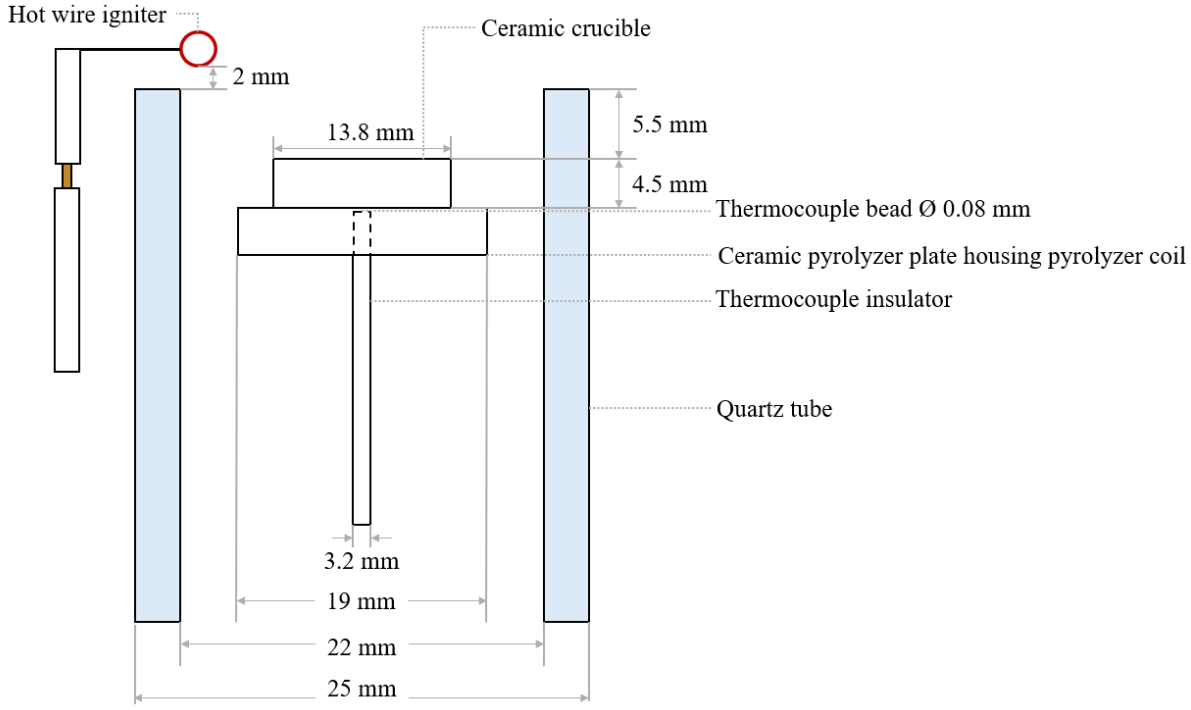

Figure 2.3 Schematic of crucible, pyrolyzer, inner quartz tube, and igniter setup (not to scale).

Table 2.1 Dimensions in mm of crucible, pyrolyzer, and inner quartz tube in updated and previous versions of MFC

	Updated MFC	Previous MFC
Crucible Inner Diameter [mm]	13.9	8
Crucible Height [mm]	4.5	4.5
Pyrolyzer Plate Diameter [mm]	19	11.7
Quartz Tube Inner Diameter [mm]	22	13
Quartz Tube Outer Diameter [mm]	25	15.8

2.2 Heating Element Manufacturing Methods

Increasing the size of the MFC crucible and pyrolyzer allowed for the opportunity to explore new manufacturing methods for the pyrolyzer. The previous MFC pyrolyzer assembly was so small that many automatic heater manufacturing techniques, such as 3D printing, were impractical or impossible to implement, and a hand coiled wire was the only method available for heating. At the larger size, however, it became possible to explore a variety of potential heater manufacturing techniques that could be implemented in the pyrolyzer.

In the previous iteration of the MFC design, the pyrolyzer is produced in the lab by hand. To make the heater, a 10 cm length of 0.4 mm x 0.4 mm square 80-20 nickel-chromium (NiCr) wire is cut and then coiled into a flat spiral [9]. An example of the pyrolyzer coil is shown in Figure 2.4. An ohmmeter is used to check the resistance of the wire before and after coiling to check if an electrical short has developed due to the wire touching itself. The resistance of the pyrolyzer coil is 0.7 Ω. When the coil has been created and tested to verify there are no electrical shorts, it is placed carefully into the ceramic pyrolyzer plate. A coating of Autocrete ceramic cement is applied on top of the wire to insulate the wire and hold it in place in the ceramic element. An Omega 0.08 mm diameter K-type thermocouple, insulated by a ceramic rod, is inserted into the center of the

ceramic heater, and also held in place using cement. When the cement is partially hardened, the thermocouple insulator must be adjusted to ensure it is perfectly vertical and the bead of the thermocouple is aligned flush with the top surface of the ceramic heater. Once the cement is hardened, the ends of the pyrolyzer coil are fitted with female D-sub socket contact crimps with a 20 – 24 AWG gauge. The entire process takes over 24 hours, including the 24 hour drying process for the cement. Making the coil itself can be laborious, can require several attempts to create a working heater, and often leads to reproducibility issues with the pyrolyzer temperature [9] [14].

Figure 2.4 Heating coil made of square 0.4 x 0.4 mm nickel chromium wire in ceramic heater [9].

Developing a new method for manufacturing the MFC's pyrolyzer that reduces the time and labor required to construct each heater would be a significant improvement to the apparatus. Additionally, a new type of heater could provide more consistent heating across the surface of the heater, whereas the current coil method can create uneven heating depending on the tightness of the coils. A more consistent heating profile across the surface of the pyrolyzer plate would alleviate concerns over exact crucible placement during testing. Furthermore, other construction methods may be more reproducible compared to the hand coiled wire method leading to more consistent

test results in terms of temperature profile between tests using different heaters. Five techniques for heater manufacturing were explored:

- Hand coiling square NiCr wire
- Hand coiling Kanthal ribbon wire
- 3D printing Inconel
- Copper printing and wire bonding
- Carbon paper

The hand coiled NiCr method is a scaled-up version of the method used in the smaller MFC design and is the simplest method to implement in the new version of the apparatus. The Kanthal ribbon wire has a rectangular cross section and can be coiled tightly with mica tape, to act as insulation to prevent electrical shorting, to create a heater. Printing the coils out of Inconel would reduce the labor required to make heaters and would allow for tighter coils, leading to more consistent heating and increased repeatability across tests and heaters. Copper printing and wire bonding is a heater manufacturing technology that is commonly used in nano-technology applications that could be expanded to a larger scale for use with the MFC. Carbon paper is a conductive paper that has been used to create heaters in other research applications and could be used as the MFC pyrolyzer.

All methods were evaluated based primarily on ease of manufacturing. New pyrolyzer construction methods that require significant by-hand labor were less desirable than more automated methods. The durability of each method of heater construction across multiple heating and cooling cycles was also considered, as the re-useability of a heater is important to the function of the MFC. Additionally, the methods were evaluated based on their ability to provide a consistent heating profile across the surface of the pyrolyzer plate. The five possible heater construction

techniques were also evaluated based on their ability to integrate into the current set-up of the MFC apparatus. The heater must fit within the ceramic plate of the pyrolyzer and the pyrolyzer and all electrical connections must fit inside the quartz tube providing the N_2 flow. The cost of each method was also an important factor in evaluating new methods of heater construction.

2.2.1 Nickel Chromium Coil

The simplest method to increase the size of the pyrolyzer was to continue the current hand coiling method at a larger scale to fit the new 19 mm ceramic pyrolyzer plate. This required no investment in new manufacturing techniques and was the fastest way to produce a larger coil for the modified version of the MFC. Additionally, it required no changes to the setup of the pyrolyzer plate and quartz tube, as those parts of the apparatus were already designed to incorporate the electrical connections used in this method of heater construction.

A 20 cm wire length was required to create a coil that fit within the new 19 mm pyrolyzer plate. The 20 cm length also included leads used to connect the pyrolyzer to the power supply. Because these larger coils required double the length of wire as the previous coil size, a slightly larger 0.5 mm x 0.5 mm square NiCr wire was used, rather than the previous 0.4 mm x 0.4 mm wire, in order to keep the resistance of the coils similar between the two coil sizes. The new, larger coils had a resistance of 0.9 Ω, just 0.2 Ω greater than the resistance of the smaller coils for the previous version of the MFC. The similarity in their resistances is advantageous, as the same power supply for the pyrolyzer can be used with the larger NiCr coils. Only adjustment of the voltage to optimize the heating profile would be required to begin using these coils.

At the larger size it was easier to hand coil the wire and to prevent it from touching itself and creating electrical shorts. Furthermore, a plastic version of the 19 mm pyrolyzer plate was 3D printed through the University of Maryland STEM Library with the same dimensions as the

ceramic pyrolyzer plate. This allowed the coil size to be tested using the plastic version, rather than the delicate ceramic piece. Furthermore, during construction, the coil could be placed in the plastic plate and adjusted using tweezers to create space between turns, allowing for the easy prevention of electrical shorts from wires touching. Similar to the method used in manufacturing the previous, smaller pyrolyzer, the coil and thermocouple rod in the updated iteration were held in place with Autocrete cement and the ends of the coil were fitted with female D-sub socket crimps. The coil and completed version of the heater assembly are shown in Figure 2.5.

Figure 2.5 Left: Heating coil made of square 0.5 x 0.5 mm nickel chromium wire in ceramic heater. Right: Heater apparatus for updated MFC with attached thermocouple and wire leads.

2.2.2 Kanthal Ribbon Wire

Ribbon wire is an easy to coil, flat wire that was investigated as a possible method to simplify heater construction. By coiling the wire tightly together with insulating tape between coil turns, it would be possible to create a denser and more consistent heating profile than coiling square wire with only an air insulator.

Kanthal A1 ribbon wire was purchased from WireOptim in two sizes: 0.8 mm wide x 0.1 mm thick and 3.17 mm wide x 0.32 mm thick. The 0.8 mm x 0.1 mm wire had a resistance of 5.76 Ω/ft while the 3.17 mm x 0.32 mm wire had a much lower resistance of 0.6 Ω/ft. Kanthal A1 wire was

selected as its thermal properties make it a popular material for use in heating applications. The purchased wire is rated for operation at temperatures up to 1400 °C. A 300 m roll of 4.76 mm wide mica tape was purchased from Axim Mica. This tape was selected to act as an electrical insulator. It has a dielectric strength greater than 20 kV/mm and is rated for operation at temperatures up to 800 °C.

Coiling the ribbon wire tightly with mica tape as the insulator, instead of air, allows for the creation of a much denser coil, which, in turn, should allow for more consistent heating across the surface of the ceramic heater. This would improve the consistency and repeatability of the heating profiles across the surface of the pyrolyzer. Additionally, using the mica tape between each coil of the wire prevents the wire from touching, even when it expands during heating. This addresses an issue with the current NiCr square wire manufacturing technique in which the wires expand when subjected to repeated heating and cooling cycles and may develop electrical shorts over time. Additionally, coiling the wire with mica tape instead of air as the insulator is intended to reduce the time required to manually produce coils as less precision will be required to ensure there is no electrical shorting.

The 0.8 mm x 0.1 mm Kanthal A1 wire was coiled manually using a quilling tool. The 0.8 mm x 0.1 mm wire was extremely easy to coil using this technique and the coils were manufactured much more quickly than the coils made out of the square NiCr wire. The hand-coiled NiCr coils take approximately 30 to 45 minutes to make and adjust to eliminate electrical shorting and maximize their heating density. The Kanthal A1 ribbon wire coils made with the 0.8 mm x 0.1 mm wire took approximately 5 minutes to construct. A coil made using this technique with the 0.8 mm x 0.1 mm wire is shown in Figure 2.6. The coil pictured fit into the 19 mm OD 17 mm ID pyrolyzer

ceramic heating plate. Making this coil required 175 cm of Kanthal A1 0.8 mm x 0.1 mm wire and resulted in a resistance of 32.1 Ω for the coil.

Figure 2.6 Kanthal A1 0.8 mm x 0.1 mm wire coiled using quilling tool.

While easy to coil, the 0.8 mm x 0.1 mm Kanthal A1 wire coils did not maintain their shape once coiled and needed to be held into place using high temperature tape before being transferred to the ceramic plate. Applying Autocrete cement or high temperature tape was required to permanently keep them in the coiled shape.

Another issue with the construction of coils using the 0.8 mm x 0.1 mm Kanthal A1 wire was the width of the ribbon wire was much less than the 4.76 mm width of the mica tape. It was challenging to keep the wire at a consistent height within the mica tape during coiling. It was easiest to coil the wire with the mica tape when the wire was centered on the width of the mica tape. However, because the mica tape is significantly wider than the ribbon wire, creating a coil with the wire centered in the tape could mean that the wire would not be in contact with the surface of the pyrolyzer plate when the coil is placed in the ceramic piece. This could result in difficulty

heating the pyrolyzer surface, and in turn the crucible, to the desired temperature as well as difficulty in achieving uniform heating profiles across the surface of the pyrolyzer plate.

Testing to determine the required voltage to heat this coil to 700 °C using the MFC pyrolyzer power source showed that the 32.1 Ω resistance was too high and that the wire could not be heated to the required 700 °C using the current power source. The current power source for the MFC is a Cotek AE-800-36 variable output power supply with a maximum power rating of 800 W and a maximum voltage output of 36 V. The LabVIEW setting of 1 V translates to 7.2 V on the supply output. The previous MFC coils were able to supply enough power to sufficiently heat samples during the pyrolysis ramp to the desired temperature of 695 °C. The power supplied to the heater in the previous version of the MFC can be calculated using the following equation:

$$P = \frac{V^2}{R} \qquad (2.1)$$

Assuming a resistance of 1 Ω for the coils in the previous version of the MFC and a supply output of 7.2 V, corresponding to a LabVIEW setting of 1 V, the power supplied was calculated as 51.8 W. Assuming that 51.8 W is the required power needed to heat samples during the pyrolysis ramp, using the maximum voltage that can be supplied by the power source of 36 V, the maximum possible resistance of a pyrolyzer coil for use with the current MFC power source is calculated using equation 2.1 to be 25 Ω. With a greater resistance than 25 Ω, the current power supply, even at its maximum voltage, would deliver less power than delivered in the previous version of the MFC. Shorter wire lengths and looser coils would be required to lower the resistance of a coil made using the 0.8 mm x 0.1 mm Kanthal A1 wire to be able to use the current power supply for the MFC pyrolyzer. This would, however, eliminate the benefits of the tight coil in terms of heating density and consistency.

Coils made using the 3.17 mm x 0.32 mm Kanthal A1 wire were difficult to shape due to the thickness and stiffness of the wire. For this size wire, it was necessary to hold the quilling tool with a drill, or otherwise clamp it to maintain stability, while coiling the wire with the tape. Creating tight coils using the 3.17 mm x 0.32 mm Kanthal A1 wire and mica tape allowed for more loops of wire to fit within the ceramic heating plate than can fit when coils are created by hand using the NiCr square wire. Heating profiles across the surface of the pyrolyzer would be more even with this method compared to the NiCr wire method. The 3.17 mm x 0.32 mm Kanthal A1 wire had a much lower resistance so coils that fit within the 19 mm OD 17 mm ID ceramic heating plate were able to be heated to the desired 700 °C using the current power supply for the MFC. Additionally, the greater width of the 3.17 mm x 0.32 mm wire allowed for it to be more evenly and neatly coiled within the width of the mica tape compared to the 0.8 mm x 0.1 mm wire. Keeping a coil of 3.17 mm x 0.32 mm wire in contact with the surface of the pyrolyzer plate would be simpler than with the 0.8 mm x 0.1 mm wire, reducing the likelihood of inconsistent heating across the surface of the pyrolyzer and between different heaters. A coil made with the large 3.17 mm x 0.32 mm Kanthal A1 wire is shown in Figure 2.7.

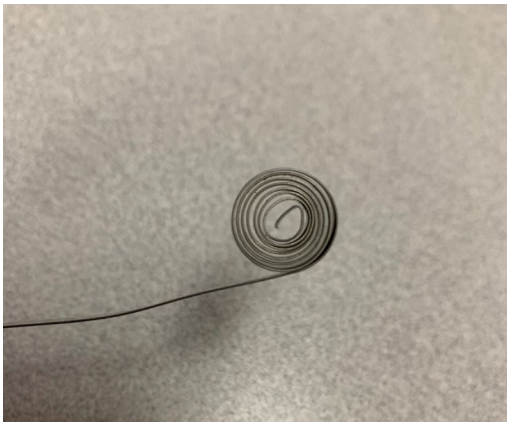

Figure 2.7 Coil made with Kanthal A1 3.17 mm x 0.32 mm wire using quilling tool.

However, the difficulty coiling the 3.17 mm x 0.32 mm Kanthal A1 wire with the mica tape made producing coils as laborious as it is to produce NiCr wire coils by hand. Another problem with the 3.17 mm x 0.32 mm wire was that it tended to expand outward once coiled, rather than holding its shape in the coil. During testing, a coil expanded and broke a ceramic heating plate. The heating plates are quite delicate and are custom printed, so a method of pyrolyzer manufacture that presents significant risk of damage to the ceramic heating plates is not desirable. Additionally, the size and stiffness of the 3.17 mm x 0.32 mm wire prevents it from being used directly as the leads to the heating coil as it was too difficult to bend out of the ceramic heating plate. Arc-welding copper wire leads to this size wire proved challenging and leads often disconnected, meaning that attaching leads was not a workable solution.

The method of coiling ribbon wires with mica tape offers some benefits compared to the current NiCr wire hand coiling method. The mica tape is a better electrical insulator than air and this method is more reliable to prevent electrical shorting. The mica tape also prevents the development of electrical problems after repeated heating and cooling of the wire. The ribbon wire method, particularly with the larger 3.17 mm x 0.32 mm wire, also could create a more even heating profile across the face of the heater as the wire can be coiled much more densely. This would allow for more even heating of the sample and reduce concerns with crucible placement affecting testing.

However, there are several drawbacks to the ribbon wire method. The 0.8 mm x 0.1 mm Kanthal A1 wire has too high of a resistance to be powered with the current power supply used for the pyrolyzer. Reducing the wire length used to create the coil would eliminate the benefit of a more even heating profile across the pyrolyzer surface. There are also construction concerns with both wire sizes. The 0.8 mm x 0.1 mm wire does not hold its shape once coiled and must be covered

with plaster immediately or held together with tape to prevent it from uncoiling. The 0.8 mm x 0.1 mm wire was also difficult to wind with the mica tape while keeping the wire at a consistent height within the width of the tape. The 3.17 mm x 0.32 mm wire holds its shape once coiled better than the smaller wire, but it too tends to expand once coiled, which damaged the ceramic heating plate. Additionally, coiling the larger wire with the mica tape was laborious and time-consuming due to the stiffness of the wire. Because of these construction concerns, this method of pyrolyzer heater construction was not pursued further for use with the MFC.

2.2.3 Inconel Printing

Inconel 625 is a nickel-chromium superalloy that can withstand high temperatures and is oxidation and corrosion resistant, making it particularly suitable for high temperature applications. It has a maximum operating temperature of 982 °C. Inconel does not deform or expand significantly when exposed to heat and also is resistant to corrosion and oxidation. Inconel 625 is commonly used in the sea-water and aerospace industries, and has increasing utility in the nuclear industry, where its high temperature applications make it suitable for use in reactor-core components [15]. Parts can easily be manufactured with Inconel using 3D printers designed for metal printing. On the University of Maryland campus, Terrapin Works uses the ProX DMP 200, a production grade 3D printer for fabricating metal and metal alloy components of sizes up to 140 mm x 140 mm x 100 mm using Inconel (Ni625). This machine can create parts with a tolerance of up to 50 microns, meaning that it is extremely well suited to create a 3D printed coil heater for the MFC.

Three different coil heaters were designed and drawn in SolidWorks 2022 and will be printed through Terrapin Works. Because the manufacturing of these parts is automated, three designs were created to test different heating densities and wire thicknesses. The resistance of each coil, R [Ω] was calculated with the following equation [16]:

$$R = \frac{\rho L}{wt} \tag{2.2}$$

where ρ is the resistivity of the wire [Ω-m], L is the length of the wire [m], t is the thickness of the wire [m], and w is the width of the wire [m]. Inconel has a resistivity of 1.29 μΩ-m [17]. The length, thickness, and width of each coil is presented, along with the calculated resistance, in Table 2.2. Reducing the thickness of the Inconel increased the resistance of the coil, as did reducing the space between coils to increase the overall coil length. Short leads, 1 cm in length, were added to the design of each coil and will also be printed of Inconel to connect the coil to wires from the power supply. The printed leads will slightly increase the resistance from the calculated resistance of the coil alone. All three coils have a resistance compatible with the power supply currently used with the MFC pyrolyzer. Images of the three heater designs are shown in Figure 2.8. The technique of Inconel printing could be applied to create heaters for the previous, smaller version of the MFC as well if the Inconel heaters work successfully at the larger size.

Table 2.2 Inconel Printed Heater Design Dimensions and Resistances

	Coil Design A	Coil Design B	Coil Design C
Length [mm]	180.47	180.47	237.55
Width [mm]	0.5	0.25	0.25
Thickness [mm]	0.25	0.25	0.25
Calculated Resistance [Ω]	1.86	3.72	4.90

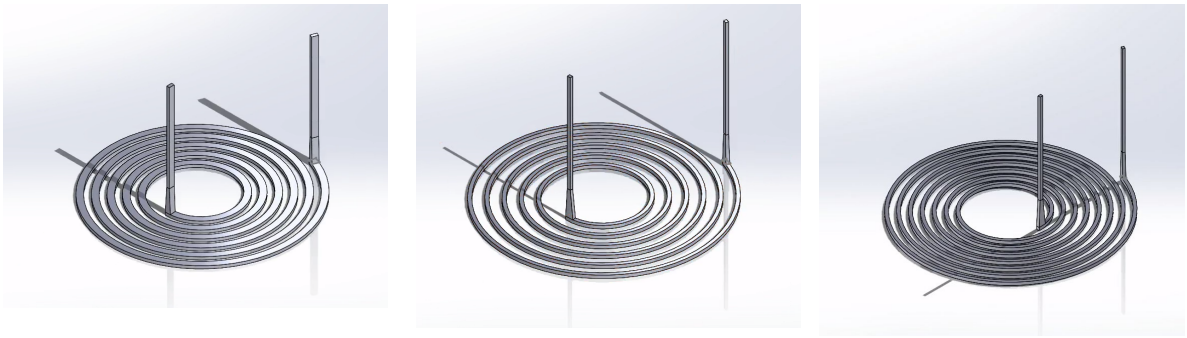

Figure 2.8 Left: Drawing of Inconel coil design A with resistance 1.86 Ω. Center: Drawing of Inconel coil design B with resistance 3.72 Ω. Right: Drawing of Inconel coil design C with resistance 4.90 Ω.

This technique significantly reduces the labor required to manufacture a single heater as the coils are printed rather than hand-coiled, a significant improvement from the current method. However, it is a more expensive method with three coils costing $186.25, meaning that re-useability and durability of the coils over multiple tests is essential for this to be a viable manufacturing method moving forward.

The Inconel printing manufacturing technique was attempted through Terrapin Works. Unfortunately, during initial manufacturing attempts there were difficulties removing the printed coils from the printer. Typically, the technicians at Terrapin Works remove Inconel pieces from the printer using a bandsaw, but this technique destroyed the coils when it was used to remove them from the printer. Because of the small diameter and thin width of the coils, they were determined to be too delicate to be removed with the bandsaw technique, so technicians reprinted them and attempted to remove them from the printer using a water-jet to preserve their shape. This technique also failed to remove the coils without causing damage. Though the Inconel printing technique shows promise, due to the desirable mechanical properties of Inconel 625 and the automatic manufacturing technique, limitations on the manufacturing process at the small scale will require the heater to be redesigned in shape or size.

2.2.4 Thin Film Deposition

Printed heaters are used on the nano-scale for a variety of applications and the technique may have applicability on the millimeter scale. Expanding this technique for use in the millimeter scale was explored through conversations with other researchers. Hongyi Sun, a Graduate Assistant in the Materials Science and Engineering department at the University of Maryland, provided valuable insight on this technique from his experience using it to create microheaters in an interview on May 2, 2024. For use as a pyrolyzer for the MFC, depositing copper at a thickness of 1 to 1.5 microns and a width of 1 mm onto an alumina substrate disk was discussed as a possible method to create a heater. As copper is highly conductive, this method would require maximizing the length of the deposited copper through a coiled shape to achieve the desired 1-10 ohm resistance. Initial calculations suggest with a well-designed wire pattern, which provides sufficient length of wire, the desired resistance could be achieved using copper, though chromium was also discussed as a secondary possibility for use in the heater.

Testing would be required to determine the adhesion of the copper to the alumina substrate. Typical microheaters use a silicon substrate that melts at temperatures greater than 1000 °C, so the ability of the copper to adhere to alumina is unknown. Transitioning from a ceramic base to a silicon base could be considered for use in the MFC if the microheater technique is pursued further. Overall, the heating element created using this method is promising for use in the MFC, although there is some concern that a heater as thin as 1 to 1.5 microns may not be able to heat the crucible sufficiently for pyrolyzing samples, particularly with samples with masses around 100 mg. Testing would also be required to determine the suitability of the heating elements and their durability after repeated heating and cooling cycles.

While the heating elements made for microheaters were promising, the electrical connections required to power and operate this type of heater would be challenging to integrate into the MFC apparatus. Typical microheaters use the wire bonding technique with gold wires to connect to an 18 mm square plate or probes are used to power the heaters. Traditional leads cannot be connected to microheaters created using this method. An 18 mm square plate would not fit in the quartz tube supplying the N_2 flow surrounding the heater, and it would be difficult to add this plate without interfering with the placement of the ceramic thermocouple probe into the heater. An alternate electrical option explored in conversation with other researchers was to use clips that directly connect the heater to a power supply. While this approach could likely successfully power the heater, the clips would have similar issues of integration into the quartz tube, pyrolyzer, and thermocouple apparatus. Future work to develop better options for electrical connection between scaled-up microheaters and the MFC power supply may be successful in finding a method to integrate this technology into the MFC.

Overall, expanding nano-scale heater printing techniques to the milligram scale for use in the MFC presents several challenges in terms of integration into the larger apparatus and electrical connection. Additionally, without significant further testing, it is difficult to know whether heaters at this thickness and with wire bonded electrical connections would be durable enough to sustain 700 °C temperatures over repeated heating cycles. Further exploration of this technology could prove to be a successful method for creating heaters for the MFC, but the significant challenges related to this method outweigh the ease of manufacturing.

2.2.5 Carbon Paper

Carbon paper is made of graphite and is highly thermally conductive. It is also electrically conductive, though less so than materials such as copper. Its flexibility and conductivity make it

popular for use in flexible electronic devices, as well as a commonly used substrate or interlayer in batteries. Carbon paper has been used as a heater for other research applications, suggesting it would likely have applicability as a heating element for use in the MFC.

Prior research by Dong, et al. using carbon heaters used strips 40 mm by 8 mm with the ends of the strips wrapped in copper foil to connect the paper to the copper wire used to supply power to the heater. An image of this type of heater used by Dong, et. al. is shown in Figure 2.9. To make these heaters, the carbon paper must be rinsed in ethanol and acetone, then dried overnight. Then, the carbon paper must be heated to a low temperature in an argon environment for two hours to remove remaining moisture. The carbon paper heaters were subject to high-voltage (16 to 72 V) electrical pulses of various durations (0.02 to 0.33 s) that allowed them to reach temperatures ranging from 1200 K to 2000 K [18].

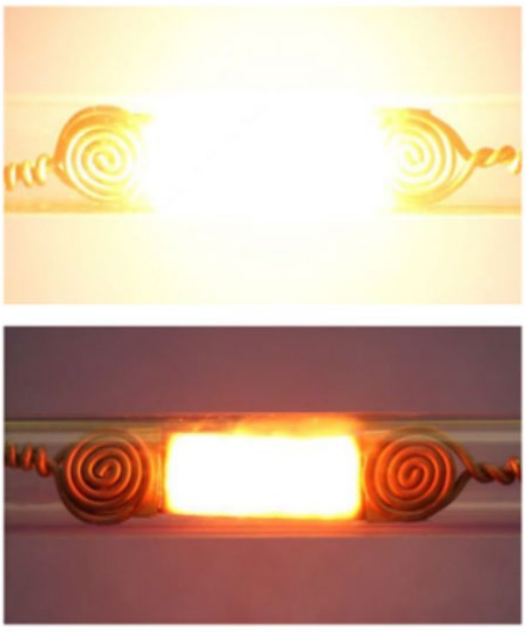

Figure 2.9 Heaters used by Dong, et. al. heated to temperatures of 2400 K and 800 K respectively [18].

A 22 cm x 30 cm sheet of Freudenberg H23 base carbon paper was purchased from Fuel Cell Store. It is 210 microns thick, making it highly flexible, and has a resistivity of 4.5 $\frac{m\Omega}{cm^2}$. This

product does not have a microporous layer and it does not have a hydrophobic treatment. For initial testing, the paper was handled with gloves and cut using scissors into a 24 mm x 4.5 mm strip. The resistance of this strip was measured to be 6 Ω. Alligator clips were used to directly connect the carbon paper to a power supply and apply increasing amounts of voltage to the sample. The voltage was increased slowly from 1 V to 6 V when the heater began to glow as seen in Figure 2.10. The voltage was further increased to 6.5 V, but the paper lost its mechanical integrity and ripped, concluding the test.

Figure 2.10 Strip carbon paper with a resistance of 6 Ω pictured during testing at 6 V as it began to glow.

A 22 mm diameter circle was also cut out of the carbon paper using scissors. A cut was made in the circle to allow it to be pulled into a spiral shape for testing. Its resistance was measured to be 17.5 Ω. Alligator clips were again connected to the test heating element and voltage was applied using the igniter power supply. The voltage was increased slowly during testing to carefully observe the effect of the increased voltage on the heater. Heat was palpable from the carbon paper spiral as the voltage was increased. Testing was stopped at a voltage of 13 V due to the presence

of a burning smell from the test heater. The heater is pictured in Figure 2.11 as its resistance was being measured. This size and shape of carbon paper heater is compatible with the current MFC power supply, which could supply sufficient voltage to provide the same amount of power as supplied to the wire coil heater in the previous version of the MFC.

Figure 2.11 Spiral carbon paper heater pictured while its resistance was measured using a voltmeter.

Carbon paper shows promise as a material that could be used to manufacture heating elements for the MFC. It is flexible and can be cut to a variety of shapes, meaning that integrating it into the apparatus would be simple and feasible. It is also a relatively low-cost material, with a 22 cm by 30 cm sheet costing $64.00 from Fuel Cell Store. A sheet of this size could be used to produce tens of heaters.

A spiral with the inner and outer parts of the coil wrapped in copper foil to connect with copper leads would mimic the current shape of the wire coil and could easily be integrated with the ceramic heater and thermocouple apparatus. Further research exploring methods of connecting the carbon paper heating element with the power supply would need to be conducted to determine the

best method for integration into the MFC apparatus. Methods of attaching the carbon paper to the ceramic pyrolyzer plate would also need to be explored further, though preliminary ideas include Autocrete cement and high-temperature glue. Attaching the carbon paper to the ceramic would address the delicacy of the paper and its tendency to rip at high temperatures by keeping the paper from moving when heated. Attaching the paper using cement would also prevent cleaned paper from being exposed to contaminants in the lab. However, the effect of cement or glue on the temperature of the heater and on its ability to heat the crucible would need to be explored through further testing.

Carbon paper heaters have been proven to reach temperatures much higher than the 700 °C required for the MFC heating ramp. However, these temperatures were achieved in past research using short electrical pulses and were not sustained for as long a duration as a standard MFC test, which has both a three minute and a four minute heating ramp. Carbon paper is also known to degrade and change in resistance with repeated heating, so further testing would be necessary to evaluate the durability of these heaters and their suitability for repeated use in the MFC. The current pyrolyzer can be used 30 to 40 times before it begins to degrade, so for carbon paper to be a suitable replacement it would need to have a similarly high number of uses before requiring replacement or have a significantly easier method of manufacture.

A final consideration that may be a drawback of carbon paper for use in the MFC is the heater preparation process. Typically, they are washed with both ethanol and acetone, dried overnight, and additionally pre-heated in an argon environment to remove moisture. This process improves the efficiency of the heaters by removing moisture and other contaminants on the heater but makes preparing the heaters time-consuming. If the heaters are found to be durable and produce consistent heating over repeated tests, a lengthy preparation process may be acceptable. However, concerns

over the durability and re-usability of carbon paper heaters make the preparation process a particular concern. Further testing of the durability of the heaters, as well as exploration of other preparation processes, is necessary to fully evaluate the suitability of carbon paper.

Carbon paper heaters show promise for use with the MFC. Cutting a carbon paper heater to the desired shape and attaching it to the ceramic heater would be much easier than hand coiling wire, making manufacturing this type of heating element simpler and quicker. This is a clear manufacturing advantage of carbon paper heaters compared to the current pyrolyzer. The flexibility of carbon paper means that integrating a carbon paper heater into the MFC apparatus would likely be simple, albeit requiring some optimization of heater shape and size. Significant further testing of carbon paper heaters would be required to determine their feasibility, particularly in terms of their durability, as the preparation required for use of this type of heater is extensive. With further testing, carbon papers may be determined to be a suitable method for manufacturing new pyrolyzers for the MFC, but due to the requirement of a new power supply and the significant heater preparation process, they were not implemented in the updated version of the MFC.

2.2.6 Selecting a Heater Manufacturing Technique

All possible pyrolyzer heater construction techniques offer unique advantages and disadvantages that needed to be considered carefully before settling on a method of heater construction. The ease of integration into the apparatus was a primary consideration for all techniques, as was the ease of manufacture. The durability of the heater and cost of each heater construction technique were also considered. Table 2.3 summarizes the positive and negative attributes of each heater manufacturing technique considered in this work and offers a recommendation on the use of each technique for future research.

Table 2.3 Evaluation of Heater Manufacturing Techniques

	Pros	Cons	Recommendation
Hand-coiled NiCr wire	• Simple, proven technique that can be easily adapted to the new increased size of the MFC • Known to be compatible with current MFC power supply • Directly comparable to the heaters used in the previous iterations of the MFC • Cost effective • Known from previous experience to last for 40 or more heating cycles	• Manual and time-consuming manufacturing process to create a coil without electrical shorts • Variability between the heating profiles produced by different coils • Sometimes develops electrical shorts after repeated heating and cooling	• Adopted for current work
Hand-coiled Kanthal ribbon wire	• Effectively prevents electrical shorts, including after repeated heating and cooling cycles • May create a denser and more even heating profile across the surface of the pyrolyzer plate • May create more repeatable heating profiles between different coils	0.8 mm x 0.1 mm Wire • Coils did not hold their shape once coiled • Resistance of coils was too high for use with current MFC power supply 3.17 mm x 0.32 mm Wire • Stiffness of the wire made it difficult to coil • Coils did not hold shape once coiled, and their expansion caused damage to the ceramic pyrolyzer plate	• Not recommended

	Pros	Cons	Recommendation
3D printed Inconel	• Automatic manufacturing technique • Printing allows for significant design flexibility • Printing allows for denser coils and more even heating profile than hand-coiled NiCr without requiring the use of an insulator • Suitable for high temperature applications and durable • Compatible with current MFC power supply	• Expensive • Construction challenges require redesign of coils to allow printing to be successful	• Recommended with additional research
Thin Film Deposition	• Design flexibility • Suitable for the small scale of the MFC	• Difficult to integrate into current MFC apparatus geometry • Difficult to connect to MFC power supply • Time-consuming to print using this technique • Heaters may be too thin to provide enough power to heat the samples in the MFC	• Not recommended

	Pros	Cons	Recommendation
Carbon paper	• Highly thermally conductive • Could create a more even heating profile across pyrolyzer surface than wire coils • Operates at temperatures well above the required 700 °C • Flexible and easy to cut to shape • Easy to integrate with current MFC pyrolyzer geometry • Cost effective	• Loses mechanical integrity at high temperatures • Resistance changes with repeated heating and cooling • Heater preparation requires a time-consuming, multi-step drying process • Durability of heaters with repeated heating cycles is unknown	• Recommended with additional research

After significant exploration of other methods, it was decided that hand coiling nickel chromium wires was ultimately the best method of heater construction for immediate implementation with the updated version of the MFC. This method required no significant testing or further development, making it easy to implement. Additionally, at the larger size, it was easier to construct coils, meaning that this method did not present as significant of a construction challenge as on the smaller scale. Thus, for simplicity, the hand coiled wire method was expanded for the updated version of the MFC.

3. Design Optimization

Altering the size of the crucible and pyrolyzer plate to allow for increased testing samples with greater mass required updates to the rest of the MFC apparatus. Changes made to the base, supports, and connections to the air and nitrogen supply are outlined in this chapter. Additionally, the increased size of the apparatus required adjustments to the air and nitrogen flow rates, as well as to the position of the pyrolyzer in the inner quartz tube, to ensure accurate, well-ventilated test results.

3.1 MFC Apparatus Updates

Altering the size of the crucible and the pyrolyzer resulted in updates being required throughout the rest of the MFC apparatus. The dimensional changes to the base, stand, and fittings of the MFC will be discussed in this section.

3.1.1 Fittings and Base of MFC

With the crucible and the pyrolyzer plate increasing in diameter, the diameter of the inner quartz tube also needed to increase to accommodate the larger pyrolyzer plate. To accommodate the larger quartz tube diameter, larger fittings were required in the base of the MFC apparatus. Larger diameter fittings have an increased length, so the length of the inner quartz tube was also increased to keep the top of the tube in the same position relative to the base as in the smaller version of the apparatus. A schematic of the smaller version of the apparatus can be viewed in Figure 1.4 in Chapter 1.1.4. The updated and original dimensions of the crucible, pyrolyzer plate, and quartz tube are given in Table 3.1.

Table 3.1 Dimensions in mm of crucible, pyrolyzer, and inner quartz tube in updated and previous versions of MFC

	Updated MFC	Previous MFC
Crucible Inner Diameter [mm]	13.9	8
Crucible Height [mm]	4.5	4.5
Pyrolyzer Plate Diameter [mm]	19	11.7
Quartz Tube Inner Diameter [mm]	22	13
Quartz Tube Outer Diameter [mm]	25	15.8
Quartz Tube Length [mm]	195	145

The increased OD of the inner quartz tube required adjustments to the brass base of the MFC, which is pictured in Figure 3.1. The base was remade to be used with the new 25 mm OD inner quartz tube, which was compatible with 1” fittings. The NPT fitting that connects the brass base of the MFC to the tubing that supplies the N_2 flow and houses the electrical connection for the pyrolyzer was increased from a ½” fitting in the previous version of the MFC to a 1” fitting in the updated version of the MFC. Otherwise, the base of the MFC was not changed dimensionally. The base of the MFC is screwed tightly to a flange that compresses an O-ring to securely hold the outer quartz tube in place without air leaks. A dimensioned drawing of the flange is shown in Figure 3.2.

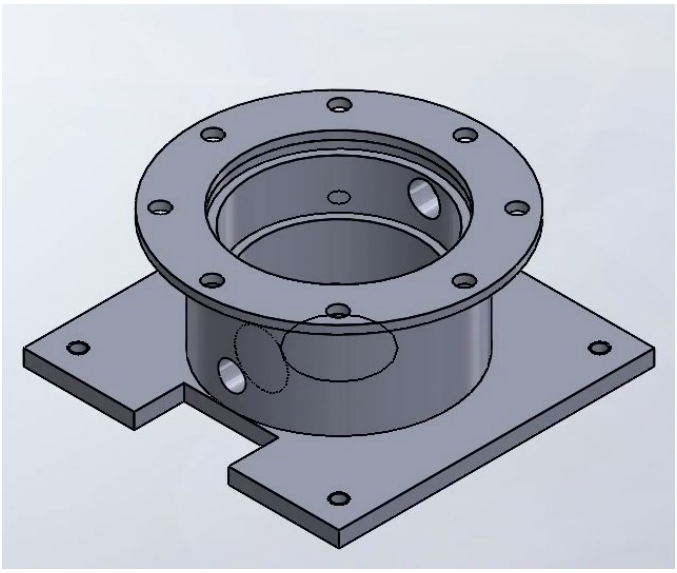

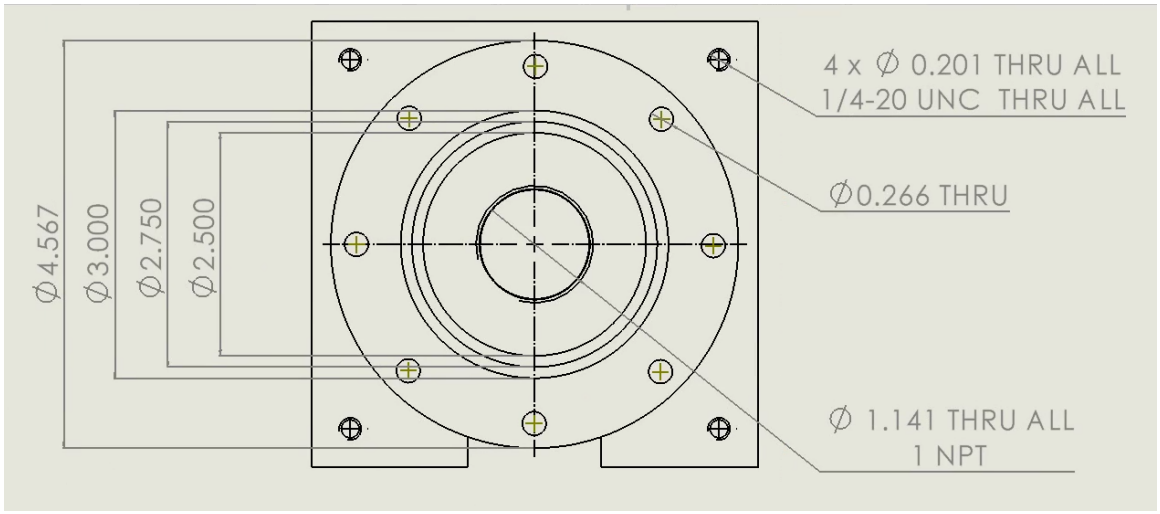

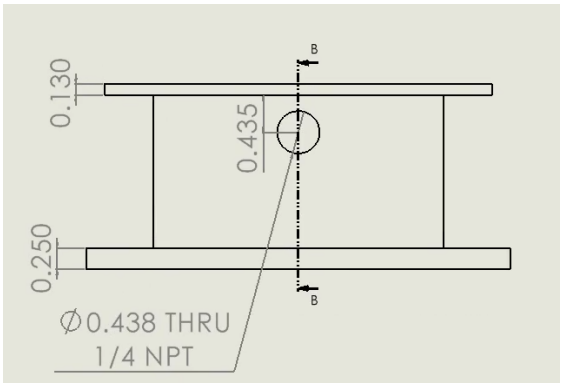

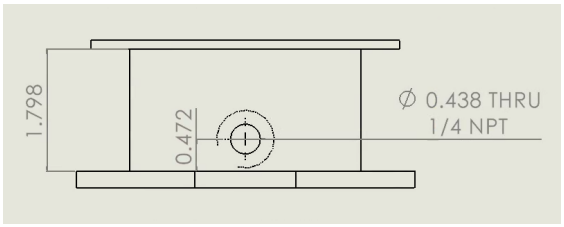

Figure 3.1 Dimensioned drawing of brass base of MFC. Dimensions in inches.

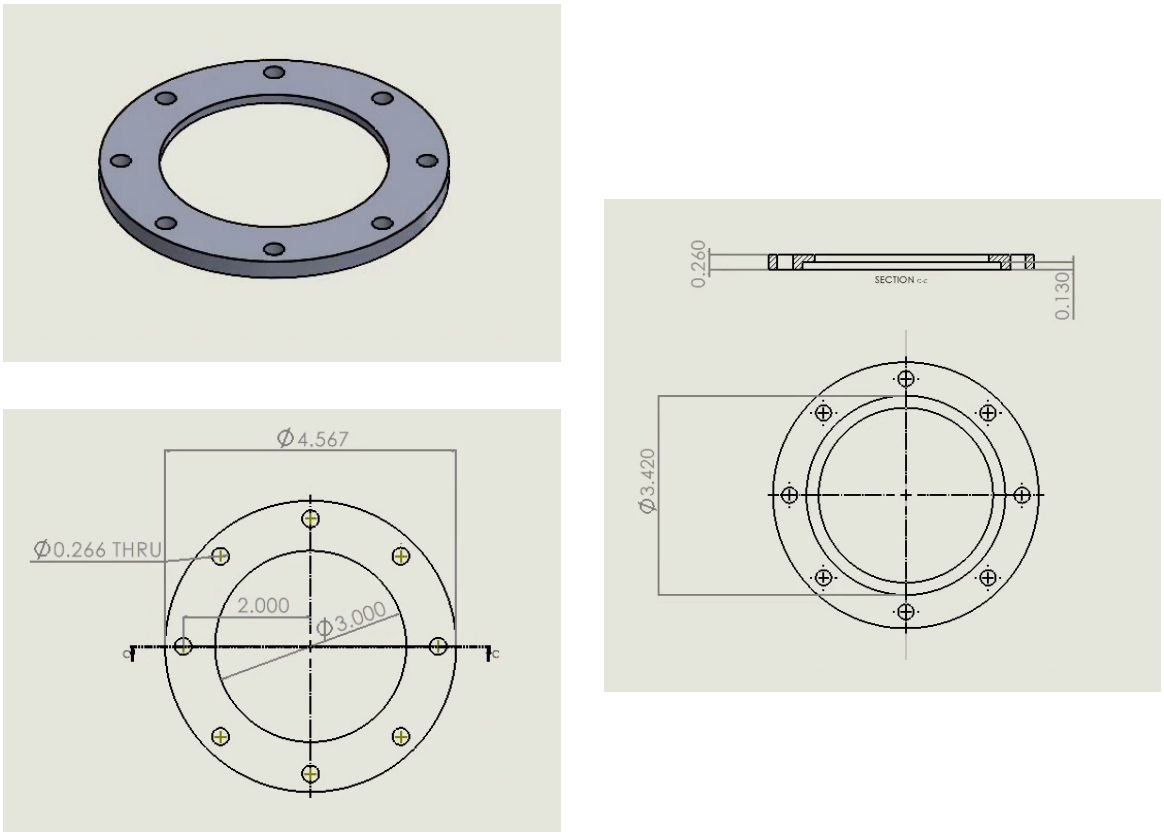

Figure 3.2 Dimensioned drawing of the brass flange that connects to the base of the MFC. Dimensions in inches.

Increasing the size of the fittings connected to the base of the MFC required adjustments to the fittings upstream. A schematic of the updated version of the MFC, showing the layout of the fittings is provided in Figure 3.3.

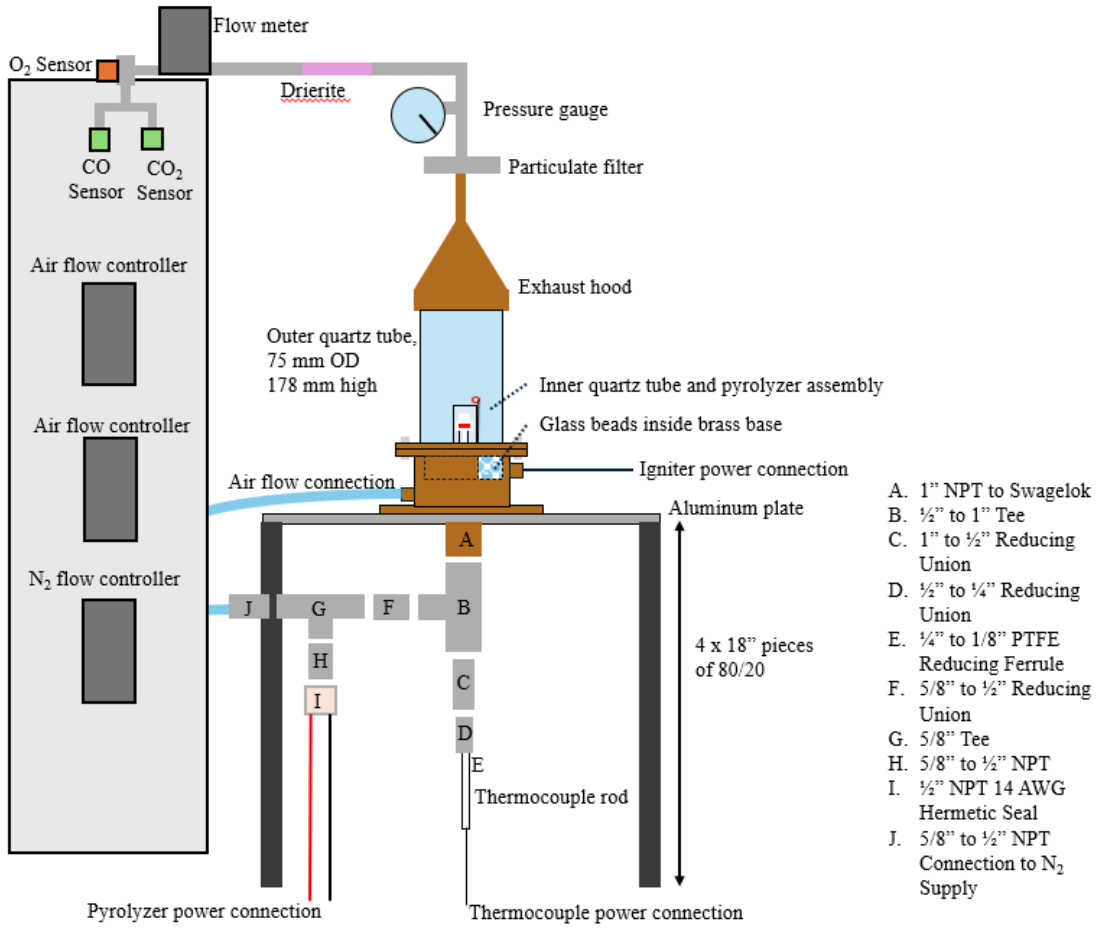

Figure 3.3 Dimensioned schematic of the version of the MFC used in this work, including the base, exhaust and gas analyzer system, fittings, and control system.

The thermocouple rod that is inserted into the pyrolyzer plate is held in its vertical position by a single fitting, as shown in Figure 3.3. Because the fitting at the base of the MFC is a 1" fitting in the updated version of the MFC used for this work, several reducing unions were required: from 1" to ½", from ½" to ¼", and a Swagelok PTFE reducing ferrule from ¼" to 1/8". This was one additional fitting compared to the number used in the previous version of the MFC, and required larger, and therefore longer, fittings. Thus, the length of the ceramic thermocouple rod was increased from 12" in the previous version of the MFC to 18" in the version of the MFC used in this work. This increased length provided enough length for the rod to extend through all required fittings, up into the inner quartz tube to the desired pyrolyzer plate position, as well as leaving

approximately 4” exposed below the fittings, which allowed for easy adjustment of the pyrolyzer plate position.

As shown in the schematic in Figure 3.3, the tee connection splits the fittings between the fittings used to hold the thermocouple rod and the fittings that connect to the N_2 inflow and that also house the electrical connection for the pyrolyzer. The fittings connecting to the N_2 inflow were re-used from the previous version of the MFC, though an additional reducing union was required to connect these 5/8” fittings with the ½” tee. On this side of the tee there is also the fitting connecting the pyrolyzer to the MFC power supply. To prevent leaks of N_2 at this connection, a hermetically sealed ½” 14 AWG fitting is used. The hermetically sealed fitting could not be reused from the previous version of the MFC as the changes in fitting size, and the addition of the reducing union, required longer wires to reach from the fitting to the location of the pyrolyzer plate. A new hermetically sealed fitting was purchased from RH Seals and the wires were measured and cut to the desired length for compatibility with the version of the MFC used in this work.

As seen in the schematic in Figure 3.3, the base of the MFC is attached to the top of a large aluminum plate that connects to 80/20 to create the stand for the MFC. This stand creates the space for the fittings and for adjustments to be made to the apparatus if necessary. Because of the increased number and length of fittings, the 80/20 used to create the stand was cut to an increased length of 18” to ensure that there was sufficient room below the apparatus for all fittings and supports.

The fittings for the MFC were previously all physically supported by the quartz tube. With the larger fittings and increased number of fittings, there were concerns the quartz tube would not be able to support the weight of the fittings without breaking. A support was developed to reduce the weight of the fittings on the quartz tube. It was 3D printed through Terrapin Works out of PETG,

a plastic recommended by Terrapin Works for structural elements. A dimensioned drawing of the part is shown in Figure 3.4.

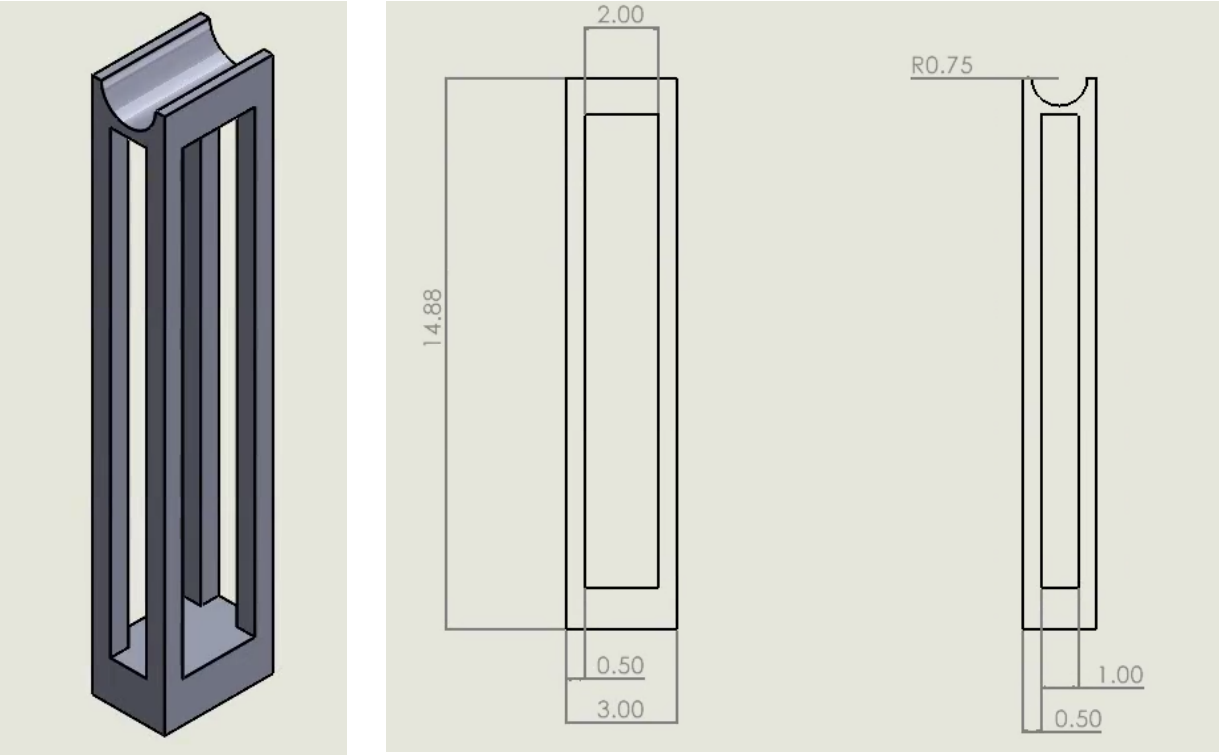

Figure 3.4 Dimensioned drawing of PETG support developed to support weight of MFC fittings. Dimensions in inches.

3.1.2 Igniter Coil

Because the diameter of the inner quartz tube was increased for the version of the MFC used in this work, the length of the igniter coil was also required to be increased. The igniter coil sits approximately 2 mm above the opening of the quartz tube. It sits off center from the quartz tube but extends across the opening of the tube to ignite the volatile gases exiting the inner quartz tube during testing. The length was increased to extend across the opening of the new 25 mm OD quartz tube. The igniter coil is made by hand, by coiling round NiCr wire into the threads of a screw. This allows for consistent manufacturing when the igniter coil requires replacement. For the updated version of the MFC, the wire was coiled around the screw 20 times, compared to 13 for the

previous version of the MFC. The igniter coil is pictured, along with the pyrolyzer plate and inner quartz tube, in Figure 3.5.

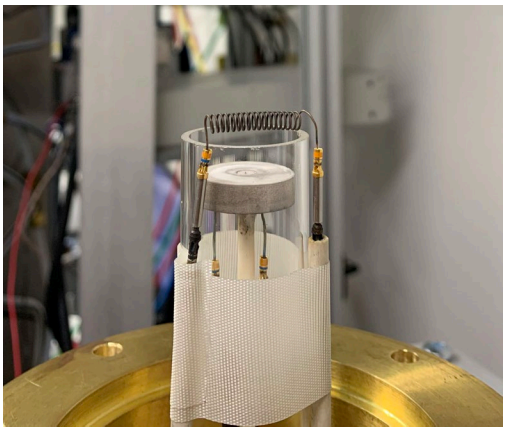

Figure 3.5 Igniter coil, shown positioned above inner quartz tube and pyrolyzer plate, in preparation for testing.

The igniter coil in the previous version of the MFC supplied 50 W of power when used during testing. This amount of power was sufficient for use of the coil as an ignition source and was the desired power output for the updated, longer version of the igniter coil used in this work. The igniter coil is powered by a separate power source from that used by the rest of the MFC. This power source is adjusted manually during tests if needed to maintain a constant level of power throughout testing. To determine the approximate voltage required to provide 50 W of power during testing, the power supply to the igniter coil was turned on and adjusted until the coil was supplying 50 W. For an igniter coil utilized with the version of the MFC used in this work, an approximate voltage of 10.80 V is sufficient to supply enough power to the igniter coil, though some adjustments may be required during testing to maintain a constant 50 V. Additionally, as the igniter coil oxidizes over time, a higher voltage may be required to achieve the same power.

3.2 Pyrolyzer Voltage Optimization

Creating the new, larger pyrolyzer coils used a greater length of wire than used for the previous version of the MFC. However, the coils for the MFC used in this work were made with square 0.5

x 0.5 mm NiCr wire, compared to the smaller 0.4 x 0.4 mm square NiCr wire used to create the heating coils in the previous version of the MFC. The longer wire length, but greater wire cross-sectional area meant that the resistance of the new MFC pyrolyzer coils, 0.9 Ω, was similar to that of the pyrolyzer coils used in the previous version of the MFC, 0.7 Ω. However, this change in resistance still necessitated an increase in the voltage output from the MFC power source for the heater to supply enough power to heat a sample during testing.

During an MFC test, the pyrolyzer is first heated from room temperature to a temperature of 47 °C during a 3-minute pre-heating ramp. This ensures that all samples begin the pyrolysis heating ramp at the same initial temperature, regardless of lab conditions on any given day. After pre-heating, the voltage output is increased for the pyrolysis ramp which over 4 minutes heats the pyrolyzer from 47 °C to its peak temperature of 695 °C. Next, the power to the pyrolyzer is turned off and the pyrolyzer is allowed to cool. Data collection continues for 2 minutes during the cooling period, leading to a total MFC test time of 9 minutes between the pre-heating ramp, pyrolysis ramp, and cooling period.

The goal for the new, larger MFC pyrolyzer was to replicate the heating ramp used in the previous version of the MFC by achieving the same temperatures at the end of the pre-heating and pyrolysis ramps. To find the correct voltage to achieve the desired temperatures, a series of open air, empty crucible tests was performed at various voltages. During these tests, N_2 was flowed through the inner quartz tube at 200 sccm to cool the pyrolyzer and prevent oxidation. Initially, the voltage settings in LabVIEW were set to the approximate voltage settings used for the previous version of the MFC: 0.557 V for the pre-heating ramp and 0.985 V for the pyrolysis ramp. Testing these voltages with the new pyrolyzer coil showed that the temperature did not reach 47 °C during the pre-heating ramp and only reached a maximum of 375 °C during the pyrolysis ramp. From

there, the voltage settings were increased and decreased to optimize the temperature until the tests achieved the desired peak temperatures at the end of the pre-heating and pyrolysis ramps reached the desired 47 °C and 695 °C. The process was conducted on two different pyrolyzers coils and the LabVIEW voltage settings initially used for each pyrolyzer are reported in Table 3.2. For pyrolyzer one, there were eleven repeated tests, while for pyrolyzer two there were five repeated tests at the final voltage settings. As the pyrolyzer ages, it becomes necessary to increase the voltage settings slightly to combat the effects of fatigue, which develop from repeated heating and cooling cycles, and lead to inconsistent heating and lower peak temperatures.

Table 3.2 Voltage Settings for Pyrolyzer Heating Ramps

	Pre-heating Ramp LabVIEW Voltage [V]	Power Source Voltage Output [V]	Pre-heating Ramp Final Temperature [°C]	Pyrolysis Ramp LabVIEW Voltage [V]	Power Source Voltage Output [V]	Pyrolysis Ramp Final Temperature [°C]
Pyrolyzer 1	0.605	4.356	48.6 ± 1.7	1.200	8.640	696.5 ± 3.0
Pyrolyzer 2	0.595	4.284	47.0 ± 0.7	1.183	8.518	695.6 ± 4.3

Once the initial voltage setting was selected for the first pyrolyzer, ten additional empty crucible, open-air tests were performed to examine the repeatability of the temperature profiles produced during heating. The average temperature across the eleven repeated tests with pyrolyzer one and the five repeated tests with pyrolyzer two are plotted over time with error bars representing two standard error is shown in Figure 3.6. The standard error is calculated for this plot, and for all other values in this work, using the following formula:

$$Standard\ Error = \frac{\sigma}{\sqrt{n}} \qquad (3.1)$$

Where σ is the population standard deviation and n is the sample size. Variation between the tests is partially due to the tests being conducted over two days. Based on experience with the previous

version of the MFC, the first test run of the day is generally colder than subsequent tests. Additionally, the crucible position was adjusted slightly between tests to replicate testing conditions in which the crucible would be removed and replaced during testing for sample measurement and cleaning. Though all efforts are made to center the crucible on the pyrolyzer plate, it is difficult to perfectly center so slightly altering its position during the voltage tests more accurately reflected the conditions of real MFC tests. There is some variation also between the two different pyrolyzers, as seen in Figure 3.6. This variation is due to minor differences in the density of the coil in the pyrolyzer plate, as well as the slight differences in the resistance of the two coils and the voltages used to produce the final temperatures for each heating ramp.

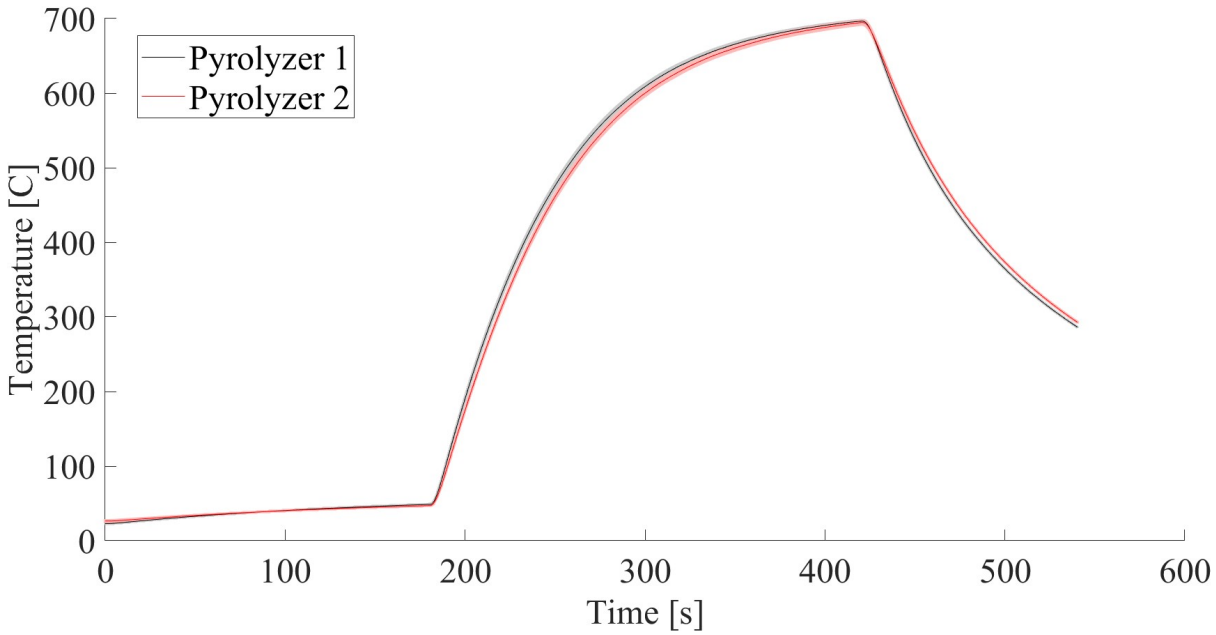

Figure 3.6 Average temperature profile of eleven empty crucible tests using pyrolyzer one and of five tests with pyrolyzer two plotted over time with error bars showing two standard errors.

Beyond achieving the same peak temperatures at the end of the pre-heating and pyrolysis ramps, it is important to match the heating rate of the previous version of the MFC. The heating rate of the previous version of the MFC mirrors the heating rate used during cone calorimeter tests, making MFC test results very comparable to cone calorimeter test results. The temperature profiles

over time for the two new pyrolyzers and for the previous version of the MFC are shown in Figure 3.7. The heating rates over time of the two new, larger MFC pyrolyzers are plotted along with the heating rate of the previous MFC pyrolyzer in Figure 3.8.

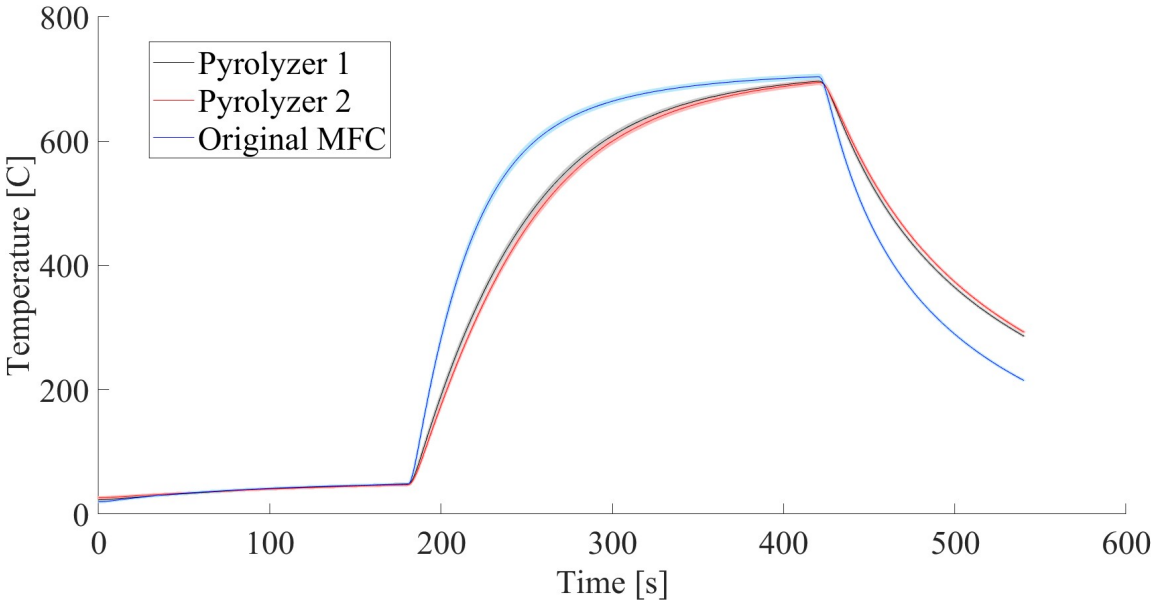

Figure 3.8 Average temperature plotted over time for the eleven empty crucible tests with pyrolyzer one, the five empty crucible tests with pyrolyzer two, and tests conducted with the previous version of the MFC.

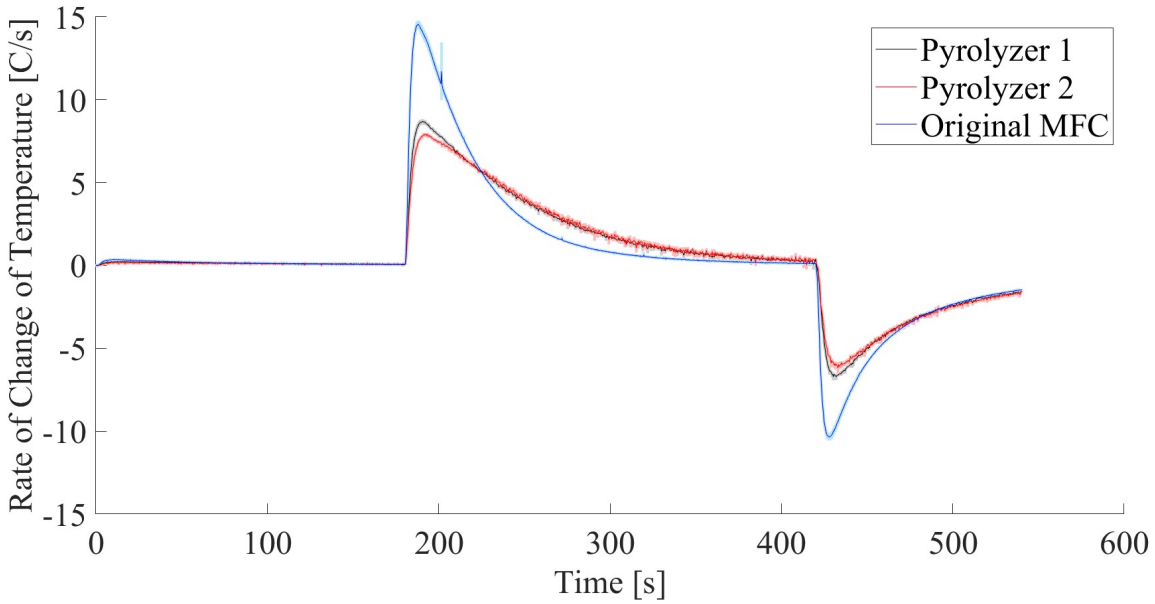

Figure 3.7 Average rate of change of temperature plotted over time for the eleven empty crucible tests with pyrolyzer one, the five empty crucible tests with pyrolyzer two, and tests conducted with the previous version of the MFC.

3.3 Consistency of Temperature Profile

One of the goals of changing the manufacturing technique used to create the pyrolyzer coil for use in the current version of the MFC was to increase the consistency of the heating profile across the surface of the pyrolyzer plate. While the hand-coiled NiCr wire manufacturing technique was selected for use in this work, rather than the Inconel printing or carbon paper techniques which showed promise for improving heating consistency, it was still of interest to examine the heating profile produced by the coil. An IR camera was used to examine the temperature of the surface of the pyrolyzer plate during the preheating ramp, pyrolysis ramp, and cooling period of a test run.

The camera was positioned above and to the right side of the MFC, viewing the surface of the pyrolyzer plate at an angle. For accurate temperature measurement, the FLIR camera relies on knowledge of the emissivity of the target surface which, for the case of the pyrolyzer plate, is unknown. The plate experiences color changes from its original white to various shades of gray after repeated testing, so the emissivity is difficult to estimate given the color variation across the surface which may or may not affect its emissivity in the spectral region of interest. For a qualitative examination of the temperature variation across the surface of the plate, the emissivity was assumed to be 1. The FLIR is limited to reading temperatures from 0 °C to 650 °C, so for the time during the pyrolysis ramp when the plate temperature exceeds 650 °C, the temperature readings from the camera will be saturated and artificially read 650 °C even though the actual temperature is higher. A selection of images showing the temperature distribution at various times during the test run is shown in Figure 3.9.

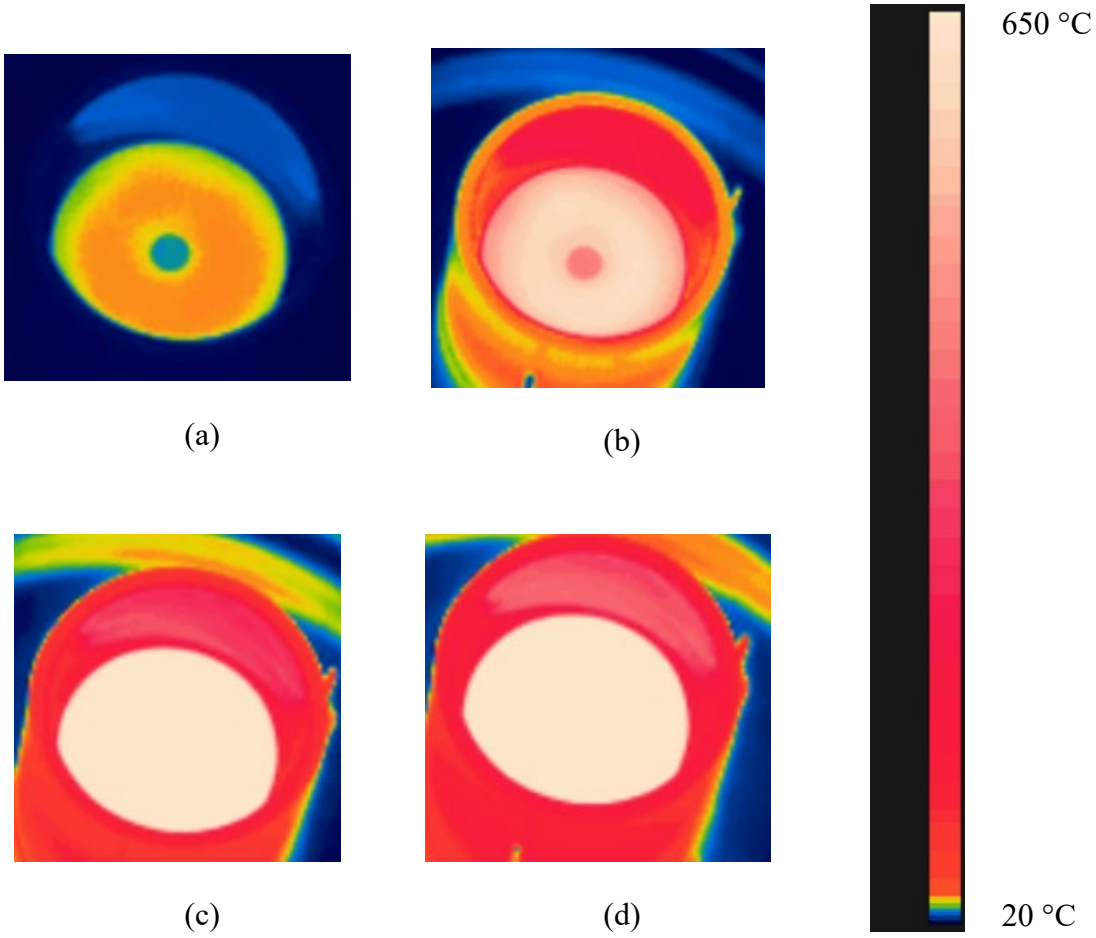

Figure 3.9 Selection of images showing the variation of temperature across the surface of the pyrolyzer plate at (a) 180 s, (b) 240 s, (c) 300 s, and (d) 360 s into the duration of the MFC test. The scale shows the temperature represented by the colors in the images, ranging from 20 °C represented with dark blue to 650 °C represented with white.

For a more detailed examination of the variation of temperature across the surface of the plate, nine points were selected on the surface of the plate and the temperature data from each point was examined. The FLIR captures data at a rate of 30 fps, providing a highly detailed look at the temperature variation in time. The points selected are shown in Figure 3.10. Because the emissivity is assumed, rather than specified, the numeric value of the temperature reported at each point is

estimated. The data reflects the variation between different locations on the pyrolyzer over time. The raw data reported by each point is plotted in Figure 3.11.

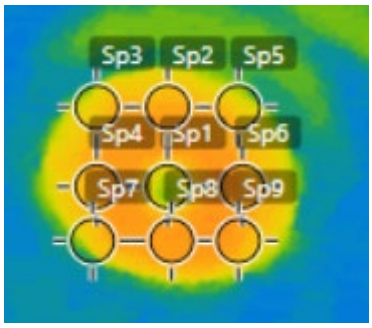

Figure 3.11 Nine points selected to provide a representative understanding of the temperature variation across the surface of the pyrolyzer plate.

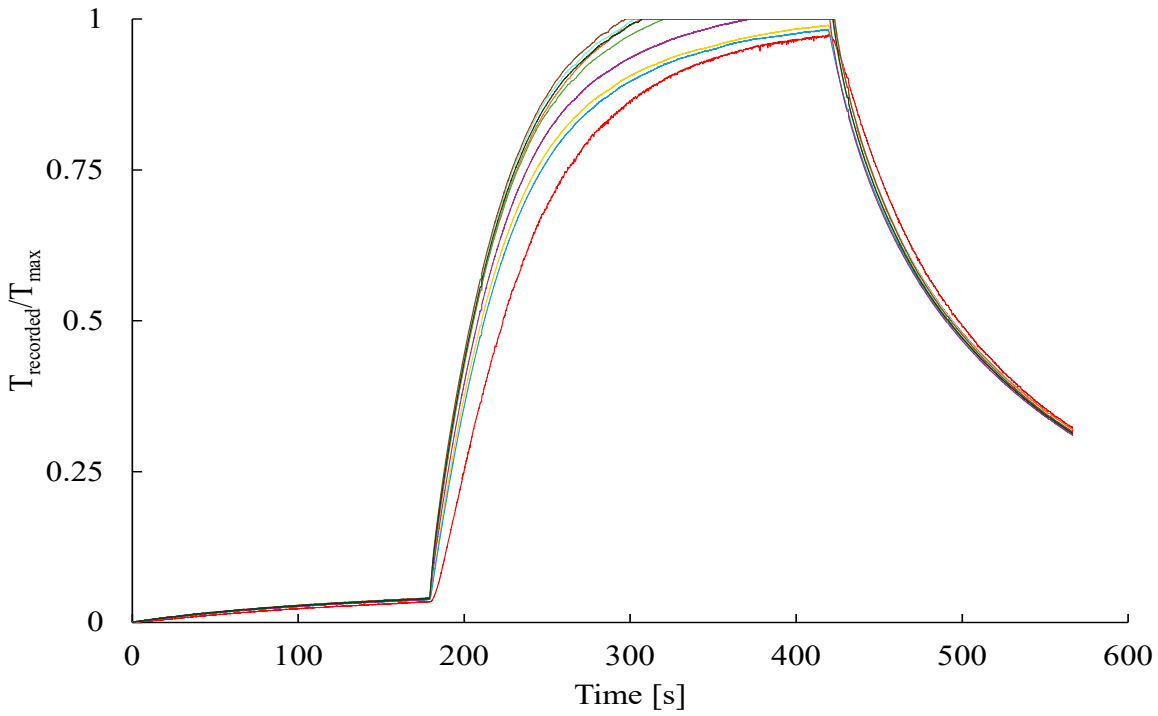

Figure 3.10 Qualitative temperature data from each of the nine representative points on the surface of the pyrolyzer normalized by the maximum recorded temperature. Times at the end of the pyrolysis ramp exceeded the maximum temperature that can be read by the camera of 650 °C and are reported as the maximum temperature.

The plot of the raw temperature data shows a significant spread between the temperature of some of the points. The center point of the pyrolyzer plate, which is represented by the red line in

Figure 3.11, is expected to be colder than the other points on the surface of the pyrolyzer plate. The temperature difference between this point and others is because the wire coil does not directly heat that area of the plate as the thermocouple rod is inserted into the center of the pyrolyzer plate. The other eight points suggest similar temperatures, though the consistency worsens as the pyrolyzer plate increases in temperature. Additionally, the peak temperatures of the plate exceed the camera's maximum of 650 °C, meaning the camera reported its maximum temperature, making it impossible to examine the consistency across the surface of the plate at its peak temperature. The FLIR test revealed inconsistency in the temperature of the pyrolyzer plate across its surface that may impact sample heating and cause inconsistency in test results. As discussed in Chapter 2.2, alternate pyrolyzer construction methods may be implemented in future work to reduce inconsistency in the heating profile across the surface of the pyrolyzer plate.

3.4 Pyrolyzer Position

The pyrolyzer plate sits inside the inner quartz tube of the MFC which provides an N_2 flow to carry volatile gases out of the tube and into the air environment of the outer quartz tube where the volatiles are ignited by the igniter coil. The desired flame location for MFC tests is at the opening of the inner quartz tube, not at the top of crucible in which samples are placed. The igniter coil is located above the opening of the quartz tube to serve as an ignition source. In the previous version of the MFC, to achieve the desired flame location the top of the pyrolyzer plate was located 7 mm below the opening of the inner quartz tube. With the pyrolyzer plate in this location, the top of the crucible was located 2.5 mm below the opening of the quartz tube. This distance separated the pyrolysis process from the ignition process and meant that the volatile gases were carried up by the N_2 to the desired location before ignition. The 7 mm distance between the pyrolyzer plate and

the opening of the tube was typically sufficient to prevent air from the outer quartz tube from entering the inner quartz tube and creating conditions for flaming inside the inner quartz tube.

In the updated version of the MFC used for this work it was important to maintain the flame position at the top of the inner quartz tube. There was initial concern that the increased diameter of the inner quartz tube would allow air from the outer quartz tube to entrain into the inner quartz tube allowing flaming ignition inside the inner quartz tube. To prevent this, the location of the pyrolyzer plate was evaluated and altered to prevent the entrainment of air into the inner quartz tube. The pyrolyzer plate was initially placed 7 mm below the opening of the inner quartz tube and a series of open to atmosphere tests were conducted on polymethyl methacrylate (PMMA) powder, a well understood polymer, and polyethylene (PE) beads, a polymer that condenses heavily during pyrolysis. The crucible used in this work is the same height as the crucible used in the previous version of the MFC, so the top of the crucible was located 2.5 mm from the opening of the inner quartz tube. The open-air tests were conducted with the inner quartz tube in place and with N_2 flowing, but without the outer quartz tube in place and without a dry air co-flow. If air entrainment can be prevented in an open atmosphere, there will not be air entrainment when the air is supplied in the forced flow conditions of the outer quartz tube.

PMMA is particularly well understood, ignites easily, and burns cleanly without significant condensate or soot produced. PMMA tests with the pyrolyzer plate 7 mm below the opening of the quartz tube yielded flames that burned at the opening of the tube and saw minimal air entrainment into the inner quartz tube that could likely be addressed with an increased N_2 flow which had not been optimized at the time of the tests conducted to evaluate pyrolyzer plate location. An image from a test using 100 mg of PMMA powder is shown in Figure 3.13 with the base of the flame located at the opening of the inner quartz tube and little to no visible entrainment or recirculation

of air inside the quartz tube. However, PE is a more heavily condensing material so open atmosphere tests on 100 mg of PE beads resulted in visible recirculation of volatile gases due to entrainment of air into the inner quartz tube. This recirculation caused some variability in flame location during each test, with the flame typically located at the opening of the inner quartz tube but with the base of the flame occasionally moving lower into the quartz tube itself. The recirculating mix of volatile gases, air, and N_2 is visible in Figure 3.12.

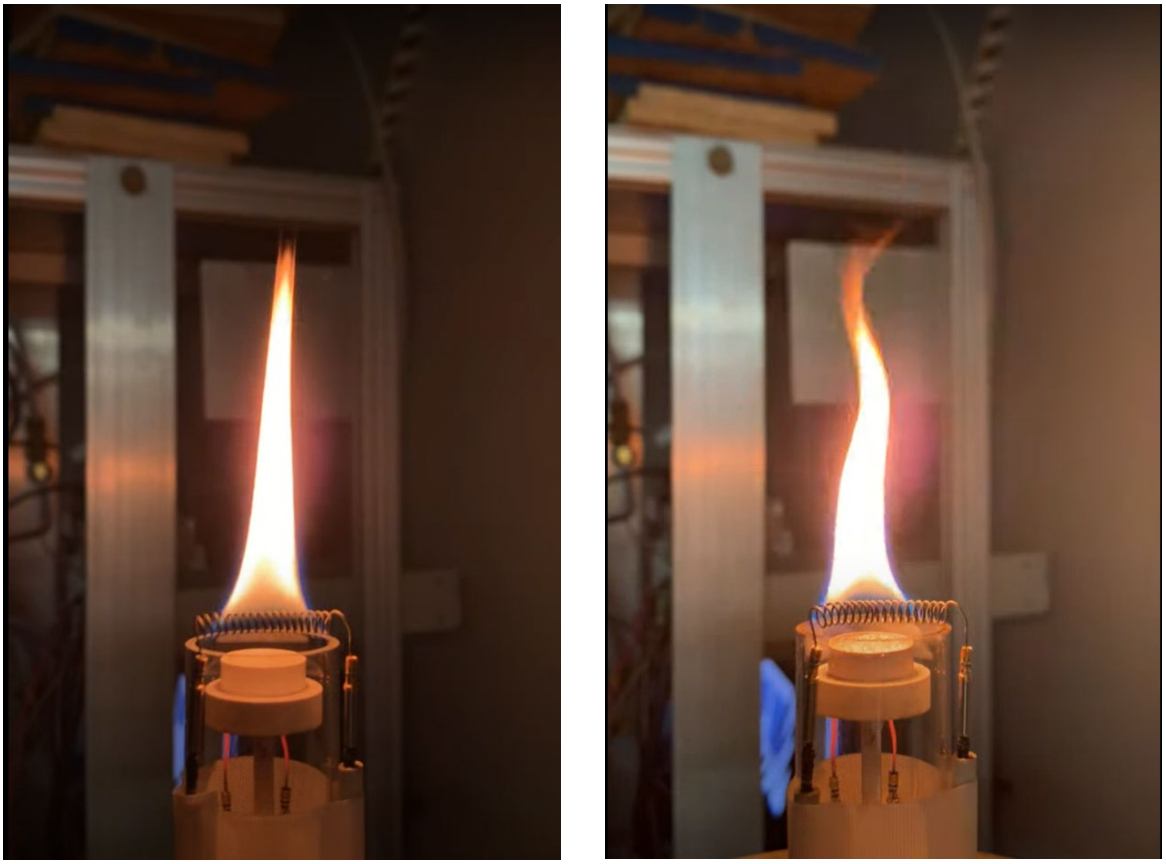

Figure 3.12 Open atmosphere test on 100 mg of PMMA powder (left) and PE beads (right) with pyrolyzer plate located 7 mm below opening of quartz tube. With the PMMA sample at left, the base of the flame is seen at the opening of the quartz tube and there is no visible recirculation of volatile gases in the inner quartz tube. With the PE sample at right, the base of the flame is located close to the opening of the quartz tube and there is visible recirculation of volatile gases in the inner quartz tube.

To prevent entrainment of air into the inner quartz tube and recirculation of the volatile gases, the pyrolyzer plate was lowered to a new location with the top of the pyrolyzer plate located 10

mm below the opening of the inner quartz tube. With the pyrolyzer plate in this location, the top of the crucible is located 5.5 mm below the opening of the quartz tube. The tests on 100 mg of PMMA powder and 100 mg of PE beads were conducted to evaluate the flame location and level of air entrainment with the pyrolyzer plate in the new location 10 mm below the opening of the inner quartz tube. The tests on PMMA showed flames burning at the opening of the inner quartz tube and no significant recirculation of volatile gases, suggesting minimal air entrainment into the inner quartz tube, as can be seen in Figure 3.14. Tests on PE also showed flame locations at the opening of the quartz tube. The PE tests also showed minimal recirculation of the volatile gases, but that the volatile gases gathered in the inner quartz tube. This was not because of air entrainment from the atmosphere into the inner quartz tube, but rather because the N_2 flow through the inner quartz tube was insufficient to prevent the collection of the volatile gases in this location. An image of an open atmosphere PE test with the flame at the opening of the inner quartz tube and with visible collection of gases in the quartz tube is provided in Figure 3.13. The flowrate of N_2 warrants optimization in order to ensure that volatiles are carried out of the inner quartz tube to prevent condensation.

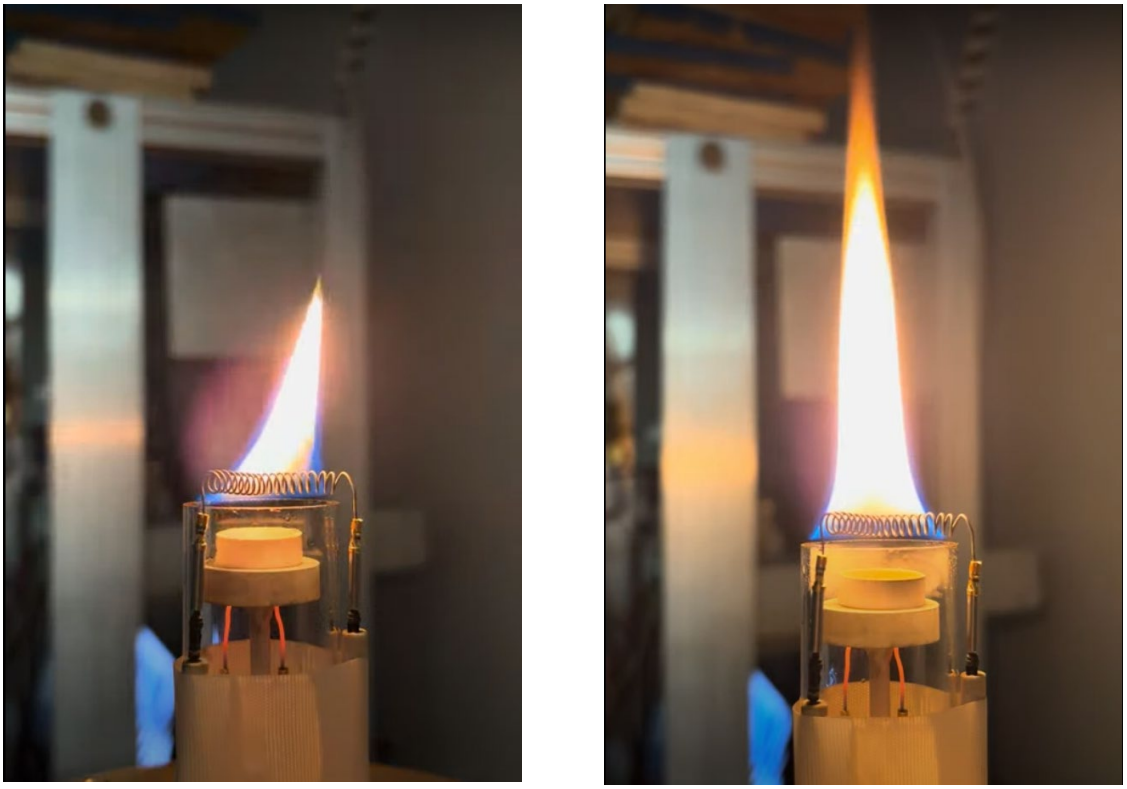

Figure 3.13 Open atmosphere test on 100 mg of PMMA powder (left) and PE beads (right) with pyrolyzer plate located 10 mm below opening of quartz tube. For PMMA at left, the base of the flame is seen at the opening of the quartz tube and there is no visible recirculation of volatile gases in the inner quartz tube. For PE at right, the base of the flame is located at the opening of the quartz tube and there is visible collection of volatile gases in the inner quartz tube, but no recirculation.

3.5 Nitrogen Flow Rate

The N_2 flow through the inner quartz tube carries the volatile gases from the crucible out into the air environment of the outer quartz tube during MFC tests. It is important that the N_2 flow be sufficient to carry the amount of volatile gases produced by heavily condensing materials like PE, without causing dilution of the volatiles to the point that ignition cannot occur. For the empty crucible tests used to optimize voltage and for the open atmosphere tests used to optimize pyrolyzer plate position, the N_2 flow was set at 200 sccm, double the flow rate used in the previous version of the MFC. This value was selected as the inner quartz tube used in this work is approximately

double the diameter of the inner quartz tube used in the previous version of the MFC. However, the open atmosphere tests on PE revealed that it was necessary to further optimize the N_2 flow to prevent the collection and condensation of volatile gases in the inner quartz tube.

To find a better value for the N_2 flow rate, an initial calculation was performed to determine the required N_2 flow rate needed to produce the same velocity of N_2 as is produced in the previous version of the MFC. The following equation was used for this calculation:

$$Q = AV \tag{3.2}$$

where Q is the flow rate of N_2 through the quartz tube in cm^3/min, A is the area inside the inner quartz tube not obstructed by the pyrolyzer plate in cm^2, and V is the velocity of the N_2 gas in cm/min. The conditions in the inner quartz tube can be approximated as standard conditions for the purpose of this calculation, this allowing for Q to be represented with the flow rate setting in sccm. The dimensions of the quartz tube and pyrolyzer plate for both the current and previous version of the MFC, as well as the flow rate and velocities calculated using Equation 3.2 are presented in Table 3.3.

Table 3.3 Dimensions and Calculated Values for N_2 Flow Rate Optimization

	Current Version of MFC	Previous Version of MFC
Pyrolyzer Plate OD [cm]	1.90	1.10
Inner Quartz Tube ID [cm]	2.20	1.30
Flow Area [cm^2]	0.97	0.38
Flow Velocity [cm/min]	265.26	265.26
Flow Rate [sccm]	256.25	100.00

For simplicity, the calculated value of 256.25 sccm was rounded to 250 sccm for testing of the ability of this level of N_2 to carry the volatile gases out of the inner quartz tube and prevent condensation inside the quartz tube. Tests were conducted on PE bead samples, as PE is a heavily condensing material that can be used to significantly test the ability of the N_2 to carry the volatile gases. Using open atmosphere tests with 250 sccm of N_2, there was less visible condensation during testing, showing the effect of the increased N_2 flow. A test on a 100 mg sample of PE beads is shown in Figure 3.14 with the flame located in the desired location at the top of the quartz tube and without condensation visible in the quartz tube.

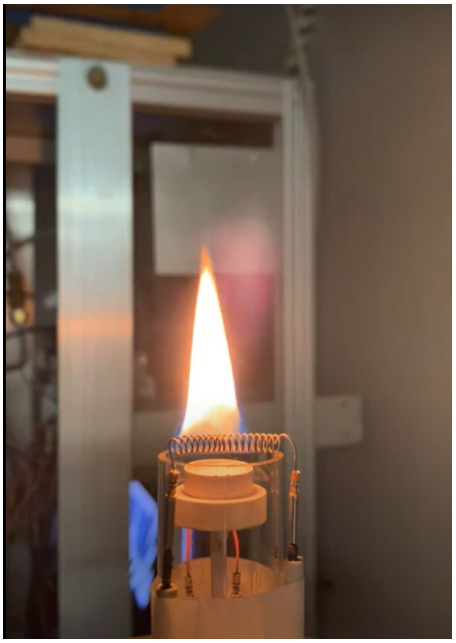

Figure 3.14 Open atmosphere test on 100 mg of PE with an N_2 flow rate of 250 sccm. The flame is located at the opening of the inner quartz tube and there is minimal visible condensation in the inner quartz tube.

However, it was also important to confirm that the increased N_2 flow did not cause dilution of the volatile gases at smaller sample sizes. Though the version of the MFC used in this work is intended for use on samples ranging in size from 90 to 150 mg, it is desirable for it to also be capable of testing the smaller sample sizes tested using the original MFC. To confirm that the N_2 flow did not cause difficulty with ignition for small sample sizes, open atmosphere tests were

conducted on 30 mg samples of PMMA powder. The PMMA tests resulted in successful ignition and burning of the 30 mg samples, but the flames were qualitatively smaller and less steady than the flames produced with tests on 100 mg samples. Additionally, the flames produced with the smaller sample sizes tended to move location more frequently between the top of the crucible and the opening of the inner quartz tube, suggesting the N_2 was causing some dilution leading to instability in combustion. However, the successful ignition of these flames reflects the increased versatility of the version of the MFC used in this work, as it is able to be used with the target sample size of 90 to 150 mg, but also with the smaller sample sizes of the previous version of the MFC. An image of a flame produced with a 30 mg sample of PMMA in an open atmosphere test is shown in Figure 3.15.

Figure 3.15 Open atmosphere test on 30 mg of PMMA powder with an N_2 flow rate of 250 sccm. Ignition was successful, but the flame location was unsteady, suggesting that samples at this small size experience some dilution from the N_2 flow.

The N_2 flow rate was also examined during closed tests using the outer quartz tube and forced air co-flow. The air co-flow created back pressure not seen with open atmosphere tests and resulted

in condensation forming on the walls of the quartz tube and running down the walls to below the level of the pyrolyzer plate during initial closed testing at an N_2 flow rate of 250 sccm. Losing volatiles as condensation on the walls alters test results for HRR, HOC, CO and CO_2 production, and soot yield. Thus, it was important to eliminate condensation and the N_2 flow was increased to 300 sccm for closed testing.

3.6 Air Flow Rate

The air flow in the outer quartz tube supplies the O_2 necessary for combustion to occur. In the previous version of the MFC, the air co-flow was supplied at a rate of 4 SLPM. Because the N_2 flow was tripled, ideally the air co-flow would also be tripled to maintain the same ratio of air to N_2. However, the air and N_2 flow controllers, as well as the flow meter, were reused in version of the MFC used in this work from the previous version of the MFC. The air controller used in the previous version of the MFC could flow a maximum of 5 SLPM of air. Fortunately, a second air controller to provide additional flow was already integrated with the MFC apparatus and could be used for the version of the MFC used in this work. The second flow controller could flow a maximum of 2 SLPM, bringing the maximum total air flow rate to 7 SLPM. Obtaining a larger flow controller was not possible given time constraints on this work. Additionally, obtaining a larger flow controller would also require a new flow meter, as the flow meter used with both this version and the previous version of the MFC is designed for up to 10 SLPM of flow. Given these limitations, tests were conducted with an air co-flow of 7 SLPM.

Flowing only 7 SLPM of air raised concerns that insufficient O_2 would be provided for combustion and that samples would be burning in under-ventilated conditions, which would affect test results for HRR; HOC; CO and CO_2 levels; and char and soot yields. The O_2 levels during testing were examined to determine the amount of oxygen being consumed by combustion to

ensure that O_2 levels never dropped below 16%, which would strongly indicate under-ventilated conditions and possibly cause flame extinction. Samples of PE caused the most significant drop in O_2 level, with 100 mg samples resulting in an average minimum O_2 concentration of 14.9%. Smaller tests using 50 mg of PE were also conducted and resulted in an average minimum O_2 concentration of 18.0%. The average O_2 level over time for the 100 mg PE tests and the 50 mg PE tests is shown in Figure 3.16. The initial O_2 level is lower for the 50 mg tests as the 50 mg tests were run with 300 sccm of N_2, while the 100 mg tests were run with 250 sccm of N_2. The other materials examined in this work burn less readily than PE and will not result in such a significant drop in O_2 concentration meaning the air flow rate of 7 SLPM was sufficient for this work. Future testing with this version of the MFC could be greatly improved by the ability to flow more air through the system to ensure well-ventilated conditions for all sample materials and sizes.

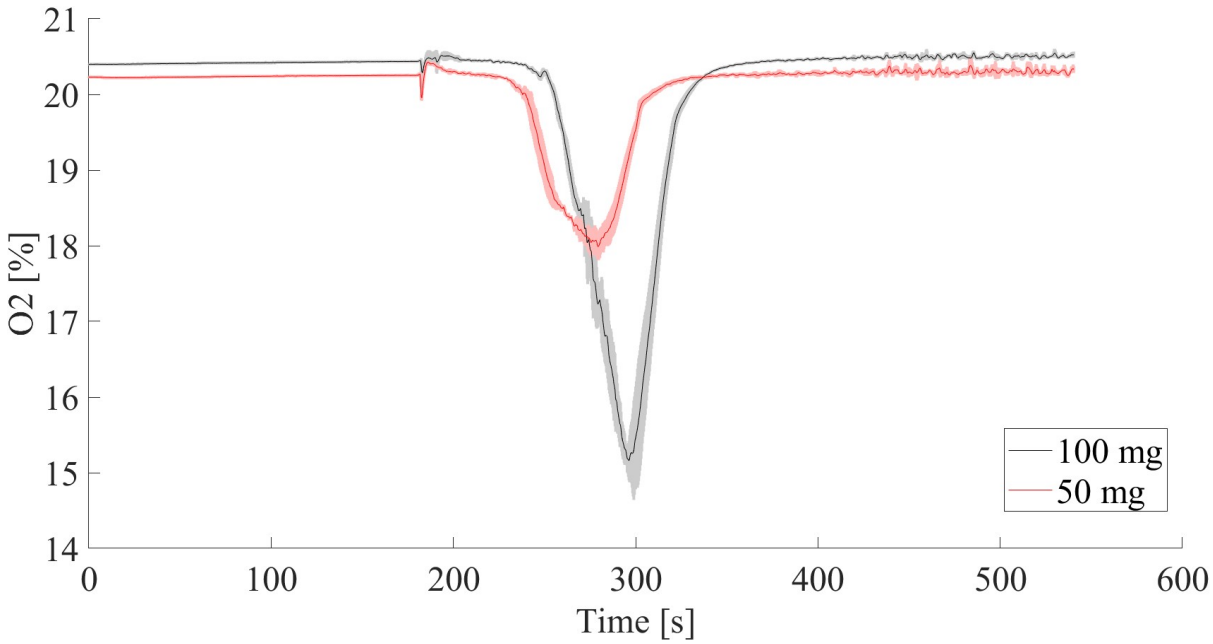

Figure 3.16 Average O_2 levels during testing of 100 mg and 50 mg PE samples.

3.7 Test Materials

Tests were conducted on four polymers and a wood-based material to compare the test results found using the new, larger version of the MFC to test results found using the original version of the MFC. The flammability parameters found through MFC tests include the heat of combustion (HOC), heat release rate (HRR), peak heat release rate (pHRR), soot yield, and char yield. The polymers selected for testing were:

- Polymethyl methacrylate (PMMA)
- Polyethylene (PE)
- Polyvinyl chloride (PVC)
- Polyether ether ketone (PEEK)

The polymers were selected as their properties are well characterized and all of them, with the exception of PE, have been studied with the original version of the MFC. Additionally, the four different polymers present different challenges in terms of flammability and burning behavior that will offer a thorough understanding of the limitations of the updated version of the MFC used in this work. PMMA is a uniquely well understood material used to characterize many bench-scale fire testing apparatuses. Because PMMA is so well understood, it is important for the results of the tests using this version of the MFC to closely match published values for PMMA to prove the accuracy of the test method. PE is a heavily condensing material with a high heat of combustion. The condensing volatiles presented design challenges to the apparatus, as discussed in Chapter 3. PVC is difficult to ignite and maintain combustion, so burning PVC in the updated version of the apparatus will prove the ability of the apparatus to burn most types of material. Additionally, PVC produces significant soot yield when burned. PEEK was selected because it is particularly difficult to ignite. It is also heavily charring, so burning PEEK will show the ability of the updated version

of the apparatus to burn even materials with non-flammable vertical flame spread test ratings. The wood-based material, oriented strand board (OSB), was selected due to its characteristic inhomogeneity which presented consistency challenges when tested in the previous version of the MFC.

3.8 Test Method

Based on the optimization, tests were run with standard conditions of 7 SLPM of air flow and 300 sccm of N_2 flow. The pyrolyzer was located 10 mm below the opening of the inner quartz tube. Some tests were conducted in conditions that deviated slightly from this standard, and any deviation will be reported with the test results.

3.8.1 Calibration and Daily Set-up

The MFC makes use of oxygen consumption calorimetry to determine the HOC and HRR of a sample, meaning that accurate measurement of the oxygen level during testing is critical to ensure quality test results. The flow meter, O_2, CO, and CO_2 sensors must be calibrated daily to ensure the accuracy of their readings. To do this, four calibration tests are performed with the flow from the flow controllers connected directly to the flow meter through a single tube, rather than through the full MFC apparatus. Before data is recorded for each test, the test is allowed to run without recording for a period of two minutes to ensure that the flow is stable and that there is no leftover gas from a previous calibration test in the system. The first calibration test is a no flow test to establish a zero condition to calibrate the flow meter. The second calibration test is a flow test in which air is flowed at 7 SLPM. The results of these tests are used to adjust the scaling for the flow meter reading in LabVIEW. The third calibration test is to create a zero value for the O_2, CO, and CO_2 sensors by flowing pure N_2 at 7 SLPM through the system. Then, a gas with known concentrations of O_2, CO, and CO_2 is flowed at 7 SLPM through the system. The percentages of

each gas are reported in Table 3.4. The values from these tests are used for scaling the sensor readings in LabVIEW.

Table 3.4 Gas Concentrations of Calibration Gas

Gas	Volumetric Percent
O_2	20.06
CO	1.012
CO_2	7.962
N_2	70.966

Moisture must be removed from the flow before it reaches the sensors. At the beginning of each test day, the Drierite desiccant must be replaced to ensure that it sufficiently dries the flow. Additionally, at the end of the tube that holds the Drierite there is a small plug made of a piece of insulation that prevents dust from the Drierite from reaching the flow meter and sensors. This piece of insulation must also be replaced at the beginning of each day of testing.

3.8.2 Test Procedure

The first step in an MFC test is to weigh a new, clean 2-micron filter to record its initial mass before placing the filter in its place in the exhaust system. Next, a clean, empty crucible must be weighed, and its initial mass recorded. The sample is added to the crucible and the full crucible is weighed and its mass is recorded. The filled crucible is placed onto the pyrolyzer plate in the inner quartz tube and its position is adjusted until the crucible is centered on the plate. Next, the outer quartz tube and attached exhaust hood are placed in the base of the MFC. The screws that connect the flange to the base of the MFC are tightened to compress the O-ring to securely hold the outer quartz tube in place. When tightening the screws, it is important to alternate between sides of the flange so that the quartz tube does not crack due to uneven forces on the walls of the tube. Once the quartz tube and attached exhaust hood are securely in place, the remainder of the exhaust system, including the components that hold the filter and the Drierite, is attached to connect the

exhaust hood to the flow meter. The camera used to record the flame during MFC testing must be positioned and focused. The room should be darkened to allow for the best possible video recording of the flame.

Once all components are attached and the camera is in position, it is important to confirm the file name and settings before beginning an MFC test and recording sensor data. The test begins with a three minute pre-heating ramp from ambient conditions to 47 °C. During the pre-heating ramp, 150 seconds after the beginning of the MFC test, the camera is turned on to begin the video recording. Then, 180 seconds after the beginning of the test, the igniter coil must be manually turned on at the same time that the voltage is automatically increased by LabVIEW to begin the pyrolysis ramp. When turning on the igniter coil, it may be necessary to adjust the voltage output slightly to achieve the desired 50 W power output. The igniter coil remains on until steady flaming combustion is observed for 5 seconds. If a sample never achieves steady flaming combustion, the igniter coil may be turned off when the sample is no longer visibly off-gassing or the igniter coil may be left on until the end of the pyrolysis ramp. The video recording may be ended when flame extinction is observed, or the recording may continue until the end of the pyrolysis ramp. The pyrolysis ramp is four minutes long and heats the sample from 47 °C to 695 °C. At the end of the pyrolysis ramp, the power to the pyrolyzer is turned off by LabVIEW and the sensors continue to record temperature and gas data for an additional two minutes during the cooling period of the test.

After the cooling period ends and data collection from the thermocouple and sensors stops, the exhaust system of the MFC is disconnected and the outer quartz tube and attached exhaust hood are removed. When removing the outer quartz tube, it is advised to loosen screws on opposite sides of the flange to prevent uneven pressure from the O-ring from cracking the quartz tube. Then, the crucible is carefully removed from its position on the pyrolyzer plate using tweezers and weighed

to determine the final mass of the crucible and any char yield remaining after the test. After recording the final mass of the crucible and any char yield, any mass inside the crucible must be removed using tweezers and compressed air. Sometimes, there is residue on the inside and outsider surfaces of the crucible that must be burned away using a butane torch. When cleaning the crucible with the butane torch, it is important to apply the flame only to the walls of the crucible or evenly across the bottom of the crucible to prevent the heat from breaking the delicate ceramic crucible. To complete an MFC test, the filter must be removed from the exhaust system and weighed. Its final mass is recorded to obtain information on soot yield during testing. For repeated testing, the pyrolyzer must be allowed to cool until the temperature read by the thermocouple is below 23 °C, showing a return to ambient conditions. This ensures repeatability between tests by beginning the two heating ramps at ambient conditions.

4. Results

The results of testing conducted on four polymers (PMMA, PE, PVC, and PEEK) and OSB at a variety of sample masses are presented in this section. Tests were conducted in triplicate for each material and sample mass. The tests were conducted at the test conditions outlined in Chapter 3.8, with 7 SLPM of air flow and 300 sccm of N_2 flow. Some tests were conducted under varied conditions, which is reported along with the results and the reason for the variation.

4.1 PMMA

Polymethyl methacrylate (PMMA) is a commonly studied polymer in fire science research. Its behavior and properties are well understood, and it has been tested using the previous version of the MFC. The popularity of PMMA as a material for fire science research makes it an optimal polymer to test to compare test results found with the version of the MFC used in with work with results from the previous version of the MFC.

The PMMA used for this research was in powder form. Samples were prepared using a small scoop to transfer the powder into the crucible. The crucible was weighed, and powder was added or removed until the sample mass reached the desired size. Samples were tested at three sizes: 100 mg, 70 mg, and 40 mg. The 100 mg sample size was selected as this size falls within the target sample size range for the version of the MFC used in this work. The 40 mg sample size was selected to ensure that this version of the MFC remains versatile enough to test the small sample masses tested in the previous version of the MFC. The 70 mg sample size was tested as the 100 mg size resulted in O_2 levels reduced slightly below the minimum 16% required for well-ventilated combustion.

During PMMA testing, the sample produces large bubbles that stretch across the area of the crucible opening, creating short initial bursts of flame as the bubbles pop and the gases make

contact with the igniter coil. Eventually, the short bursts of flame develop into steady flaming conditions. The larger sample masses resulted in larger flames with longer burn durations than the smaller sample mass tests. The results of the PMMA tests on the three sample sizes are shown in Table 4.1, along with results on PMMA from tests conducted by DeBeer using the previous version of the MFC [9]. Soot yield was not recorded for the 40 mg and 100 mg tests, and is reported as not measured (NM). The ignition time reported in this work is relative to the time at which the igniter coil was turned on, a different time than the ignition times reported by DeBeer. To avoid confusion, the times recorded by DeBeer are not reported (NR) in this work. The average HRR normalized by mass for each sample size is plotted over time in Figure 4.1 and over temperature in Figure 4.2. The error bars shown represent two standard error, using three tests per sample mass. The raw HRR plots for the individual tests can be found in Appendix A.

Table 4.1 MFC Experimental Results on PMMA using Current Version of MFC and Previous Version of MFC

		40 mg	70 mg	100 mg	DeBeer [9]
Sample Mass	[mg]	40.42 ± 0.41	70.60 ± 0.88	99.38 ± 0.63	34.51 ± 0.66
Time to Ignition	[s]	50 ± 2	45 ± 3	52 ± 2	NR
Char Yield	[%]	0.26 ± 0.18	0.25 ± 0.16	0.23 ± 0.03	0.33 ± 0.09
Soot Yield	[%]	NM	0.69 ± 0.19	NM	1.12 ± 0.46
Ignition Temperature	[°C]	331 ± 10	323 ± 15	328 ± 4	439 ± 11
Peak HRR	[kW/g]	916.0 ± 19.5	930.0 ± 30.1	961.0 ± 82.7	1123 ± 6
Average HRR	[kW/g]	608.0 ± 22.4	473.0 ± 16.9	501.0 ± 30.2	507 ± 5
HOC (initial mass)	[kJ/g]	24.10 ± 0.75	25.20 ± 0.18	26.40 ± 0.32	24.18 ± 0.70
HOC (gasified mass)	[kJ/g]	24.20 ± 0.37	25.30 ± 0.07	26.40 ± 0.17	24.27 ± 0.68

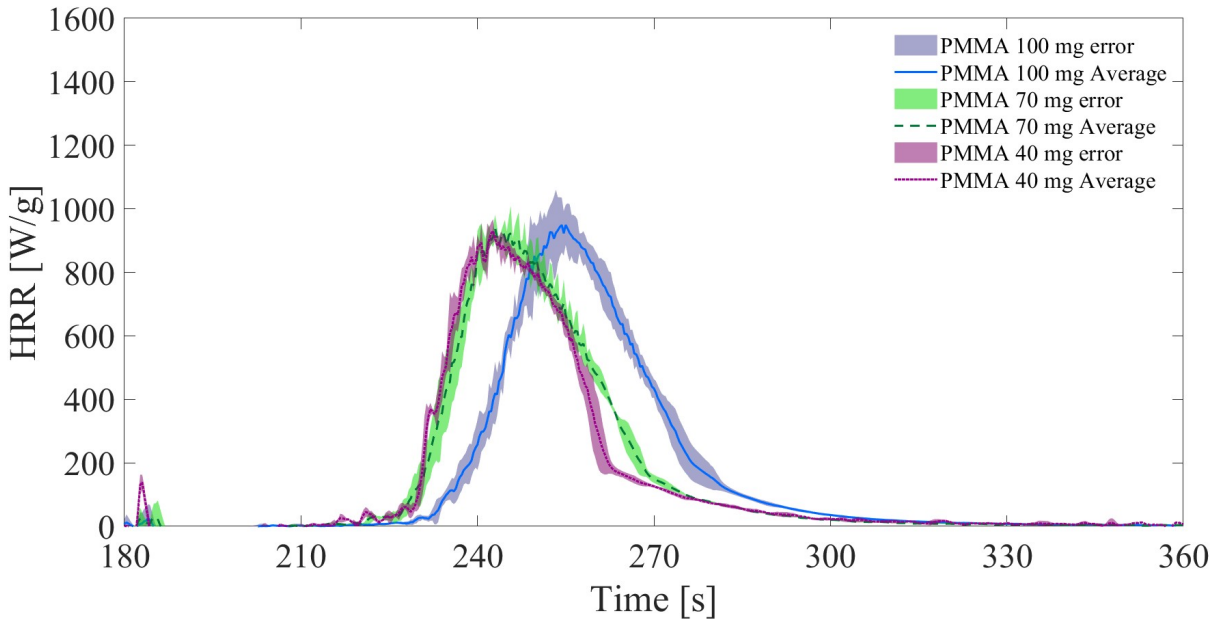

Figure 4.1 Average HRR with error plotted with respect to time for sets of three tests on three different sample masses of PMMA.

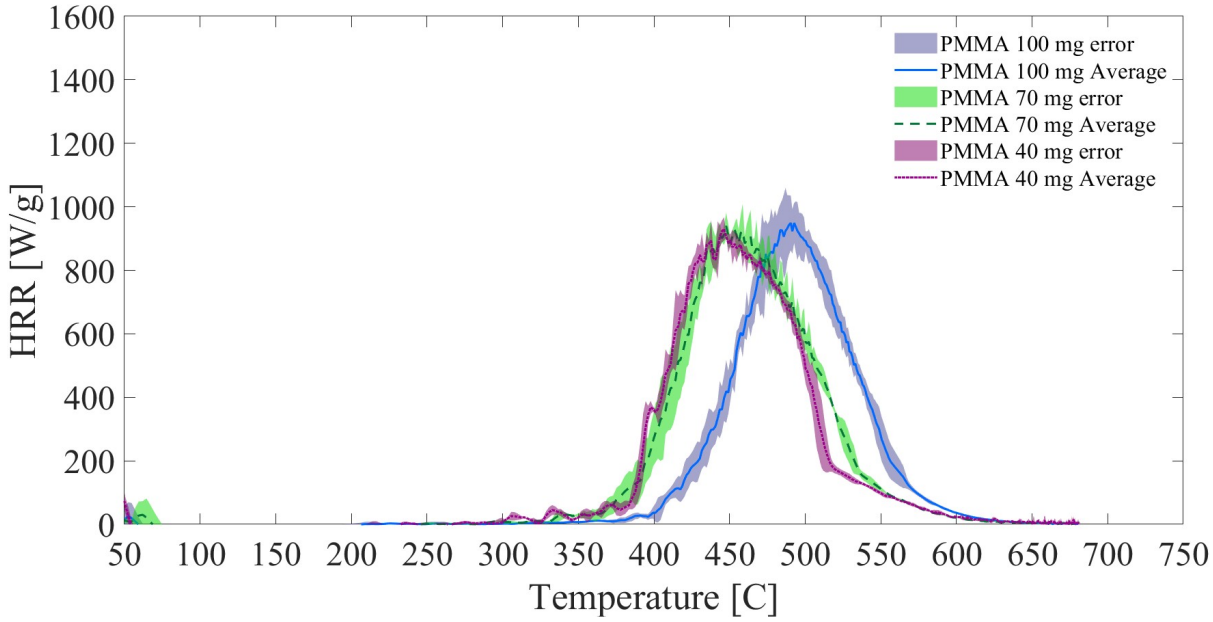

Figure 4.2 Average HRR with error plotted with respect to temperature for sets of three tests on three different sample masses of PMMA.

The HRR for the 40 mg and 70 mg sample tests closely align in terms of pHRR and ignition time, as seen in Figure 4.1and Figure 4.2, though the 70 mg sample ignites slightly later on average than the 40 mg sample. The 100 mg samples ignite later than both the 40 mg and 70 mg samples,

which is partially due to thermal inertia. It requires more time to heat greater mass, resulting in a later ignition time for the larger sample size. The pHRR normalized by mass for all three sample sizes is similar and reflects consistency during testing. The pHRR for all tests using the current version of the MFC is less than the pHRR seen in tests using the previous version of the MFC. This is likely due to the differences in the heating profile between the pyrolyzer used in this work and the pyrolyzer used in the previous version of the MFC, which is discussed in Chapter 3.2. The average HRR varies more widely for the different sample masses, reflecting differences in the burning time for each sample mass. The average HRR for the tests conducted with this version of the MFC aligns with the average HRR seen in tests with the previous version of the MFC.

The early spikes in HRR seen around the 180 second mark in Figure 4.1 are not caused by sample burning. This spike occurs throughout testing, regardless of material or sample mass, and is also seen in tests conducted using the previous version of the MFC. The spike in HRR at this early time in testing coincides with the beginning of the pyrolysis heating ramp and with the time at which the igniter coil is turned on. Most likely, when the igniter coil is turned on, the heat of the coil forces some air out of the inner quartz tube. Additionally, when turned on, the igniter coil is at a high temperature which speeds oxidation, so the air forced out of the tube when the coil is turned on carries some of the products of that oxidation to the gas sensors. This theory is supported as a small decrease in the O_2 level reported by the gas sensors is seen at the beginning of the pyrolysis heating ramp.

The HOC is calculated based on both initial and gasified mass. For PMMA, which does not char, these values are near identical for the two calculation methods. The value of HOC for the 40 mg tests conducted with this version of the MFC matches well with the results found with the previous version of the MFC. The value for HOC found with the current version of the MFC

increases with sample size, likely because the limited air flow of 7 SLPM is insufficient to provide enough oxygen for well-ventilated conditions for larger sample masses. With increased air flow, there would be greater consistency in the HOC calculated for the different sample masses.

PMMA does not leave char or residue in the crucible in any of the tests conducted with this version of the MFC or in tests using the previous version of the MFC. The soot yield was not measured for the 40 mg or 100 mg sample masses, and for the 70 mg test the soot yield is comparable for the soot yield reported in tests using the previous version of the MFC. The similarities between the values found using the current version of the MFC and the previous version of the MFC supports the reliability of the current version of the MFC as a test method.

4.2 PE

Polyethylene (PE) is a polymer that is widely used in a variety of consumer products. It is highly combustible and produces significant amounts of soot when burned. It was selected for this study for its properties as a material with a high HOC and the significant amount of condensate that it produces when it burns. The condensate gases produced during the burning of PE were a challenge to the apparatus as discussed in Chapter 3. A set of three tests was conducted with polyethylene at three different sample masses: 50 mg, 70 mg, and 100 mg. The PE burned for this work was in the form of beads. For 50 mg samples, 3 beads were used, while 4 beads and 6 beads were used for the 70 mg and 100 mg samples respectively.

When heated, the PE samples off-gassed and produced small bubbles that created some unsteady initial flaming, though to a lesser degree than with the PMMA samples. After a short unsteady period, the PE tests resulted in steady flames, with the larger flames and longer burn durations seen for the tests on larger sample masses. The results of the tests are presented in Table 4.2. The average HRR normalized by mass over time is presented in Figure 4.3 and the average

HRR normalized by mass is plotted with respect to temperature in Figure 4.4. The plots of the raw HRR normalized by mass are available in Appendix A.

Table 4.2 MFC Experimental Results using Current Version of MFC

		50 mg	70 mg	100 mg
Sample Mass	[mg]	50.52 ± 1.77	70.55 ± 0.47	101.87± 2.45
Time to Ignition	[s]	58 ± 2	68 ± 3	68 ± 2
Char Yield	[%]	0.26 ± 0.18	0.25 ± 0.16	0.23 ± 0.03
Soot Yield	[%]	NM	1.89 ± 0.07	NM
Ignition Temperature	[°C]	368 ± 7	411 ± 3	377 ± 8
Peak HRR	[kW/g]	955.0 ± 56.1	1480.0 ± 71.1	1100.0 ± 39.1
Average HRR	[kW/g]	640.0 ± 11.5	740.0 ± 11.5	537.0 ± 3.3
HOC (initial mass)	[kJ/g]	44.30 ± 0.33	45.60 ± 0.66	43.20 ± 0.12
HOC (gasified mass)	[kJ/g]	44.40 ± 0.15	45.70 ± 0.37	43.20 ± 0.05

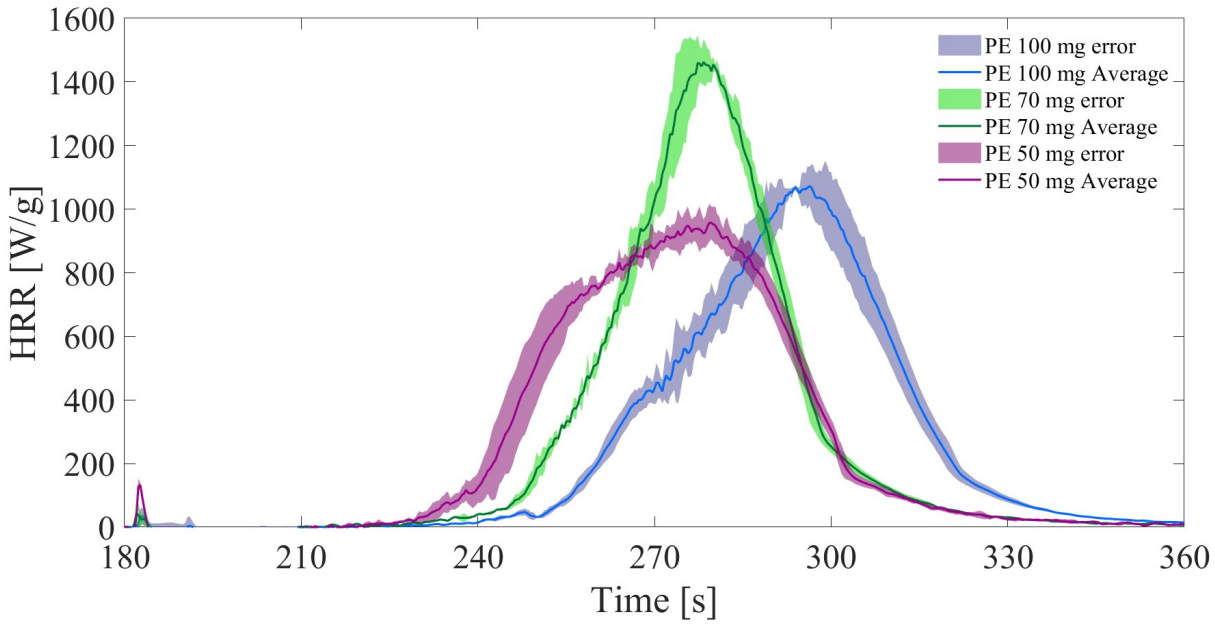

Figure 4.3 Average HRR with error plotted with respect to time for sets of three tests on three different sample masses of PE.

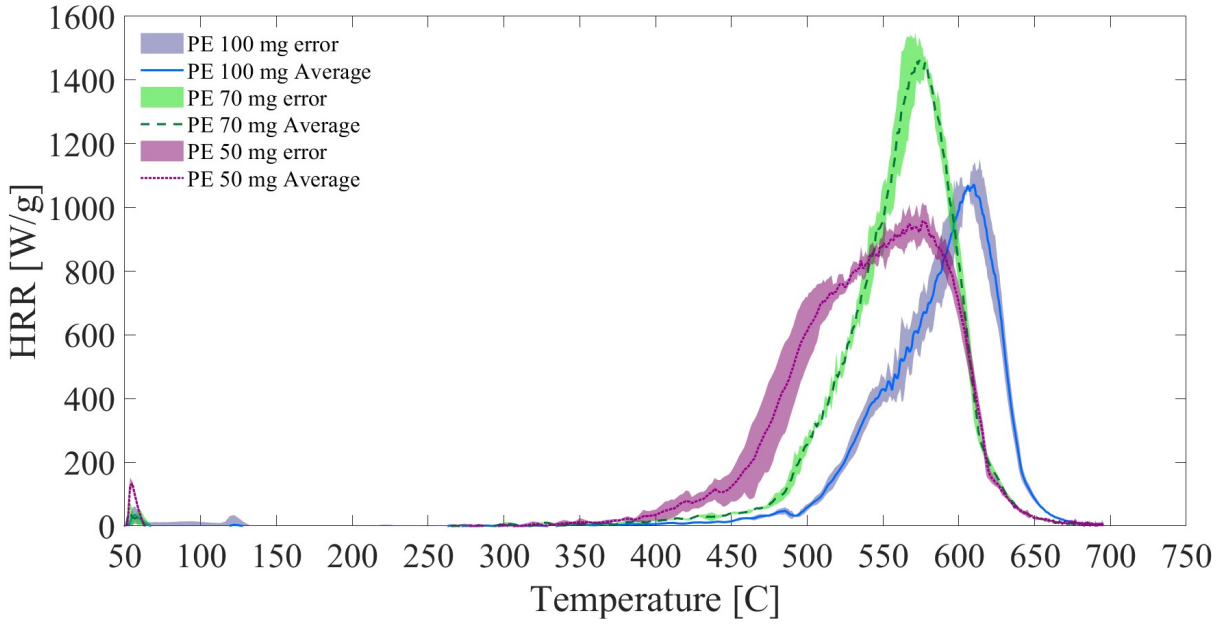

Figure 4.4 Average HRR with error plotted with respect to temperature for sets of three tests on three different sample masses of PE.

As seen in Figure 4.3 and Figure 4.4, there is inconsistency between the HRR plots for the three sample masses of PE plotted with respect to time and temperature. The 50 mg samples ignite before the 70 mg samples, which ignite before the 100 mg samples. This is likely due to the thermal inertia of the sample as more heat is required to bring a larger mass to its ignition temperature. This may also be due to inconsistency in pyrolyzer plate temperature across the surface of the plate, as discussed in Chapter 3.3. Inconsistent pyrolyzer plate temperature would create uneven heating of the sample, resulting in discrepancies in burning behavior between samples of different masses and different numbers of beads. The 70 mg tests have a significantly higher HRR normalized by mass compared to the tests on 50 mg and 100 mg sample masses. This is caused by a number of factors. The first is the limitation on the airflow through the system to 7 SLPM due to the flow controllers, as discussed in Chapter 3. The 100 mg tests likely do not burn as completely as the tests on smaller sample masses as there may be insufficient air flow to maintain fully well-ventilated conditions for the duration of the test. Additionally, in the videos for the 100 mg tests,

it is possible to observe some condensation forming on the walls of the inner quartz tube and dripping below the level of the pyrolyzer plate. This condensation occurred because the 100 mg tests were run with 250 sccm of N_2 and the formation of the condensation resulted in all tests performed subsequently to be run with a flowrate of 300 sccm of N_2. The 70 mg tests likely have the most accurate HRR when normalized per mass as there is sufficient N_2 flow to prevent condensation on the walls of the inner quartz tube and the sample mass is small enough for the 7 SLPM air flow to supply sufficient amounts of O_2 for complete combustion. It is unclear why the 50 mg tests have a lower peak and average HRR, as there was not visible condensation and at a smaller sample size the air flow would have been sufficient. One theory is that the 50 mg test mass was too diluted by the N_2 flow for ideal burning behavior and that there may be a lower limit on the sample masses that can be tested in the MFC. However, the ability to burn 40 mg of PMMA is a counterpoint to this theory as PE is significantly more combustible than PMMA. Further research could be conducted to understand whether condensation, air flow, sample mass, or a combination of factors creates the inconsistency in the results of the PE tests.

PE has not been tested comprehensively with the previous version of the MFC, so MFC data was not available for comparison. However, the maximum HOC in ideal stoichiometric conditions was calculated from the stoichiometric burning equation of PE in oxygen. From the balanced chemical equation, the ratio of mass of O_2 consumed to mass of PE consumed during burning can be found and multiplied by 13.1 kJ/g to determine the HOC. For PE, this value was calculated to be 44.9 kJ/g of PE. The results for HOC calculated for each set of tests at the different sample masses is close to this ideal value for HOC which suggests that despite inconsistencies in HRR, the test results on PE still provide strong insight into the burning behavior of the material. The values were close to ideal for both the HOC calculated using the initial sample mass and the HOC

calculated based on gasified mass, the values of which are similar for PE since PE does not produce significant char yield. Resolving issues with flow and heating consistency would likely bring the values of HOC even closer to the ideal value.

PE is not a charring material, as seen across all tests. It does produce significant amounts of soot, which was measured only for the 70 mg test. It would be valuable to examine the soot yields for other sample masses to determine whether the soot yield has been affected by potentially under-ventilated conditions.

4.3 PVC

Polyvinyl chloride (PVC) is a polymer widely used to make consumer plastic products. It is difficult to ignite and can achieve a non-flammable rating in UL-94 vertical flame spread tests. PVC is also self-extinguishing because it produces hydrogen chlorine gas as it decomposes [19]. The hydrogen chlorine gas slows combustion reactions and displaces O_2, both of which lead to flaming ignition being difficult to sustain on PVC. The difficulty of achieving ignition and steady flaming made PVC an ideal polymer to test to challenge the ability of the version of the MFC used in this work to provide sufficient power for ignition and burning. Furthermore, PVC has been studied using the previous version of the MFC, making it an ideal material to test for direct comparison between the results from the two versions of the apparatus. PVC was tested in multiple sample sizes. It was tested in disks at 3 different sizes: 70 mg, 100 mg, and 200 mg. An 8 mm drill was used to cut the disks from a sheet of PVC. The disks were sanded down and weighed periodically until the desired mass for testing was achieved.

PVC is highly intumescent, meaning that when heated it swells and deforms significantly. Samples off-gassed significantly before ignition and once ignited, PVC samples had difficulty achieving steady flaming conditions. Occasionally, PVC samples would ignite, extinguish, and reignite, due to the hydrogen chloride gas produced by decomposing PVC making it difficult to sustain ignition. The results of the tests on the various sizes, as well as the results of tests from the previous version of the MFC by DeBeer [9], are presented in Table 4.3. The HRR normalized by mass is plotted against time in Figure 4.5 and against temperature in Figure 4.6. The plots of the raw HRR normalized by mass are available in Appendix A.

Table 4.3 MFC Experimental Results using Current Version of MFC and Previous Version of MFC

		70 mg Disks	100 mg Disks	200 mg	De Beer [9]
Sample Mass	[mg]	74.60 ± 2.37	106.23 ± 1.94	211.64 ± 5.07	57.08 ± 5.80
Time to Ignition	[s]	79 ± 2	92 ± 4	105 ± 8	NR
Char Yield	[%]	16.10 ± 0.44	17.03 ± 1.39	16.10 ± 0.43	17.27 ± 2.12
Soot Yield	[%]	5.63 ± 1.68	8.40 ± 0.37	7.71 ± 0.88	4.06 ± 2.18
Ignition Temperature	[°C]	361 ± 7.28	347 ± 30.9	403 ± 24	392 ± 8
Peak HRR	[kW/g]	249.0 ± 24.4	269.0 ± 26.0	162 ± 42	269 ± 2
Average HRR	[kW/g]	58.5 ± 15.2	30.7 ± 2.7	35 ± 15	221 ± 20
HOC (initial mass)	[kJ/g]	7.79 ± 1.6	6.08 ± 0.23	6.61 ± 0.13	7.42 ± 0.48
HOC (gasified mass)	[kJ/g]	9.27 ± 0.93	7.24 ± 0.14	7.91 ± 0.07	9.27 ± 0.21

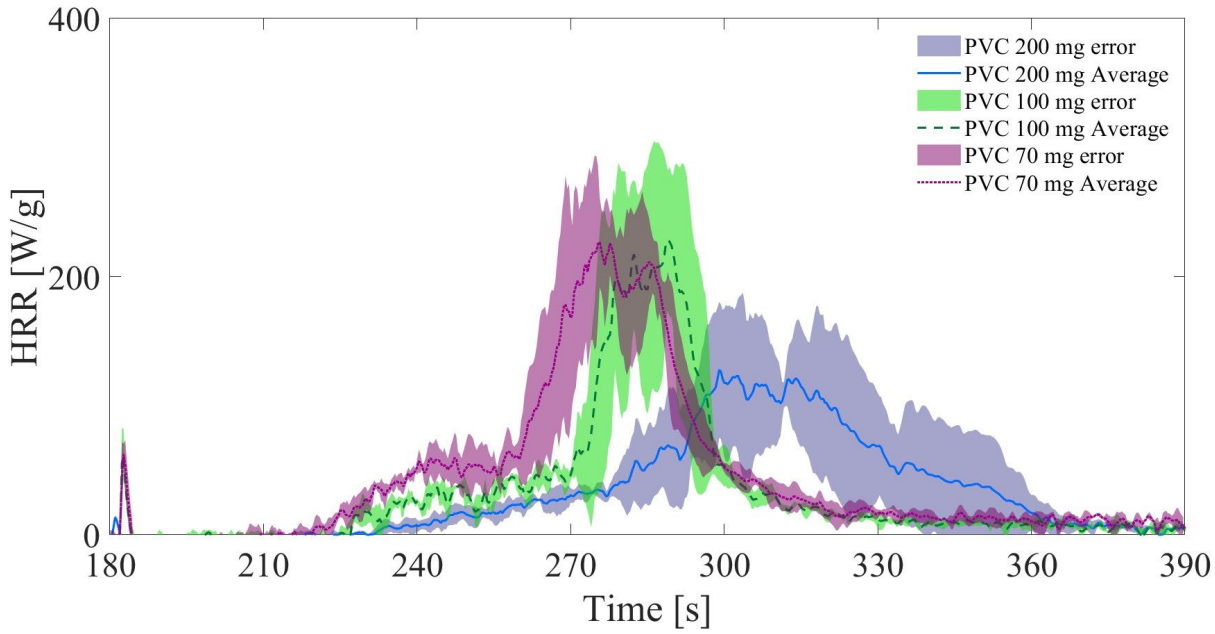

Figure 4.6 Average HRR with error plotted with respect to time for sets of three tests on three different sample masses of PVC.

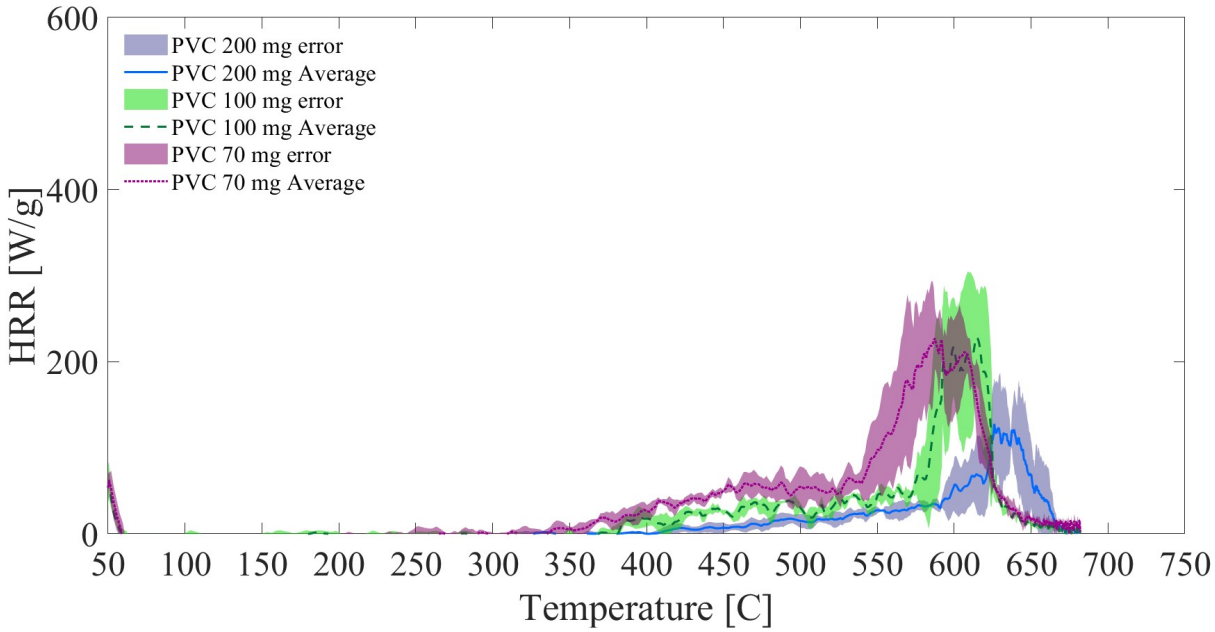

Figure 4.5 Average HRR with error plotted with respect to temperature for sets of three tests on three different sample masses of PVC.

The tests on PVC disks produced qualitatively unsteady flames. To ensure continued combustion during testing, the igniter coil was left on until full extinguishment of the flame was observed. The pHRRs of the PVC tests at the 70 mg and 100 mg sample masses were comparable

to the pHRR observed by DeBeer in tests using the previous version of the MFC. The pHRR for the 200 mg test was significantly reduced, likely due to an issue observed with the air flow and conditions in the outer quartz tube. PVC is a heavily sooting material and the smoke produced by the samples at the 200 mg size made visible a problem in the exhaust system of the MFC. Smoke began to build up in the outer quartz tube and there was significant recirculation of the air and smoke in the outer quartz tube. An image of this phenomena is shown in Figure 4.7. The recirculation likely occurred because the increased air flow at 7 SLPM was more than the exhaust system could handle. The recirculation of the air and smoke created under-ventilated conditions in the outer quartz tube and affected the burning of the 200 mg PVC samples, leading to their lower HRR when normalized by sample mass. To confirm that the exhaust system was the cause of this recirculation, a test was performed in which only the outer quartz tube and exhaust hood were in place without connecting to the gas sensors and flow meter. A test was also performed with the outer quartz tube without the exhaust hood to provide nearly open conditions for exhaust. There was recirculation visible in the test with the exhaust hood and minimal recirculation visible in the test with only the outer quartz tube. Figure 4.8 shows the conditions in the quartz tube during these tests with varied exhaust conditions.

Figure 4.8 Smoke and air recirculation visible during MFC test on 200 mg of PVC with air co-flow of 7 SLPM.

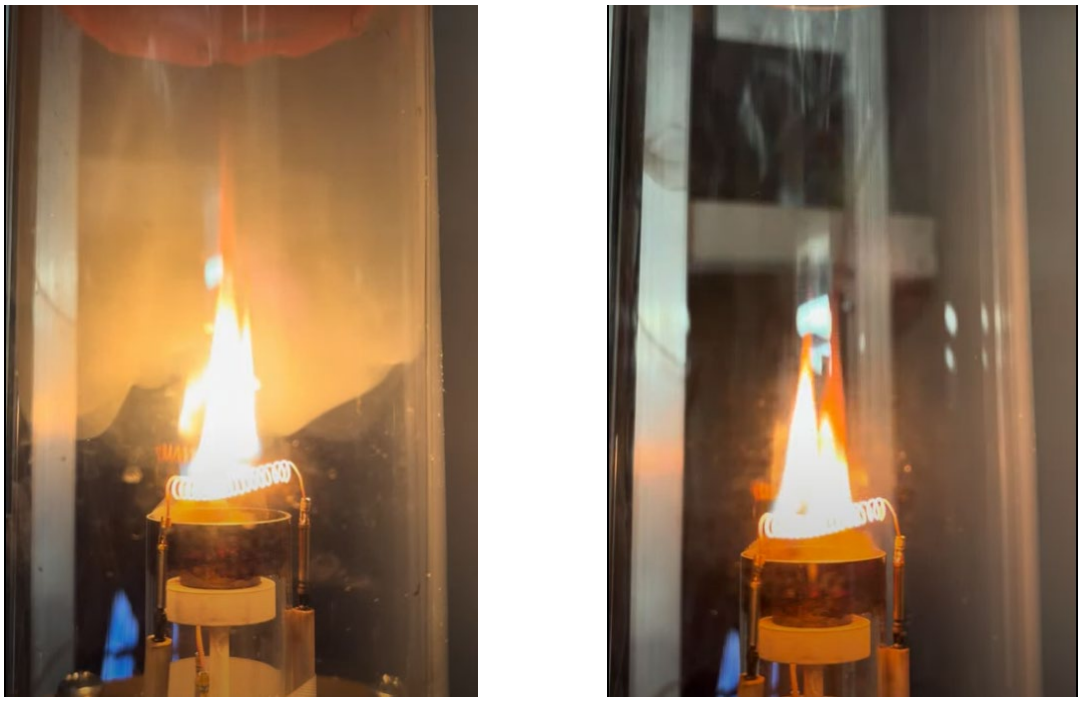

Figure 4.7 Smoke and air recirculation visible during MFC tests on 200 mg of PVC with air co-flow of 7 SLPM. Left: Quartz tube and exhaust hood in place without connection to sensors. Right: Open quartz tube, without exhaust tube or connection to sensors.

The tests on various sample sizes of PVC showed relative consistency in the HOC calculated between different sample sizes. The 70 mg tests provided results particularly close to those seen with the previous version of the MFC. This continues to further the argument that increased air flow to ensure well-ventilated conditions would make the MFC results more accurate and consistent with the previous version of the apparatus. However, this argument must be considered with the knowledge that a larger exhaust system must be explored to prevent the recirculation of combustion products and air in the outer quartz tube seen in the 200 mg PVC tests. The soot yield from the tests using the current version of the MFC is slightly higher than the soot yield from the previous version of the MFC, likely due to the possibility of slightly under-ventilated conditions. The ignition temperature of the different sample sizes varies as, like with PMMA and PE, the larger samples require more heating to achieve their ignition temperature and the thermocouple measures only the temperature of the bottom of the crucible which continues to rise even as the sample is heated. Additionally, inconsistency in ignition times between the different sample masses may be caused by inconsistency in the pyrolyzer plate temperature, as discussed in Chapter 3. The tests using this version of the MFC showed a comparable char yield to the tests conducted by DeBeer using the previous version of the MFC. This was promising, as past experience testing PVC in the previous version of the MFC resulted in char yields below the expected value due to excess oxidation of material in the crucible. The char yields found in the tests for this work were as expected, suggesting that there is not air entrainment into the inner quartz tube causing additional oxidation of sample material during testing.

The tests on PVC disks were inconsistent in their results and HRR profiles, as can be seen in the large error bars in Figure 4.5 and Figure 4.6. One potential explanation for this inconsistency was that the highly intumescent behavior of the PVC meant that the disks were not maintaining

strong thermal contact with the crucible during testing. The swelling and deformation of the samples may have resulted in uneven heating of the sample and, therefore, in inconsistency in burning behavior. To evaluate the effect of sample presentation on test results and consistency, PVC was also tested as shavings at the 70 mg and 100 mg sizes. The shavings were produced by filing a sheet of PVC and collecting the filings. The filings were placed in the crucible using a small scoop and were tamped down to ensure strong initial thermal contact between the sample and the crucible. The test results from the shavings tests are reported in Table 4.4 along with the data from the 70 mg and 100 mg disk tests for comparison. The HRR normalized by mass for the shavings and disks tests is plotted against time in Figure 4.9 and against temperature in Figure 4.10. The plots of the raw HRR normalized by mass over time are available in Appendix A.

Table 4.4 MFC Experimental Results for Disk and Shaving Sample Preparation Methods

		70 mg Disks	70 mg Shavings	100 mg Disks	100 mg Shavings
Sample Mass	[mg]	74.60 ± 2.37	70.10 ± 0.88	106.23 ± 1.94	99.70 ± 1.82
Time to Ignition	[s]	79 ± 2	70 ± 1	92 ± 4	73 ± 2
Char Yield	[%]	16.10 ± 0.44	19.48 ± 0.25	17.03 ± 1.39	19.50 ± 0.01
Soot Yield	[%]	5.63 ± 1.68	4.89 ± 0.64	8.40 ± 0.37	4.61 ± 0.68
Ignition Temperature	[°C]	361 ± 7.28	298 ± 12	347 ± 30.9	292 ± 5
Peak HRR	[kW/g]	249.0 ± 24.4	237.0 ± 39.8	269.0 ± 26.0	254.0 ± 16.1
Average HRR	[kW/g]	58.5 ± 15.2	60.4 ± 0.1	30.7 ± 2.7	53.6 ± 2.7
HOC (initial mass)	[kJ/g]	7.79 ± 1.6	5.94 ± 0.12	6.08 ± 0.23	7.02 ± 0.50
HOC (gasified mass)	[kJ/g]	9.27 ± 0.93	7.38 ± 0.07	7.24 ± 0.14	8.67 ± 0.27

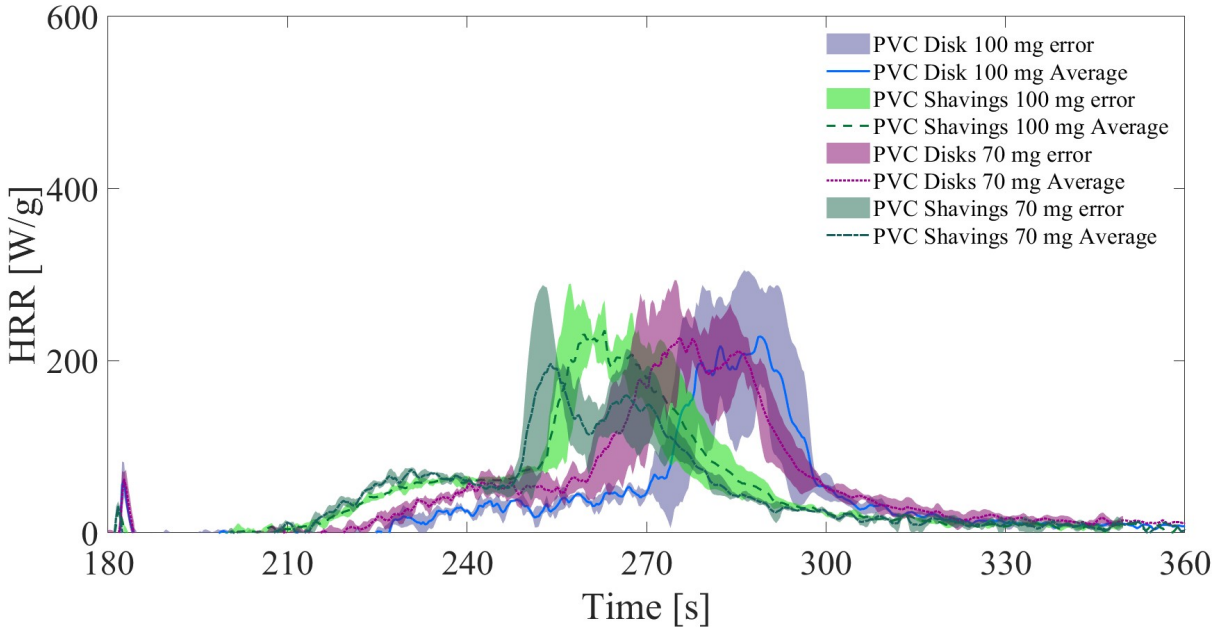

Figure 4.10 Average HRR with error plotted with respect to time for sets of three tests on two different sample preparations of PVC.

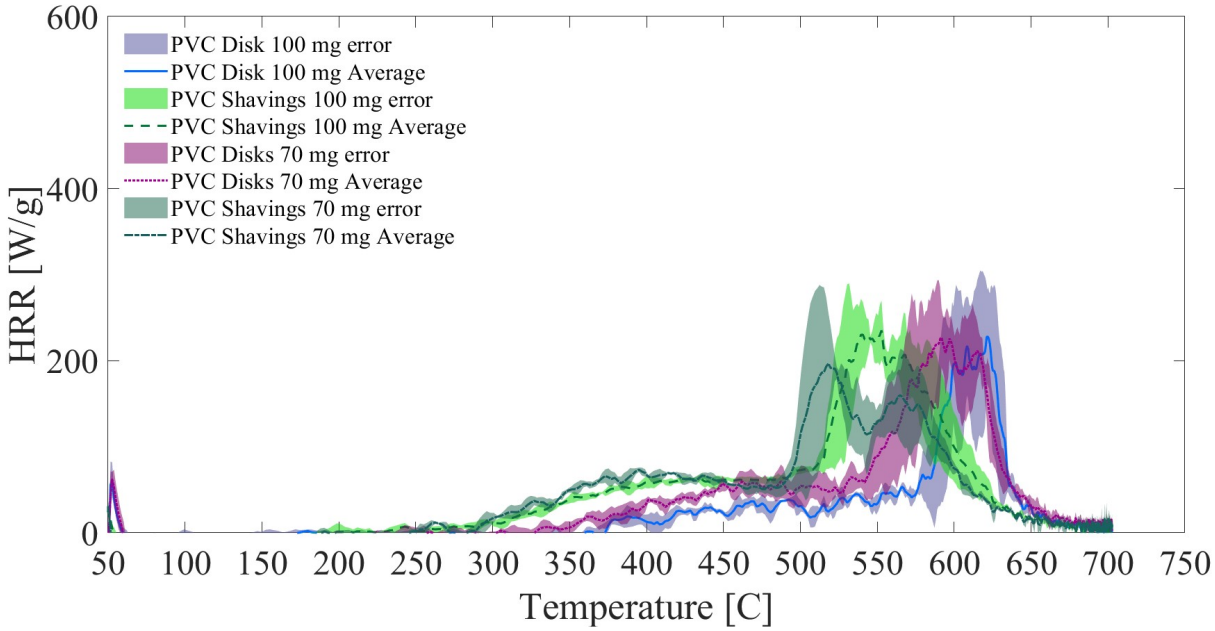

Figure 4.9 Average HRR with error plotted with respect to temperature for sets of three tests on two different sample preparations of PVC.

The shavings ignited earlier and at a lower temperature reading than the disk tests for both the 70 mg and 100 mg sample size. However, the large error bars in the plots show that inconsistency was not eliminated by changing the sample presentation. The inconsistency is likely due to

inconsistent heating across the surface of the pyrolyzer plate. The soot yield for the shavings tests was lower than for the tests on disks, whereas the char yield for the tests on shavings was higher than the char yield for tests on disks. This suggests that there was less oxidation of the material in the crucible and that the material that did pyrolyze was burned more completely with the shavings than with the disks.

4.4 PEEK

Polyether ether ketone (PEEK) is a polymer that is used for engineering applications due to its It is highly resistant to thermal decomposition and has a melting point of around 350 °C [20]. PEEK is rated as non-flammable by UL-94 testing, meaning that the samples self-extinguish when the ignition source is removed [21]. PEEK is a difficult material to burn successfully, making it an ideal polymer to test the limits of the ability of the updated version of the MFC to heat and burn samples. PEEK has been studied using the previous version of the MFC, making possible the direct comparison of results between the two versions of the apparatus. For this work, samples of PEEK were prepared as disks using a 12 mm drill. Samples were sanded down to various thicknesses to achieve their desired masses. PEEK was initially tested at the 70 mg size but failed to ignite at this size. The sample mass was increased to 120 mg, which also failed to ignite. Finally, the sample mass was increased to 250 mg, which resulted in successful ignition and burning. Additionally, in an attempt to more completely burn the samples of PEEK, three tests were conducted at increasing voltages. This resulted in peak temperatures of up to 745 °C at the end of the pyrolysis ramp and more rapid heating rates at the beginning of the pyrolysis ramps.

The flames seen with the PEEK samples were difficult to achieve. The samples decomposed slowly and off-gassed significantly before igniting at temperatures well over 600 °C. Once ignited, the flames were small and, for most samples, blue. The flames were unsteady and

sometimes extinguished before reigniting. The igniter coil remained on during the duration of testing to allow sustained combustion. The results of the PEEK tests are presented in Table 4.5. The average HRR normalized by mass and plotted over time is shown in Figure 4.11 and plotted with respect to temperature in Figure 4.12, along with the results from the tests at higher voltage. Raw plots of the HRR normalized by sample mass are provided in Appendix A.

Table 4.5 MFC Experimental Results for Tests Using Varied Voltage Settings with Current Version of Apparatus and Results for Tests Using Previous Version of MFC

		250 mg	1.23 V	1.235 V	1.245 V	DeBeer [9]
Sample Mass	[mg]	253.68 ± 2.53	252.88	252.07	253.77	55.38 ± 3.50
Time to Ignition	[s]	143 ± 4	129	131	127	-
Char Yield	[%]	84.75 ± 1.57	84.9	84.8	84.9	49.91 ± 2.85
Soot Yield	[%]	0.54 ± 0.13	0.69	0.79	0.68	1.81 ± 1.37
Ignition Temperature	[°C]	647 ± 5	647	630	642	652 ± 11
Peak HRR	[kW/g]	56 ± 1	41	65	65	448 ± 13
Average HRR	[kW/g]	37 ± 2	24	41	40	249 ± 43
HOC (initial mass)	[kJ/g]	2.17 ± 0.06	1.37	2.29	1.96	8.49 ± 0.23
HOC (gasified mass)	[kJ/g]	14.20 ± 0.79	11.9	15.1	13	17.57 ± 0.53

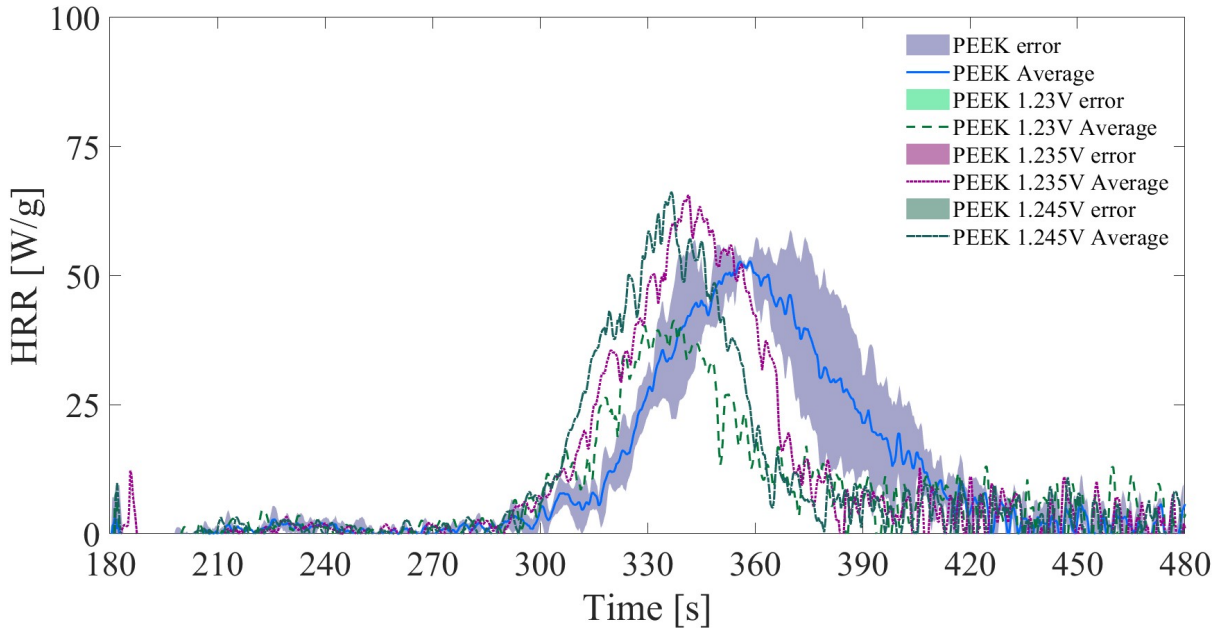

Figure 4.11 HRR normalized by mass for 250 mg PEEK samples and for tests on 250 mg PEEK samples at varied higher voltage settings plotted with respect to time.

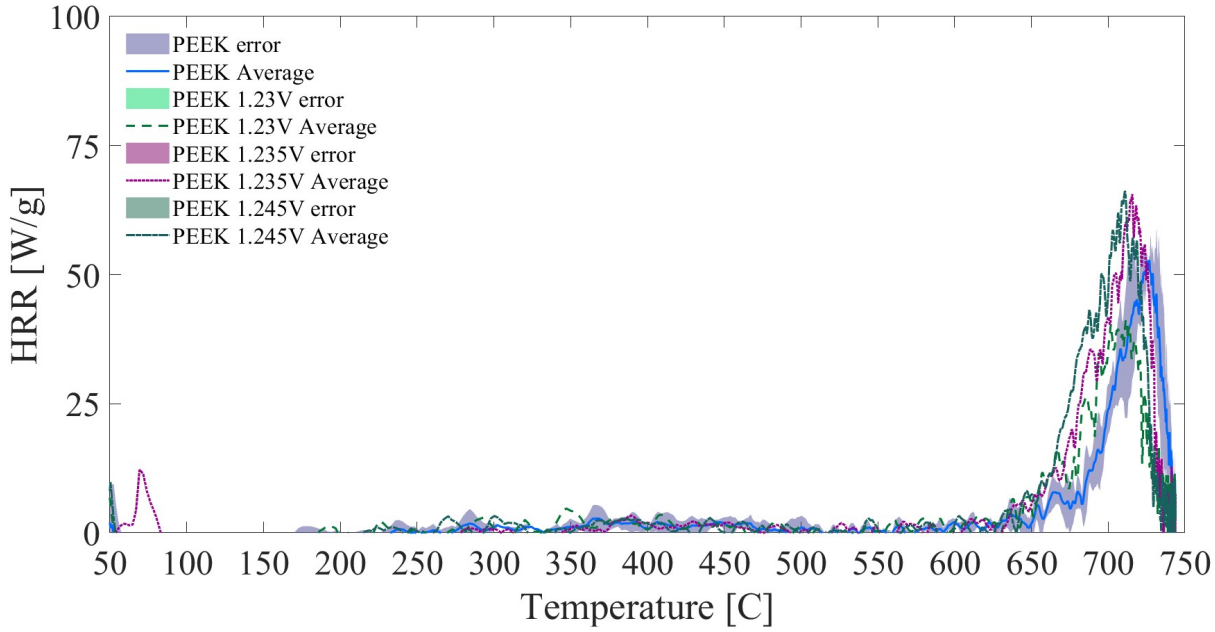

Figure 4.12 HRR normalized by mass for 250 mg PEEK samples and for tests on 250 mg PEEK samples at varied higher voltage settings plotted with respect to temperature.

The HRR curves for the PEEK tests are reasonably consistent, given the unsteady flaming observed during testing and occasional extinction and reignition of some of the samples. The tests at 1.235 V and 1.245 V have higher pHRR values than the tests conducted at lower voltages, but the average HRR values for all tests are similar. However, both the average HRR and pHRR values for all tests conducted for this work are significantly lower than the values found during tests using the previous version of the MFC. Similarly, though there is consistency between the HOC calculated across all tests conducted for this work, there is a significant discrepancy between the values of HOC calculated using initial mass in this work and in work using the previous version of the MFC. The tests conducted at a higher voltage ignited earlier in time and at lower temperature readings, suggesting that a faster heating rate improves the ignition and burning behavior when testing difficult to ignite materials, like PEEK.

The discrepancy between the values found using the version of the MFC used for this work and the previous version of the MFC is likely due to a combination of factors. First, the heating

rate for the pyrolyzer plate in this version of the MFC is slower than in the previous version of the MFC, meaning that samples are heated more gradually which may have resulted in more inconsistent burning behavior or a longer period of time in which the sample off-gassed but did not ignite. Additionally, as discussed in Chapter 3.3, there are inconsistencies in the temperature profile across the surface of the pyrolyzer plate. For samples presented as disks, this may cause uneven heating, resulting in reduced HRR and HOC values. This also may explain the high char yield, around 80%, of the PEEK samples tested in this work, as the samples may not have been exposed to sufficient and consistent heating. More consistent and rapid heating would likely achieve the expected char yield of around 50%, as was seen during tests conducted by DeBeer using the previous version of the MFC [9]. Finally, the samples of PEEK were large, and, like with the other polymers tested, may have been experiencing under-ventilated conditions in the outer quartz tube due to the limited 7 SLPM of air flow. Increased air flow would likely improve burning conditions for PEEK samples, as with the other polymers.

4.5 OSB

Oriented strand board (OSB) is a wood-based material commonly used in residential construction and furniture fabrication. OSB was selected for testing in this work to diversify the types of materials tested using the updated version of the MFC to reflect the versatility of the apparatus. Additionally, OSB is an inhomogeneous material and testing OSB will offer insight into the ability of the updated version of the MFC to accurately reflect the burning behavior of inhomogeneous materials. As discussed in Chapter 1.2.3, the previous version of the MFC struggled to provide consistent results on samples from inhomogeneous materials due to the small crucible size and it was a goal of this work to improve the results of testing on inhomogeneous materials. OSB samples were prepared as disks at two sample masses: 70 mg and 175 mg. The 70 mg disks were prepared

using an 8 mm drill, while the 75 mg samples were prepared using a 12 mm drill. Once drilled, samples were cut or filed until they were the desired mass. From experience with the previous version of the MFC, preparing the larger 175 mg samples was easier as the amount of filing or cutting to size was significantly reduced.

OSB ignited easily and burned steadily during testing. The results of testing on the 70 mg and 175 mg samples are presented in Table 4.6, along with results from tests conducted using the previous version of the MFC for comparison with this work. The HRR normalized by sample mass is plotted against time and temperature in Figure 4.13 and Figure 4.14.

Table 4.6 Experimental Results Using Updated and Previous Version of MFC

		70 mg	175 mg	40 mg (Original MFC)
Sample Mass	[mg]	70.22 ± 2.39	177.13 ± 5.65	47.38 ± 0.56
Time to Ignition	[s]	63 ± 2	64 ± 2	NR
Char Yield	[%]	14.95 ± 0.06	16.73 ± 2.24	15.31 ± 0.55
Soot Yield	[%]	3.45 ± 1.87	1.67 ± 0.33	NM
Ignition Temperature	[°C]	379 ± 8.62	371 ± 10.4	407 ± 8.55
Peak HRR	[kW/g]	419.0 ± 20.6	329.0 ± 19.8	433.0 ± 33.1
Average HRR	[kW/g]	286.0 ± 24.0	219.0 ± 9.6	282.0 ± 13.4
HOC (initial mass)	[kJ/g]	9.73 ± 1.19	10.20 ± 0.17	9.99 ± 0.42
HOC (gasified mass)	[kJ/g]	11.40 ± 0.70	12.70 ± 0.10	11.80 ± 0.26

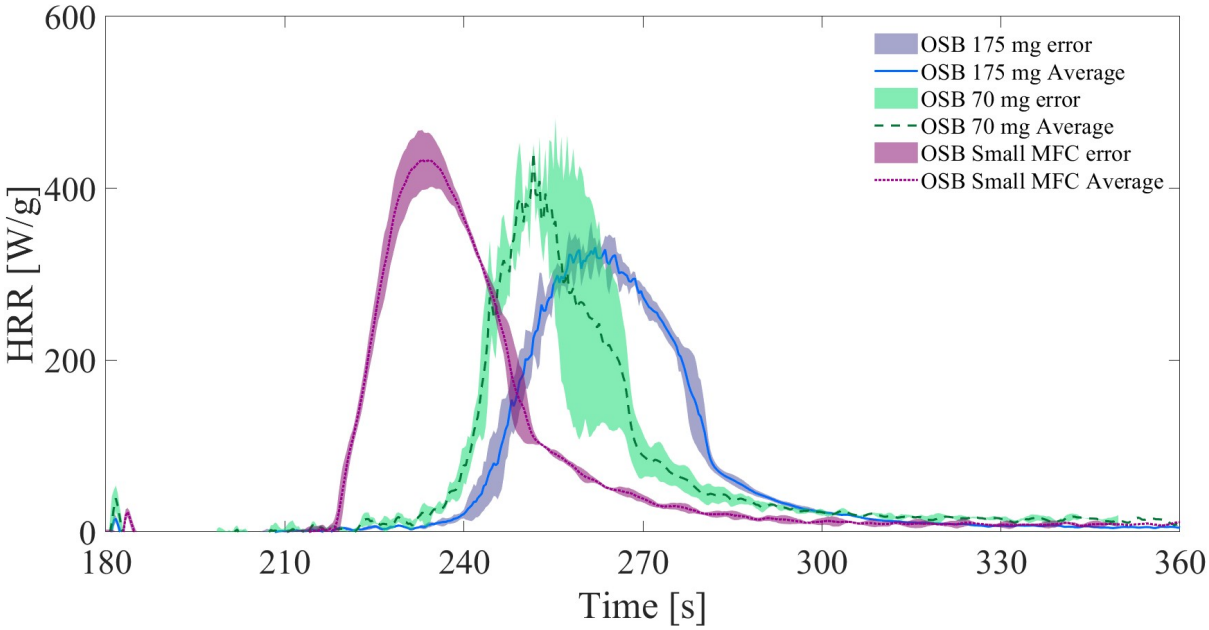

Figure 4.14 HRR normalized by mass plotted over time for tests conducted using the updated and previous versions of the MFC.

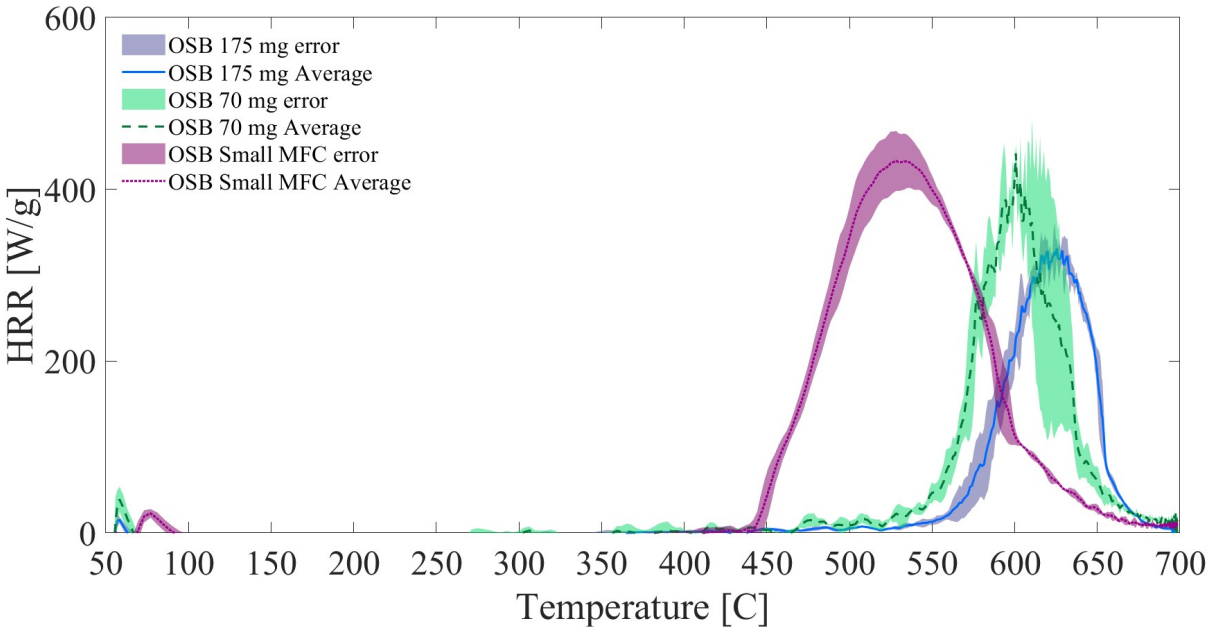

Figure 4.13 HRR normalized by mass plotted with respect to temperature for tests conducted using the updated and previous versions of the MFC.

The OSB tests were consistent, though the large error observed with the 70 mg sample tests is a result of an extinction and reignition related to the igniter coil being mistakenly turned off early. The tests had similar pHRR and average HRR for both sample sizes tested using the updated

version of the apparatus and were also consistent with the tests conducted using the previous version of the apparatus. Similarly, the HOC calculated using initial and gasified mass was consistent across tests conducted at all sample masses and with both versions of the apparatus.

The greatest inconsistency between the tests using the updated and previous version of the MFC lies in the ignition temperature, as seen in Figure 4.14. The higher ignition temperature seen in the tests using the updated version of the MFC may be due to inconsistent heating across the surface of the pyrolyzer plate. The increased mass of the samples additionally will require more heat to cause ignition, potentially leading to higher thermocouple readings at the bottom of the crucible as the heat is transferred through the crucible to the sample and through the sample mass.

4.6 Summary of Test Results

The tests conducted for this work on four polymers and OSB showed the functionality and versatility of the updated version of the MFC, but also began to reveal the limitations of the apparatus and areas for future work and improvements. The apparatus was successfully able to ignite and burn materials with a variety of burning behaviors, ranging from highly combustible materials, like PE, to difficult to non-flammable materials, like PVC and PEEK. The results of testing were not impacted significantly by sample presentation, which varied for the different materials and included powder, shavings, beads, and disks. Additionally, the updated version of the apparatus successfully burned samples with masses as high as 250 mg and as low as 40 mg, giving it a much broader ability for testing than the previous version of the apparatus.

There was general consistency with the results of work conducted using the previous version of the apparatus, and inconsistency between the two versions of the MFC can be addressed through increasing the air flow through the outer quartz tube to improve ventilation conditions at larger samples sizes. This would address the variety of evidence presented that at the current 7 SLPM the

conditions in the outer quartz tube become slightly under-ventilated when burning larger sample masses. Furthermore, increasing the size of the exhaust system would also address the under-ventilated conditions seen in the outer quartz tube by eliminating recirculation of air and smoke during testing. Additionally, improvements in pyrolyzer coil consistency would result in more consistent heating across the surface of the pyrolyzer plate which would likely improve the results of testing using the updated version of the apparatus.

5. Conclusion

Updating the MFC apparatus by increasing the crucible size to allow testing of larger samples offered a variety of benefits to improve upon the drawbacks of the MFC outlined in Chapter 1. Tests conducted with the updated version of the apparatus demonstrated the ability of the updated MFC to test a wide variety of sample sizes, ranging from the sizes tested in the previous version of the apparatus around 40 mg to sample masses as large as 250 mg. This increased the versatility of the apparatus for testing and allowed for easier sample preparation. Samples of PVC, PEEK, and OSB were prepared as disks for testing in this work. Preparing disk samples in the previous version of the apparatus required significant sanding or cutting to achieve the desired sample mass, a process which added significant time to testing. With the updated version of the apparatus, samples were drilled using a larger drill and required only moderate amounts of sanding or cutting to achieve the desired sample size, thus reducing the amount of time required for sample preparation. Testing on OSB also showed the enhanced ability of the updated version of the MFC to test inhomogeneous materials. Because an increased crucible size allowed for samples with a greater surface area, tests on OSB, particularly at the 175 mg size, were more consistent than tests using the previous version of the MFC. Additionally, because the tests capture a larger area of sample mass, they will more accurately reflect the burning behavior of OSB during full-scale burning, showing the utility of the updated version of the apparatus for testing inhomogeneous materials. Though biomass was not tested in this work, the versatility of the updated version of the MFC to test samples at a wide range of masses and the increased crucible diameter make the updated version of the MFC well-suited for tests on biomass materials. The characteristic length of samples such as pine needles or grass could be better preserved during testing using the updated version of the MFC. Testing on biomass is particularly important and a major area of research

today due to the prevalence of wildfires, so enhancing the ability of the MFC to test biomass materials allows expansion of the use of the MFC into this area of research.

The increase in crucible size also meant increasing the size of the pyrolyzer, which allowed for the exploration of new heater manufacturing techniques. The hand-coiled NiCr wire technique was used for this work due to time constraints preventing the full development of other promising heater manufacturing techniques. It was easier to produce a heater for the larger, updated version of the MFC using the hand-coiled NiCr wire method than to produce the small heater required for the previous version of the MFC. This was an improvement over the previous version of the apparatus, and the hand-coiled NiCr wire method was easy to implement and effective for the purpose of this work. However, the hand-coiled heaters result in some inconsistency between each different heater which must be adjusted for with minor voltage optimization when the heater is replaced. Additionally, it was observed with a FLIR camera that there was some inconsistency in temperature profile across the surface of the pyrolyzer plate, which is a product of the manual manufacturing technique. By hand, it is difficult to create identical coils, meaning that there is inherent variation in the heating density due to the specific placement of the wires.

It is recommended that alternate heater manufacturing methods, as outline in Chapter 2, be explored for further research. The method of 3D printing coils using Inconel shows particular promise due to the properties of Inconel, which has a high maximum operating temperature and sufficient electrical conductivity for use as a heating element. Additionally, an automated method like 3D printing increases the repeatability of each heater which will allow for greater repeatability between tests using different heaters. Similarly, 3D printing allows for coils to be placed more closely together, allowing for greater heating density and, therefore, improved consistency of the temperature profile across the surface of the pyrolyzer plate. Carbon paper is also a method that

may be suitable for implementation in the MFC apparatus and is recommended with additional research into the heater preparation and construction process.

The optimization process for the updated version of the MFC allowed for the establishment of a base setting in LawVIEW for the pyrolyzer voltage settings. However, as the pyrolyzers are manufactured by hand and are not identical, each individual pyrolyzer will require some optimization from this setting in order to achieve the desired peak temperature at the end of the pre-heating and pyrolysis ramps. The N_2 flow was also optimized to achieve the necessary flow to propel volatile gases out of the inner quartz tube without causing dilution and preventing ignition. This process was conducted mainly using PE samples, as PE condenses heavily meaning that if there is no leftover condensation in the inner quartz tube after a PE test, there will be no condensation after a test with the same settings of a less heavily condensing material.

The increased N_2 flow and increased sample sizes resulted in a need for increased air flow through the outer quartz tube. However, due to limitations on the flow controllers and flow meter, the maximum amount of air that could be flowed through the MFC in the updated version of the apparatus was 7 SLPM. This was increased from 4 SLPM in the previous version of the apparatus but was insufficient to ensure well-ventilated conditions throughout testing for all sample masses and materials. The N_2 flow was tripled from the previous version of the apparatus so optimally the air flow would have been tripled from the previous version of the MFC, resulting in an ideal air flow of 12 SLPM. The limited airflow resulted in the O_2 levels for some tests dropping below the threshold of 16% for well-ventilated conditions. Additionally, inconsistencies in test results and lower values for HOC than found in previous research suggest under-ventilated conditions.

However, increased air flow alone cannot resolve the flow issues in the updated version of the MFC. The exhaust system was reused from the previous version of the apparatus and was not

designed to handle the quantity of air flow used in this work, or the larger quantity of air flow that would be required for future work. Tests on PVC, which produces significant amounts of smoke during combustion, revealed recirculation of the air and smoke in the outer quartz tube during testing. Two tests, one without the connection to the sensors and one without the exhaust hood, were conducted to determine the location of the cause of the recirculation. These tests revealed that the exhaust hood constricts the flow and causes recirculation, even when the sensors are not connected. For future work, the exhaust hood and overall exhaust system, including the particulate filter and tubing connecting the exhaust hood to the flow meter and gas sensors will need to be increased in size to accommodate the larger flow necessary to maintain well-ventilated conditions.

The updates to the MFC conducted in this work showed that the increased size improved the versatility and utility of the apparatus, as well as the ease of manufacture of the pyrolyzer coil. There is, however, room for future research and improvement to the apparatus. Further research into heater construction methods, particularly exploration of carbon paper or 3D printing Inconel, is an area of improvement for the apparatus. Updating the heater manufacturing technique could improve MFC test results by increasing the consistency of the heater when replaced and by improving the consistency of the temperature profile across the surface of the pyrolyzer. Additionally, there is the possibility of exploring alternate methods to improve pyrolyzer temperature consistency, such as adding a conductive material like copper foil to the top surface of the pyrolyzer plate to create more even temperatures. Another area of future work is to update the exhaust system to handle larger flow rates and increase the air flow through the apparatus. This would require testing to evaluate the O_2 levels during testing to ensure well-ventilated conditions throughout a test, as well as testing to ensure the absence of recirculation in the outer quartz tube. Making improvements to the exhaust system and flowing larger quantities of air through the MFC

would improve the consistency and accuracy of the test results using the updated version of the apparatus, particularly at larger sample masses. Another area of future work could be to explore the ability of the MFC to create a controlled atmosphere in the outer quartz tube to deliberately replicate under-ventilated burning conditions. Fires in the real world are often under-ventilated, leading them to produce greater yields of soot, CO_2, and CO, as well as other toxic products. Expanding the ability of the MFC to test in under-ventilated conditions would expand the uses of the apparatus and offer insight into burning behavior that are not gained through other fire testing methods, such as MCC tests.

The updated version of the MFC provides largely similar results to the previous version of the apparatus. However, a major concern with the updated version of the apparatus is the inconsistency in test results seen when the sample mass is changed. While there is room for future improvements on the MFC, it is a versatile and useful fire testing apparatus for tests on small sample masses in a variety of sample presentations.

Appendix A

The plots of the HRR normalized by mass for each test that resulted in the average plots shown in Chapter 4 are shown for each of the test materials. Additionally, plots showing the percent of O_2 detected by the gas sensor for each material are also shown for each material. Finally, the temperature reported by the thermocouple over time is also shown for each test for each material.

PMMA

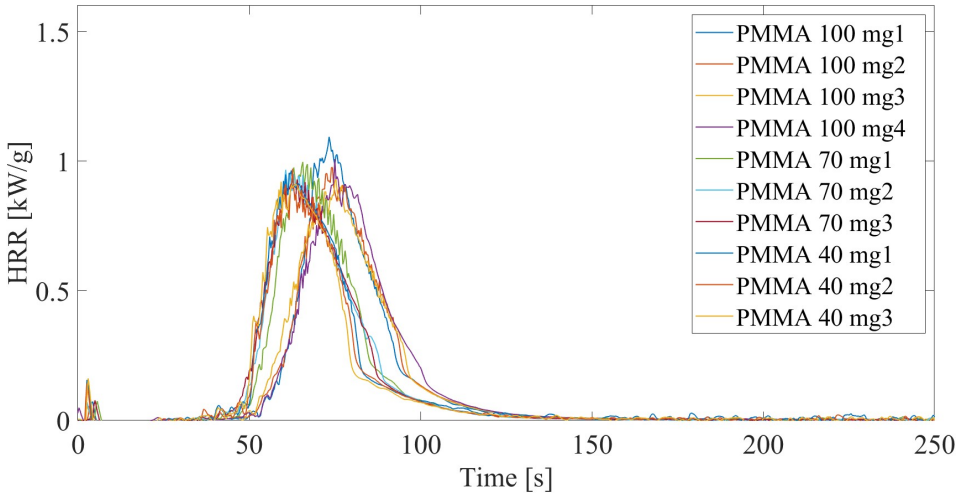

Figure A.1 Raw HRR curves normalized by initial sample mass for PMMA tests at 100 mg, 70 mg, and 40 mg sample masses.

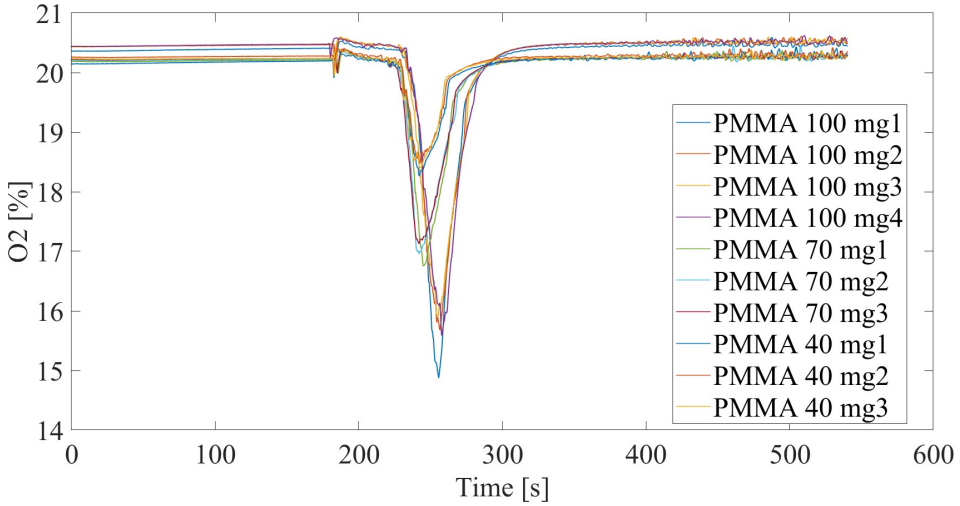

Figure A.2 Percent O_2 detected by the gas sensors during testing of PMMA at 100 mg, 70 mg, and 40 mg sample masses.

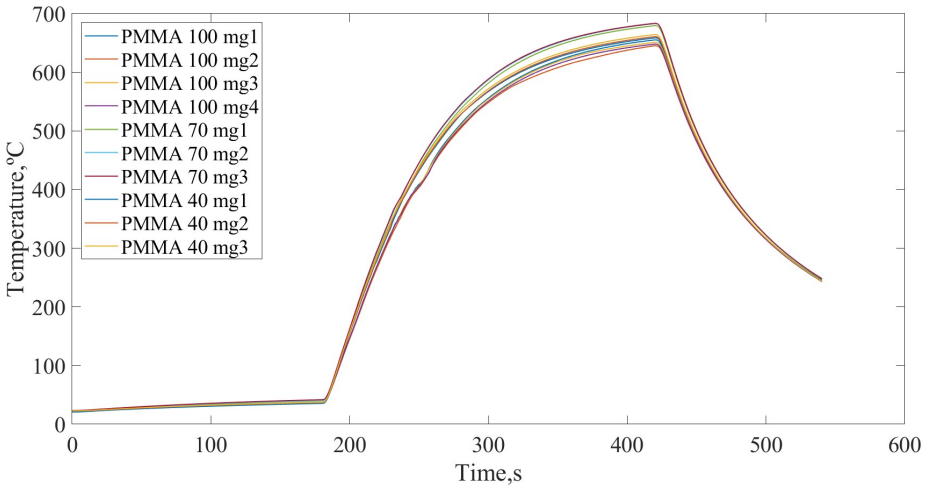

Figure A.3 Temperature reported by the thermocouple during testing of PMMA at 100 mg, 70 mg, and 40 mg sample masses. The dip seen between 200 s and 300 s corresponds to ignition of the sample.

PE

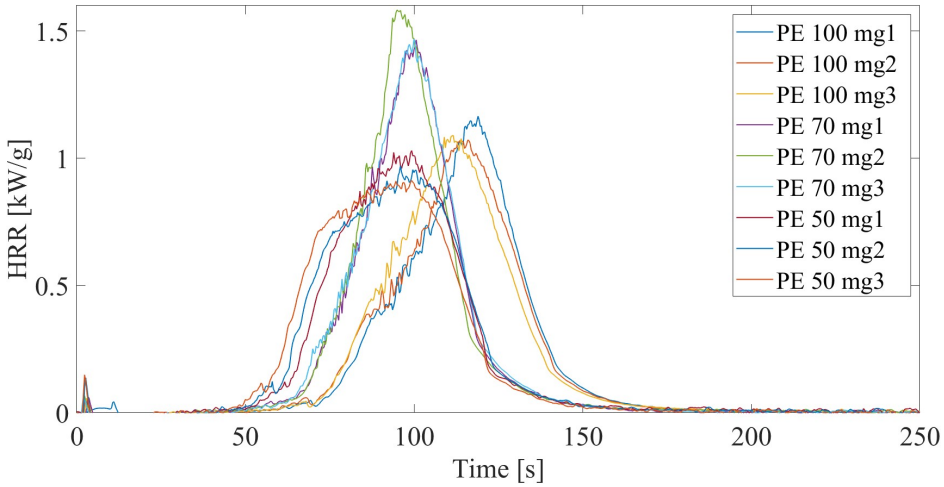

Figure A.4 Raw HRR curves normalized by initial sample mass for PE tests at 100 mg, 70 mg, and 50 mg sample masses.

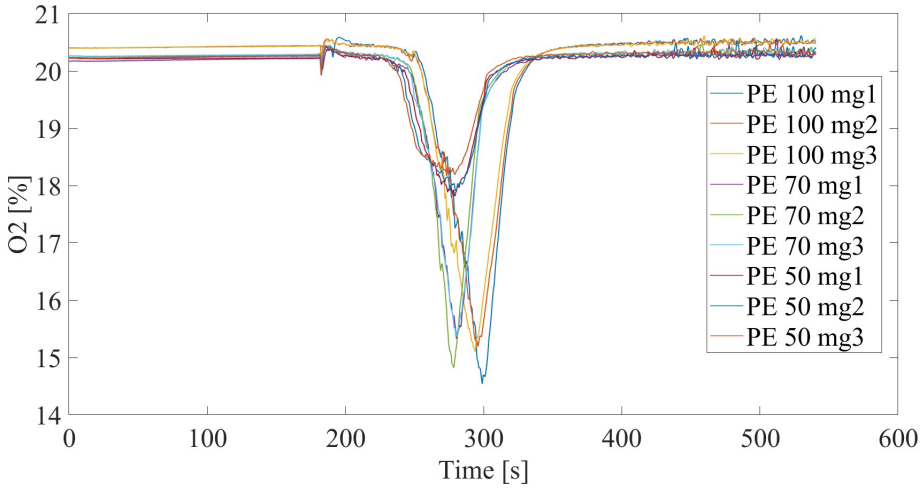

Figure A.5 Percent O_2 detected by the gas sensors during testing of PE at 100 mg, 70 mg, and 50 mg sample masses.

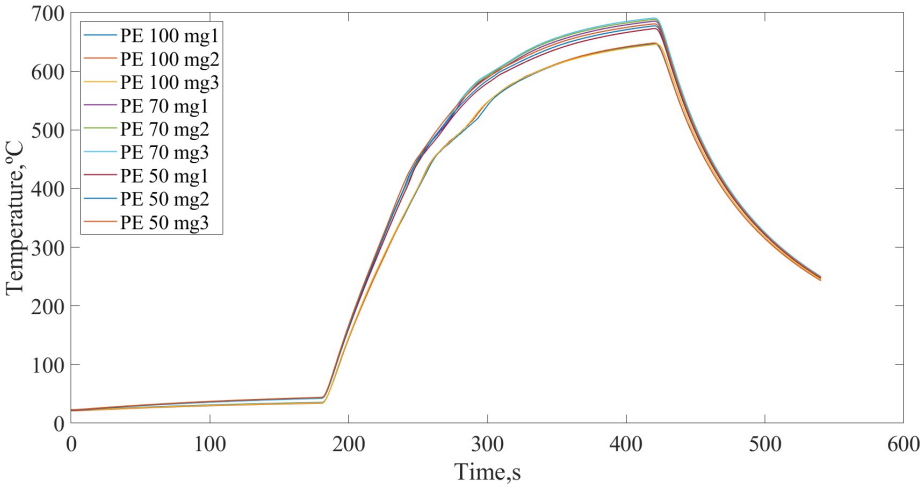

Figure A.6 Temperature reported by the thermocouple during testing of PE at 100 mg, 70 mg, and 50 mg sample masses. The dip seen between 200 s and 300 s corresponds to ignition of the sample.

PVC

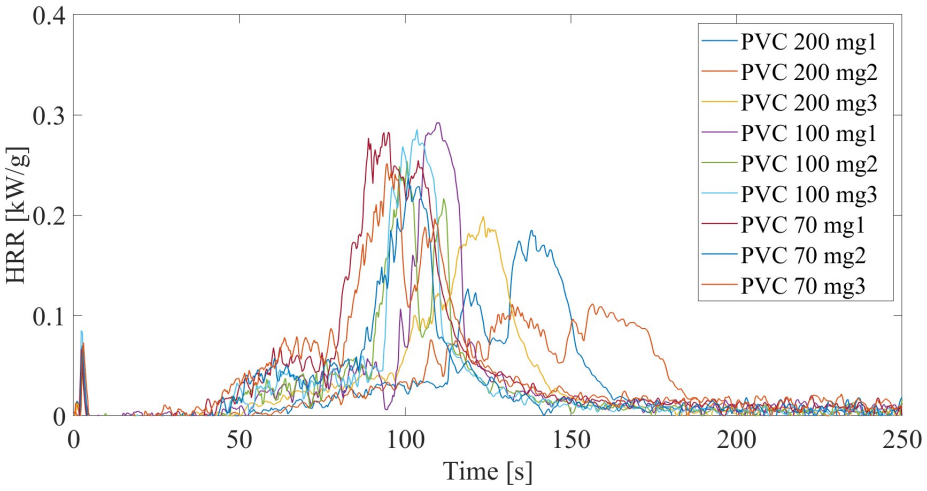

Figure A.7 Raw HRR curves normalized by initial sample mass for PVC tests at 200 mg, 100 mg, and 70 mg sample masses when burned as disks.

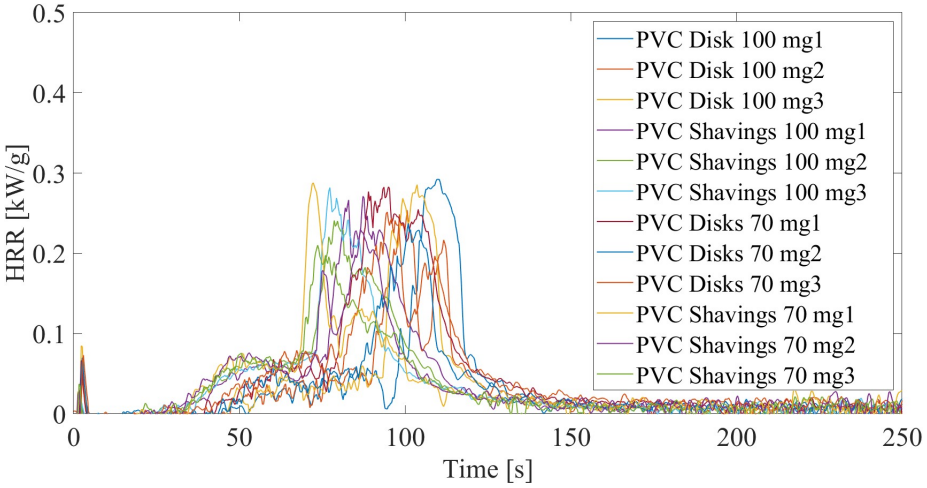

Figure A.8 Raw HRR curves normalized by initial sample mass for PVC tests at 100 mg and 70 mg sample masses when burned as disks compared to when burned as shavings.

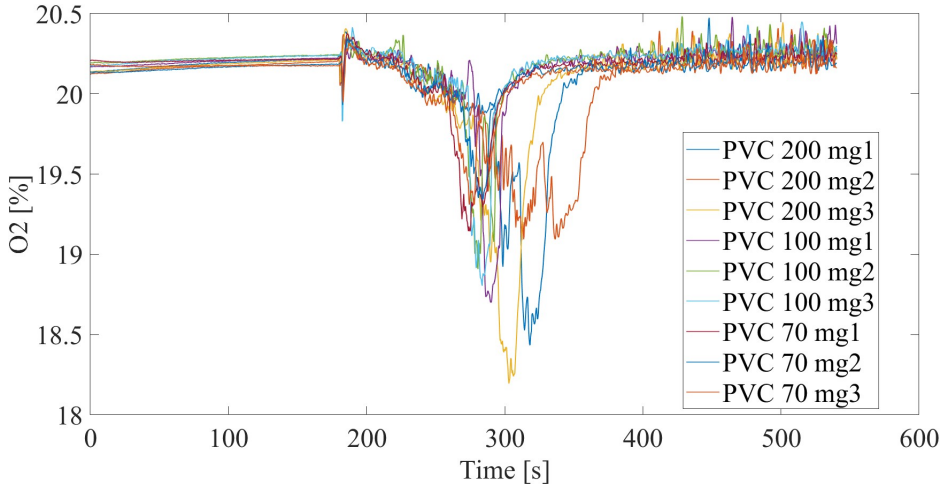

Figure A.9 Percent O_2 detected by the gas sensors during testing of PVC at 200 mg, 100 mg, and 70 mg sample masses when prepared as disks.

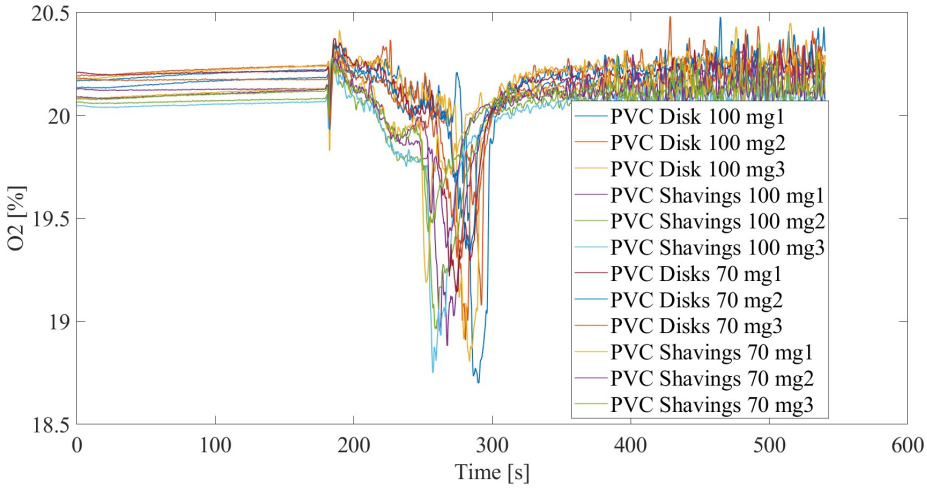

Figure A.10 Percent O_2 detected by the gas sensors during testing of PVC at 100 mg and 70 mg sample masses when prepared as disks and compared to when prepared as shavings.

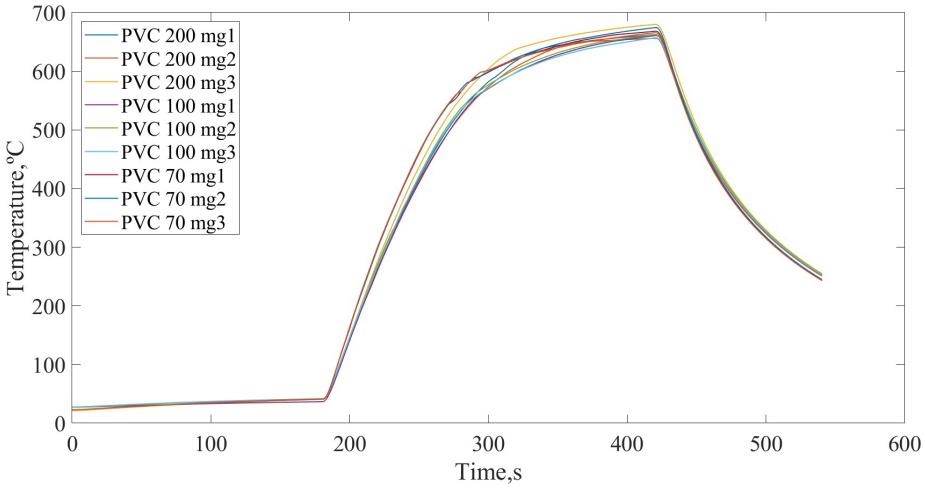

Figure A.11 Temperature reported by the thermocouple during testing of PVC at 200 mg, 100 mg, and 70 mg sample masses with samples prepared as disks. The dip seen between 200 s and 300 s corresponds to ignition of the sample.

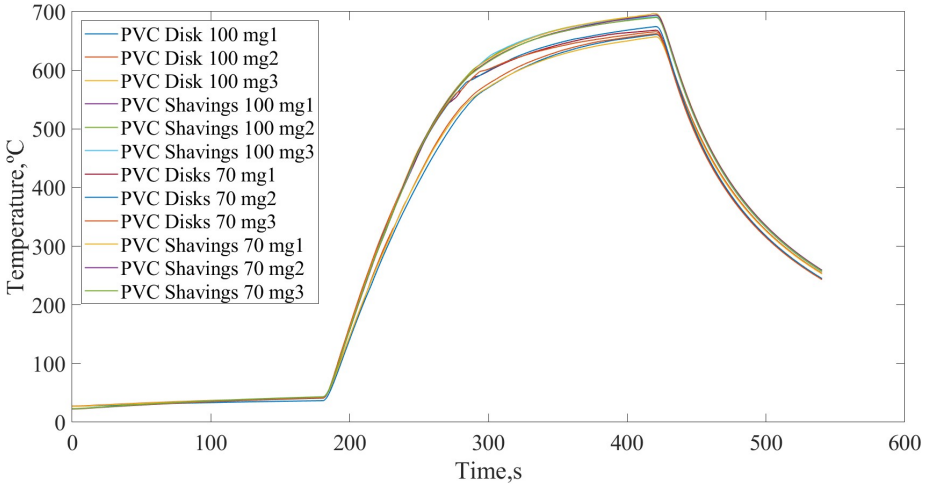

Figure A.12 Temperature reported by the thermocouple during testing of PVC at 100 mg and 70 mg sample masses with samples prepared as disks compared to samples prepared as shavings. The dip seen between 200 s and 300 s corresponds to ignition of the sample.

PEEK

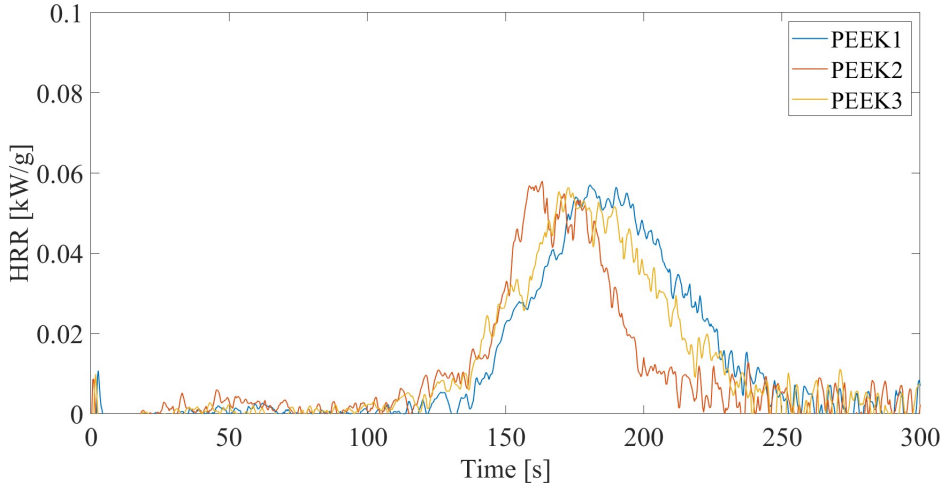

Figure A.13 Raw HRR curves normalized by initial sample mass for PEEK tests at 250 mg.

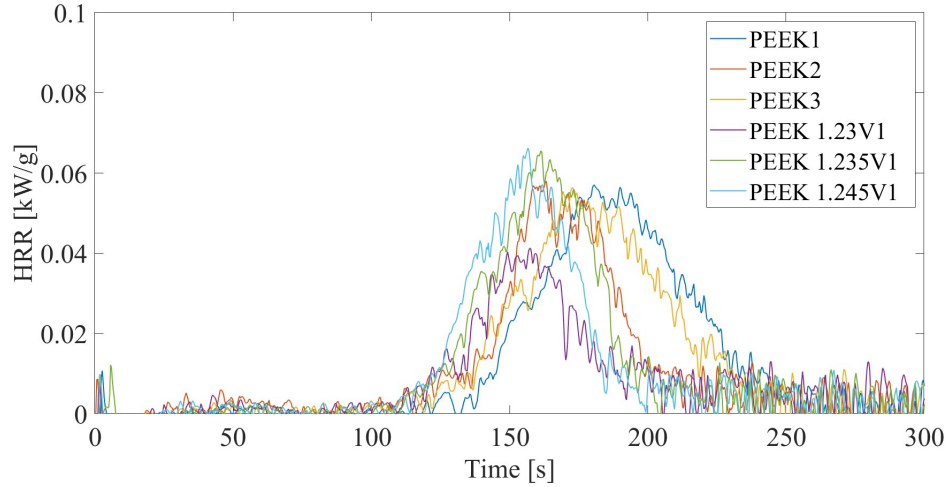

Figure A.14 Raw HRR curves normalized by initial sample mass for PEEK tests at 250 mg with 3 tests at 1.225 V, and three tests at progressively higher voltage settings.

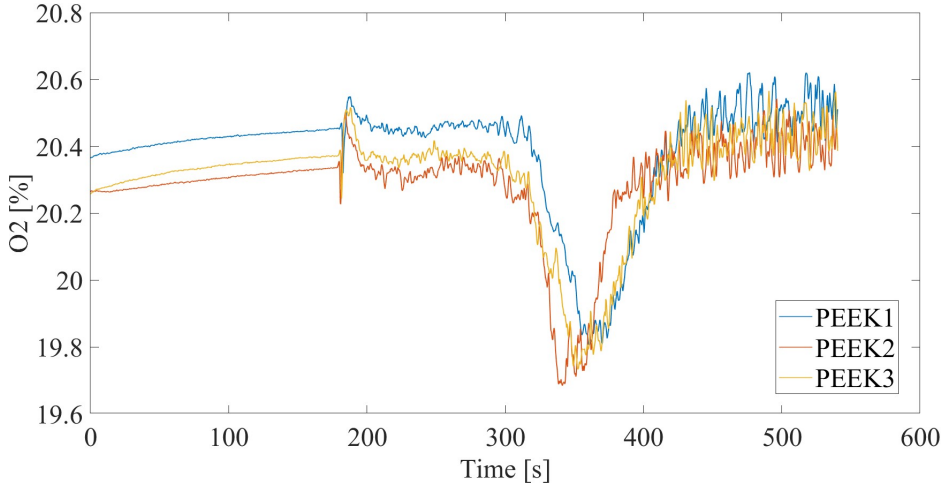

Figure A.15 Percent O_2 detected by the gas sensors during testing of PEEK at 250 mg.

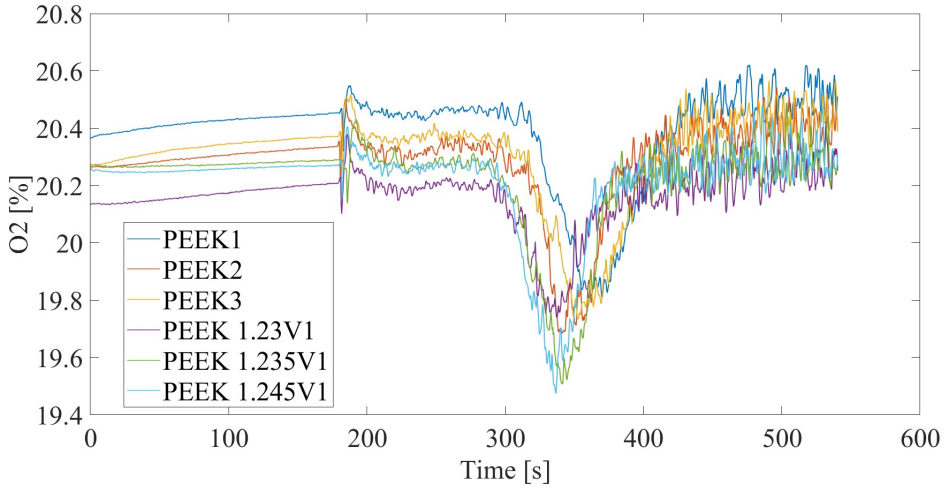

Figure A.16 Percent O_2 detected by the gas sensors during testing of PEEK at 250 mg when tested three times at 1.225 V, and at three progressively higher voltage settings.

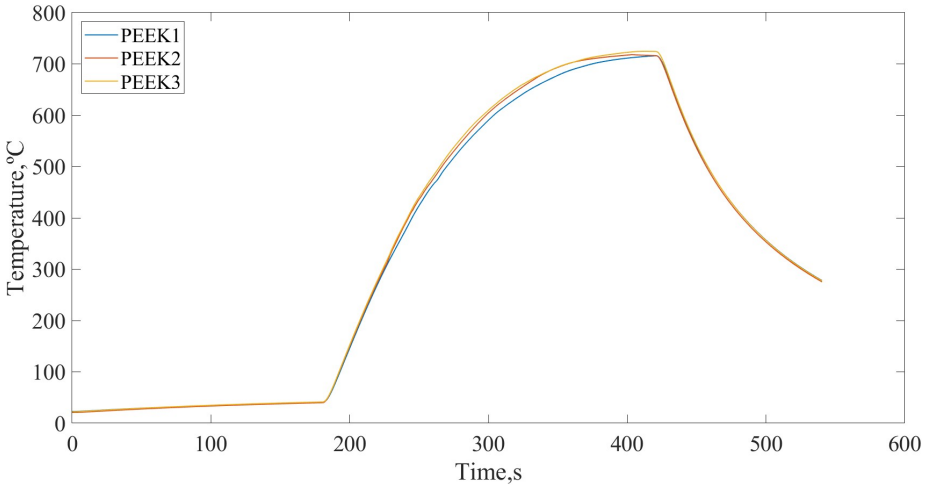

Figure A.17 Temperature reported by the thermocouple during testing of PEEK at 250 mg.

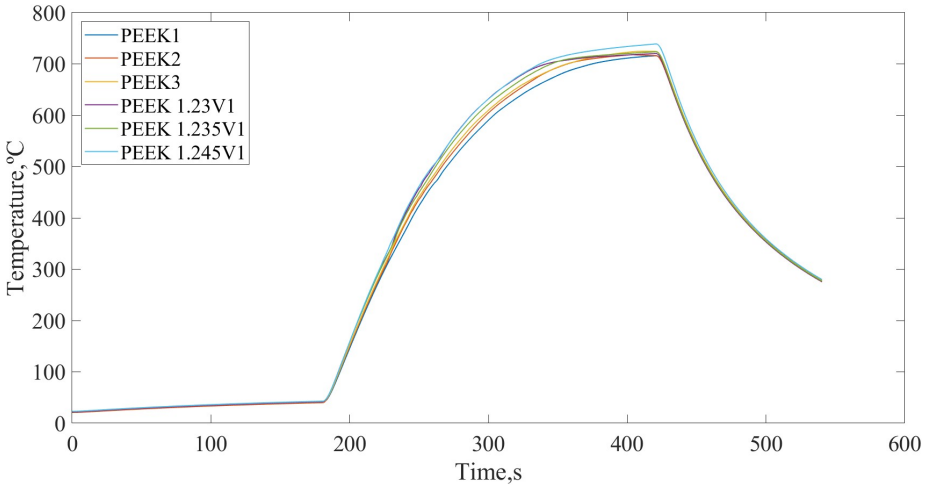

Figure A.18 Temperature reported by the thermocouple during testing of PEEK at 250 mg with three tests at 1.225 V, and three tests at progressively higher voltage settings.

OSB

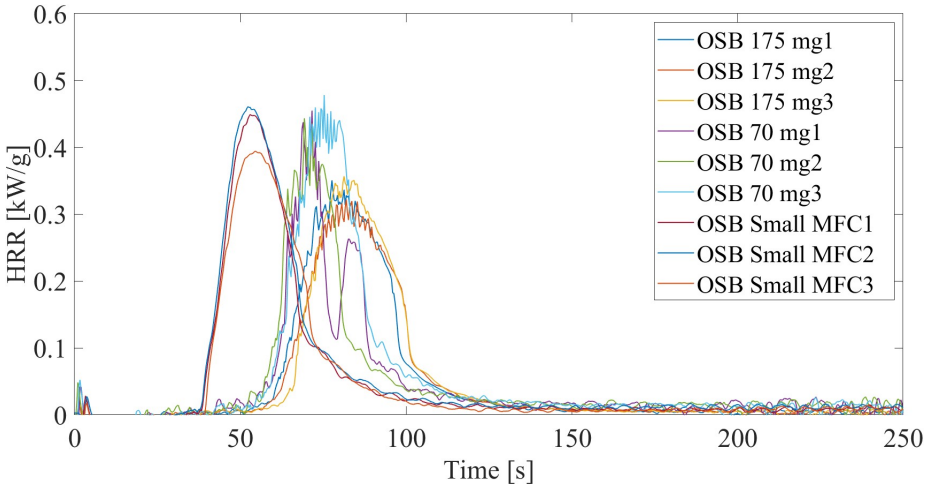

Figure A.19 Raw HRR curves normalized by initial sample mass for OSB tests at 175 mg, 70 mg, and 40 mg sample masses when burned as disks. The 40 mg samples were burned using the previous version of the MFC.

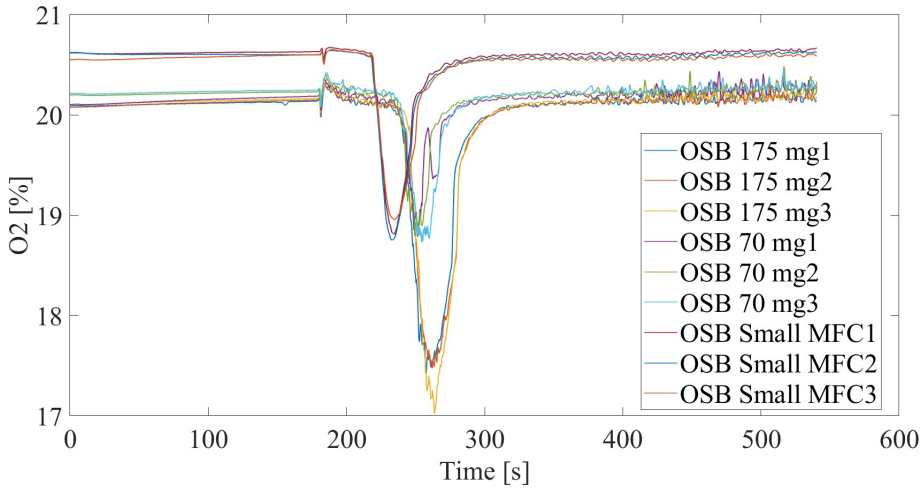

Figure A.20 Percent O_2 detected by the gas sensors during testing of OSB at 175 mg, 70 mg, and 40 mg (tested using previous version of MFC). The tests using the previous version of the MFC show a higher O_2 percentage initially due to less N_2 flow through the inner quartz tube during testing.

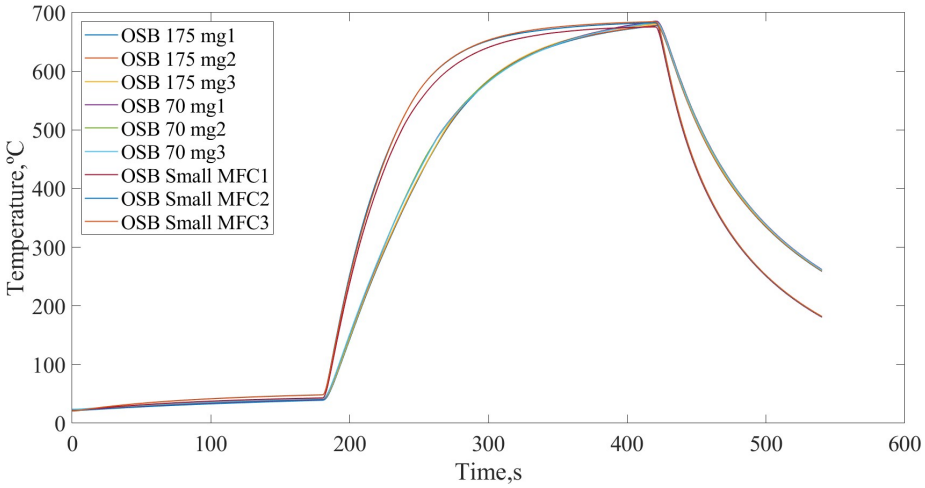

Figure A.21 Temperature reported by the thermocouple during testing of OSB at 175 mg, 70 mg, and 40 mg (tested using previous version of the MFC) sample masses.

Bibliography

[1] Hall, Shelby. “US Fire Problem: Fire Loss in the United States.” *Nfpa.Org*, NFPA Research, 1 Nov. 2023, www.nfpa.org/education-and-research/research/nfpa-research/fire-statistical-reports/fire-loss-in-the-united-states.

[2] Madrzykowski, Daniel. “New Comparison of Natural and Synthetic Home Furnishings.” *Fire Safety Research Institute*, 30 Sept. 2020, fsri.org/research/new-comparison-natural-and-synthetic-home-furnishings.

[3] ASTM E1354, Standard Test Method for Heat and Visible Smoke Release Rates for Materials and Products Using an Oxygen Consumption Calorimeter, (2019). C.

[4] Dewaghe, C.Y. Lew, M. Claes, S.A. Belgium, P. Dubois, 23 - Fire-retardant applications of polymer–carbon nanotubes composites: improved barrier effect and synergism, in: T. McNally, P.B.T.-P.N.C. Pötschke (Eds.), Woodhead Publ. Ser. Compos. Sci. Eng., Woodhead Publishing, 2011: pp. 718–745. doi:https://doi.org/10.1533/9780857091390.3.718.

[5] Babrauskas, Vytenis. “The Cone Calorimeter.” *The SFPE Handbook of Fire Protection Engineering*, Springer, New York, NY, 2016, pp. 952–980, Accessed 2024.

[6] C. Huggett, Estimation of rate of heat release by means of oxygen consumption measurements, Fire Mater. 4 (1980) 61–65. doi:10.1002/fam.810040202.

[7] Khan, Mohammed, et al. “Combustion Characteristics of Materials and Generation of Fire Products.” *The SFPE Handbook of Fire Protection Engineering*, Springer, New York, NY, 2016, pp. 1143–1232, Accessed 2024.

[8] ASTM E2058, Standard Test Methods for Measurement of Material Flammability Using a Fire Propagation Apparatus (FPA), (2019).

[9] J. A. De Beer, Milligram-scale flame calorimetry: Novel design of a pyrolyzer system used to emulate the burning behavior exhibited by coupon-sized cone calorimetry samples, ProQuest Dissertations & Theses Global, (2020), (2454590140), https://www.proquest.com/dissertations-theses/milligramscale-flame-calorimetry-novel-design/docview/2454590140/se-2

[10] R. Lyon, R. Walters, A Microscale Combustion Calorimeter, Federal Aviation Administration, February 2002.

[11] R.E. Lyon, R.N. Walters, S.I. Stoliarov, Screening flame retardants for plastics using microscale combustion calorimetry, Polym. Eng. Sci. 47 (2007) 15011510. doi:10.1002/pen.20871.

[12] ASTM D7309, Standard Test Method for Determining Flammability Characteristics of Plastics and Other Solid Materials Using Microscale Combustion Calorimetry, (2019).

[13] Raffan-Montoya, Fernando, et al. “Measurement of heat release in laminar diffusion flames fueled by controlled pyrolysis of Milligram-sized solid samples: Impact of bromine- and phosphorus-based flame retardants.” *Combustion and Flame*, vol. 162, no. 12, Dec. 2015, pp. 4660–4670, https://doi.org/10.1016/j.combustflame.2015.09.031.

[14] Roche, Thomas. “Use Of Milligram-Scale Flame Calorimetry For Characterizing Flammability Of Fabric Samples With Flame Retardant Treatments.” *University of Maryland*, 2023.

[15] “Inconel Alloy 625.” *Special Metals*, 2013, specialmetals.com.

[16] Heaney, M. “Electrical Conductivity and Resistivity” in *Electrical Measurement, Signal Processing, and Displays* John G. Webster. CRC Press (2004) pp. 7-3

[17] “Inconel 625 Technical Data.” *High Temp Metals*, 2015, www.hightempmetals.com/techdata/hitempInconel625data.php.

[18] Dong, Q., Yao, Y., Cheng, S. et al. Programmable heating and quenching for efficient thermochemical synthesis. Nature 605, 470–476 (2022). https://doi.org/10.1038/s41586-022-04568-6

[19] “Fire Retarding Properties.” *PVC South East Europe*, 2010, www.seepvcforum.com/en/content/29-fire-retarding-properties.

[20] McKeen, Laurence. “Chapter 10 High Temperature Polymers.” *The Effect of Creep and Other Time Related Factors on Plastics and Elastomers*, 2nd ed., William Andrew Publishing, 2009, pp. 337–372. *Science Direct*, https://www-sciencedirect-com.proxy-um.researchport.umd.edu/science/article/abs/pii/B9780815515852500121. Accessed 2024.

[21] “UL 94 Classification and Flame-Retardant Plastic Materials.” *Protolabs*, Mar. 2019, www.protolabs.com/resources/blog/flame-retardant-thermoplastics-and-ul-classifications/.